

OPTIMAL LIQUIDATION STRATEGIES FOR LARGE-TICK STOCKS

A THESIS PRESENTED FOR THE DEGREE OF
DOCTOR OF PHILOSOPHY OF IMPERIAL COLLEGE LONDON

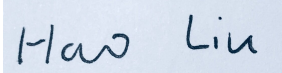
AND THE
DIPLOMA OF IMPERIAL COLLEGE

BY
HAO LIU

DEPARTMENT OF MATHEMATICS
IMPERIAL COLLEGE
180 QUEEN'S GATE, LONDON SW7 2BZ

JANUARY 2018

I certify that this thesis, and the research to which it refers, are the product of my own work, and that any ideas or quotations from the work of other people, published or otherwise, are fully acknowledged in accordance with the standard referencing practices of the discipline.

Signed: 

COPYRIGHT

The copyright of this thesis rests with the author and is made available under a Creative Commons Attribution Non-Commercial No Derivatives licence. Researchers are free to copy, distribute or transmit the thesis on the condition that they attribute it, that they do not use it for commercial purposes and that they do not alter, transform or build upon it. For any reuse or redistribution, researchers must make clear to others the licence terms of this work.

Optimal Liquidation Strategies for Large-Tick Stocks

ABSTRACT

This thesis is devoted to study the optimal liquidation strategies in a limit order book for large-tick stocks. Two frameworks are proposed.

In the first framework, we formulate a stylised limit order book that admits one-tick spread and fixed market depth cap, in which order flows arrive according to point processes with stochastic intensities. We consider an agent who wants to liquidate a position in this limit order book through market orders and pegged displayed/non-displayed limit orders within a fixed time horizon, and whose goal is to maximise the expected utility from the terminal wealth. For this optimal liquidation problem, we derive the associated Hamilton-Jacobi-Bellman quasi-variational inequality and prove a verification theorem giving sufficient conditions for the HJBQVI solution to be the value function. The optimal strategy is a combined stochastic and impulse control, and is then solved numerically using finite different scheme.

In the second framework, we formulate a stylised level-I limit order book whose spread is constantly one tick and whose dynamics are driven by the queueing races at the best prices. Order book events occur according to independent Poisson processes, with parameters depending on the most recent price move direction. Our goal is to maximise the expected terminal wealth of an agent who needs to liquidate a position within a fixed time horizon. By assuming that the agent trades through both limit and market orders only when the price moves, we model her liquidation procedure as a semi-Markov decision process, and compute the semi-Markov kernel using Laplace method in the language of queueing theory. The optimal liquidation policy is then solved by dynamic programming, and illustrated numerically.

To my family.

ACKNOWLEDGMENTS

I wish to express my heartfelt appreciation to my supervisor Dr. Antoine Jacquier for his excellent guidance and valuable suggestions throughout my PhD study.

I am deeply grateful to my parents for their considerable support and great encouragement.

I am enormously grateful to Shell Treasury Centre Ltd for providing sponsorship to my PhD study and grant me the opportunity to gain industrial experience alongside my research.

I want to sincerely thank Department of Mathematics at Imperial College for providing many well-organised reading groups, graduate courses and research seminars.

I want to warmly thank my friends, office mates and fellow postgraduate students for their pleasant company and for the many laughs we shared.

LIST OF FIGURES

1.1	a schematic diagram of a LOB (figure source: [39]).	2
2.1	examples of buy market order arrival or sell limit order cancellation.	15
2.2	examples of sell limit order placement.	16
2.3	example of sell limit order placement in the LOB with the agent's participation.	23
2.4	histogram of the best ask queue sizes (in number of shares) right before the best ask price decreases and those right after the best ask price increases.	33
2.5	YHOO: histograms of order sizes of sell limit order submissions (left) and sell limit order cancellations (right) at the best ask price.	33
2.6	histogram of the sizes of buy market order arrivals.	34
2.7	YHOO: empirical (line of circles) and the fitted (solid line) complementary cumulative distribution function of buy market order size M_1 on a doubly logarithmic plot.	36
2.8	left panel: the scatter plot of the set $\left(100\mathfrak{d}, \hat{\lambda}^\varpi(100\mathfrak{d})\right)_{\mathfrak{d}=0,1,\dots,50}$ for $\varpi \in \{m, l, c\}$; right panel: the fitted line $y = \exp\left(\hat{\beta}_0^\varpi + \hat{\beta}_1^\varpi x + \hat{\beta}_2^\varpi x^2\right)$ for $\varpi \in \{m, l, c\}$	38
2.9	optimal strategy (q^*, h^*, e^*) , namely, the optimal size of displayed limit order, non-displayed limit order and market order, as a function $QS(\cdot, \cdot, \cdot)$ of the best ask queue size (x-axis: $j = 1, 2, \dots, 20$, corresponding to 2100, 2000, \dots , 200 shares), the remaining inventory position (y-axis: $k = 1, 2, \dots, 10$, corresponding to 100, 200, \dots , 1000 shares) and the time to maturity (panels on the left (resp. right): $i = 500$ (resp. 50), corresponding to 500 (resp. 50) seconds.)	49

3.1	YHOO: histogram of the queueing race duration after a backward Insertion (left panel) and a forward insertion (right panel).	78
3.2	YHOO: f_{+1} (left) and f_{-1} (right) with no latency (top) and with one-millisecond latency (bottom).	82
3.3	optimal policy as a function of best ask volume (x-axis: $v^a = 1, \dots, 25$), best bid volume (y-axis: $v^b = 1, \dots, 25$), latency (top: $\mathbf{lat} = 0\text{ms}$; bottom: $\mathbf{lat} = 1\text{ms}$) and price move direction (left: $j = -1$; right: $j = 1$) when fixing inventory $y = 2$ and time to maturity $\lambda = 10$.	86
3.4	optimal policy as a function of best ask volume (x-axis: $v^a = 1, \dots, 25$), best bid volume (y-axis: $v^b = 1, \dots, 25$), time to maturity (top: $\lambda = 3$; bottom: $\lambda = 10$) and price move direction (left: $j = -1$; right: $j = 1$) when fixing inventory $y = 1$ and latency $\mathbf{lat} = 1\text{ms}$.	87
A.1	YHOO: direction of order price modification for event pairs in the form of ‘same-size, same-side full cancellation and submission’.	92
A.2	MSFT (top-left), INTC (top-right) and YHOO (bottom): empirical distributions of the millisecond and microsecond remainders in 2016.	94
A.3	YHOO: example of probability anomalies in the daily empirical distributions of microsecond remainders.	98

LIST OF TABLES

2.1	probability mass functions f^l and f^c on \mathcal{N}	34
2.2	estimated coefficients for the linear regression in (2.40).	38
2.3	parameter settings.	48
3.1	evolution of the semi-Markov decision process under a horizon-related Markov deterministic policy $\pi \in \Pi$	62
3.2	percentage of time with a given spread	77
3.3	percentage of forward and backward insertions.	78
3.4	average order size (in shares).	79
3.5	Poisson parameter estimation with no latency.	80
3.6	Poisson parameter estimation with 1ms latency.	80
A.1	descriptive statistics on timestamps and recorded events in 2016.	90
A.2	Cramér-von Mises test for discrete uniform distribution	96

CONTENTS

1	INTRODUCTION	1
1.1	Background	1
1.2	Classifications of Algorithmic Trading	3
1.2.1	Agency algorithms	3
1.2.2	Proprietary algorithms	5
1.3	Large-tick stocks	7
1.4	LOBSTER dataset	7
1.4.1	Source and structure	8
1.4.2	Advantages and limitations	8
1.5	Organisation of this thesis	9
2	OPTIMAL LIQUIDATION STRATEGY - FRAMEWORK I	11
2.1	Introduction	11
2.2	Problem Formulation	13
2.2.1	Underlying LOB model	13
2.2.2	Liquidation strategy	20
2.2.3	State process	23
2.2.4	Trading objective	26
2.3	Optimal liquidation strategy	28
2.3.1	Value function	28
2.3.2	Dynamic programming equation	29
2.3.3	Verification theorem	30
2.4	Parameter estimations and computational results	31

2.4.1	Parameter estimations	32
2.4.2	Numerical scheme	39
2.4.3	Optimal Strategy	47
3	OPTIMAL LIQUIDATION STRATEGY - FRAMEWORK II	50
3.1	Introduction	50
3.2	LOB and Trading Strategy	52
3.2.1	‘Level-I’ LOB model	52
3.2.2	Objective and admissible trading strategies	55
3.3	Trading process modelled by semi-Markov decision processes .	56
3.3.1	Semi-Markov decision model	57
3.3.2	Dynamics of the finite-horizon semi-Markov decision process	61
3.3.3	Value function and optimal policy	64
3.4	Semi-Markov kernel	65
3.4.1	Closed-form expressions	66
3.4.2	Laplace method	71
3.5	Existence of Optimal Policy	73
3.6	Empirical studies and computational results	76
3.6.1	Descriptive statistics	77
3.6.2	Parameter estimation	78
3.6.3	Numerical scheme	81
3.6.4	Optimal strategy	83
	APPENDIX A EMPIRICAL STUDIES FOR LARGE-TICK STOCKS	88
A.1	Concurrency	89
A.2	Clock-time Periodicity	93
	APPENDIX B APPENDIX FOR CHAPTER 2	99

B.1 Proof of Theorem 2.14	99
APPENDIX C APPENDIX FOR CHAPTER 3	103
C.1 Proof of Proposition 3.23	103
C.2 Proof of Proposition 3.24	107
C.3 Proof of Proposition 3.30	108
C.4 Proof of Proposition 3.31	109
C.5 Maximum Likelihood Estimation for the Poisson Parameters .	110
REFERENCES	111

NOTATIONS

SETS AND SET OPERATIONS

\mathbb{R} : set of real numbers; $\mathbb{R}^+ := (0, \infty)$; $\mathbb{R}_0^+ := \mathbb{R}^+ \cup \{0\}$; $\mathbb{R}^- := \mathbb{R} \setminus \mathbb{R}_0^+$.

\mathbb{Z} : set of integer numbers.

\mathbb{N} : the set of non-negative integers. $\mathbb{N}^+ := \mathbb{N} \setminus \{0\}$;

\mathbb{C} : set of imaginary numbers.

For $m, n \in \mathbb{N}^+$, $\mathcal{M}_{m \times n}(\mathbb{R})$ denotes the set of \mathbb{R} -valued $m \times n$ matrices; $\mathcal{M}_m(\mathbb{R})$ denotes the set of \mathbb{R} -valued square matrices of order m , for $m \in \mathbb{N}^+$.

Let \mathcal{S} be a set, $\bar{\mathcal{S}}$ and $\partial\mathcal{S}$ denote the closure and boundary of set \mathcal{S} .

FUNCTIONS AND FUNCTIONS SPACES

$x \wedge y := \min(x, y)$; $x \vee y := \max(x, y)$.

For any set A , the indicator functions $\mathbb{1}_A(\cdot)$ is defined by

$$\mathbb{1}_A := \begin{cases} 1 & \text{if } x \in A, \\ 0 & \text{if } x \notin A. \end{cases}$$

$C^{1,2}([0, T] \times \mathcal{O})$ is the space of \mathbb{R} -valued functions f on $[0, T] \times \mathcal{O}$ whose partial derivatives $\frac{\partial f}{\partial t}$, $\frac{\partial f}{\partial x_i}$, $\frac{\partial^2 f}{\partial x_i \partial x_j}$, $1 \leq i, j \leq n$ exist and are continuous on $[0, T]$. \mathcal{O} is an open set on \mathbb{R}^n .

$C_b(\mathcal{U})$ is the space of bounded and continuous functions on \mathcal{U} .

ABBREVIATIONS

AT: algorithmic trading

LOB: limit order book

NBBO: national best bid offer

HJBQVI: Hamilton-Jacobi-Bellman quasi-variational inequality

SDE: stochastic differential equation

a.s.: almost surely

càdlàg: right continuous with left limits

s.t.: such that

resp. respectively

1

INTRODUCTION

1.1 BACKGROUND

Algorithmic trading (AT) refers to the use of mathematical models, computers, and telecommunications networks to automate the buying and selling of financial securities [58]. Over the previous two decades, the emergence and rise of AT has been vastly facilitated by the greater complexity of the modern financial markets as well as the significant breakthroughs in quantitative modelling and information technology. In particular, the predominance of automated order-driven trading systems, the proliferation of the trading venues, and the accelerating speed of information processing jointly promote the popularity of AT.

Nowadays, most equity and derivative exchanges all over the world are at least partially providing the order-driven trading mechanism: Australian Securities Exchange, Euronext, Helsinki, Hong Kong, Shenzhen, Swiss, Tokyo, Toronto, Vancouver Stock Exchanges are pure order-driven markets and New York, London Stock Exchanges, Nasdaq are hybrid markets [39]. Different from a quote-driven market, where large market makers centralise buy and sell orders and provide liquidity to other market participants through setting

bid and ask quotes, an order-driven market is much more flexible, which allows all market participants to send buy or sell orders specifying the price and amount they want to trade into a limit order book (LOB). According to the classical terminology [39, Section 2.2], orders leading to an immediate execution upon submission based on the LOB's trade-matching algorithm are called market orders, while orders that do not result in an immediate execution and therefore are stored in the LOB are called limit orders. The highest (resp. lowest) price among all the active buy (resp. sell) limit orders is called the best bid price (resp. best ask price). The average (resp. difference) of the best bid and ask price is called the mid price (resp. spread). Figure 1.1 gives a schematic diagram of a LOB illustrating the above terms. In addition to the displayed part of a LOB, virtually all exchanges now al-

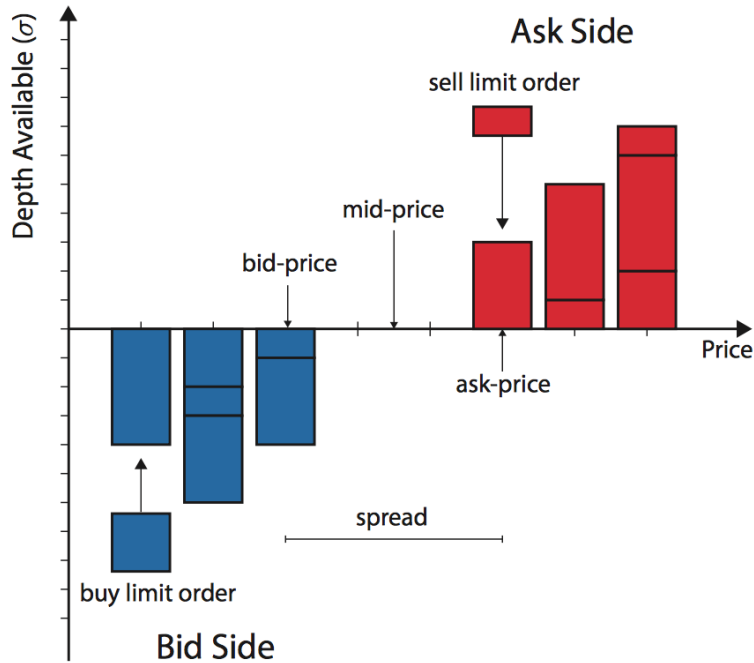


Figure 1.1: a schematic diagram of a LOB (figure source: [39]).

low market participants to submit partially or entirely non-displayed limit orders [10], also known as iceberg orders or hidden orders, resulting the LOB having a non-displayed part.

Broadly speaking, a LOB can be understood as a collection of active buy and sell limit orders stored at different price levels, and these outstanding limit orders can either get executed by subsequent counterpart market orders based on a certain priority rule or be cancelled. In particular, a priority rule regulates how active limit orders get executed. By far the most common priority rule is ‘price-visibility-time’, that is,

- price: limit orders placed at a more competitive price, namely, a price that is closer to the mid price, get higher execution priority;
- visibility: for limit orders placed at the same price, the displayed limit orders take higher execution priority over the non-displayed ones;
- time: limit orders placed at the same price and with the same display status follow the ‘first come first serve’ rule.

Throughout this thesis, we will work on LOBs that apply the ‘price-visibility-time’ priority rule.

1.2 CLASSIFICATIONS OF ALGORITHMIC TRADING

According to [44], algorithms serve for different purposes and are therefore classified into two categories: agency and proprietary.

1.2.1 AGENCY ALGORITHMS

Agency algorithms are normally used by the buy-side institutional investors (and the brokers who serve them) in order to implement long-term position changes, aiming at minimising the execution costs and market impact. Generally speaking, an agency algorithm decomposes the acquisition or liquidation process of a large parent order into three layers:

1. how to slice the parent order into child orders and schedule the child orders over the entire trading horizon;

2. what is the price, order type, visibility and timing to execute each child order within its scheduled trading horizon;
3. which venue(s) should each child order be routed to.

Literature on optimal liquidation/acquisition strategies is classified accordingly based on the above three layers. Almgren and Chriss [6], Almgren [5], Gatheral, Schied and Slynko [36] and Lorenz and Almgren [59] address the optimal execution problems by solely considering the first layer, in which case the direct interactions between the trader and the LOB are abstracted away. Some studies take the first two layers into account simultaneously and formulate the optimal strategies for executing a large position in a single LOB market. For example, Obizhaeva and Wang [67] and Alfonsi, Fruth and Schied [4] develop the optimal execution strategies entirely using market orders, assuming that the liquidity replenishes gradually over time after it is taken. Bayraktar and Ludkovski [8], Guéant, Lehalle and Fernandez-Tapia [41] design the optimal liquidation strategy that posts limit orders only, treating the liquidation process as a sequence of order fills and modelling it by a point process. Cartea and Jaimungal [19] seek to execute a large order employing both market and limit orders, and solve the optimal strategies under different scenarios. Some researchers focus on the second layer and study how to optimally execute a single child order for the purpose of incorporating information on the LOB market microstructure into their trading strategies, such as Stoikov and Waeber [76], Donnelly and Gan [32] and Gonzalez and Schervish [38] for market-order-oriented, limit-order-oriented and hybrid optimal strategy, respectively. Besides, Cebiroğlu and Horst [21] formulate and analyse the optimal submission strategy of an iceberg order, capturing the trade-off between the costs and benefits of order display. Finally, Cont and Kukanov [27] combine the last two layers together and propose a strategy that optimally distributes a child order across different order types and trading venues.

1.2.2 PROPRIETARY ALGORITHMS

In contrast to agency algorithms, proprietary algorithms are mainly adopted by high frequency traders aiming to make profits from the trading process itself. As stated in a white paper [73] by U.S. Securities & Exchange Commission, high frequency traders are typically defined as professional traders acting in a proprietary capacity that engage in strategies that generate a large number of trades on daily basis. Key characteristics associated with high frequency trading (HFT) include:

1. use of extraordinarily high-speed and sophisticated computer programs for generating, routing, and executing orders;
2. use of co-location services and individual data feeds offered by exchanges and others to minimise network and other types of latencies;
3. very short time-frames for establishing and liquidating positions;
4. the submission of numerous orders that are cancelled shortly after submission;
5. ending the trading day in as close to a flat position as possible (that is, not carrying significant, unhedged positions overnight).

In fact, HFT is regarded as one of the most dominant components of the market structure in recent years. Taking the U.S. equity market for example, HFT activities accounted for only less than 10% of all trades at the beginning of this century, but had grown significantly and represented approximately half of the trading volume by late 2012 [37]. Unsurprisingly, the prevalence of HFT has led to considerable debates about its impact on market quality, in particular after the ‘flash crash’ on May 6, 2010 [56]. There are widely different views among regulators, in the financial media, and in the rapidly growing academic literature on whether HFT is beneficial, neutral, or detrimental. See [55, 62] for HFT surveys.

There is no doubt that HFT studies highly depend on the availability and quality of the relevant market data, which is one of the toughest challenges

facing any HFT researcher. In fact, as trading anonymity is preserved in almost all modern equity markets, exchanges and regulators are the only sources of data identifying whether orders and trades originate from an HFT account, while public available data on order book activities normally do not reveal the identities of market participants. Accordingly, HFT literature is divided into the following two categories:

1. ones that analyse non-public datasets in which market activities have been attributed to HFT/non-HFT accounts;
2. ones that use various measures calculable from publicly available market data to proxy for HFT.

The U.S. Securities and Exchange Commission [74] provides an exhaustive survey on the HFT literature of the first category. Particularly, the ‘Nasdaq HFT dataset’ is the only data source available to academic researchers that directly classify HFT activities in U.S. equities: firms are categorised as HFT according to the Nasdaq’s knowledge of their customers together with the analysis of their trading styles such as inventory position, order duration, and order-to-trade ratio. See [14, 17, 48] for empirical literature employing the Nasdaq HFT dataset.

HFT literature of the second category vary depending on the selections of different HFT proxies. For instance, Hasbrouck and Saar [44] propose a measure ‘strategic run’ of low-latency activities based on Nasdaq ITCH data feed in order to approximate HFT activity. Brogaard, Hendershott and Riordan [15] use Canadian regulatory data with masked participant IDs that track market activities and remain constant across days, securities and markets, and introduce a HFT identification criteria according to trading volume and intraday inventory position. Cartea, Payne, Penalva and Tapia [20] build a measure from Nasdaq ITCH data feed that captures the ultra-fast activities in the market and study its relation with market quality.

1.3 LARGE-TICK STOCKS

When trading shares in a LOB, traders need to specify the order prices according to the platform’s tick size, that is, the smallest allowable price interval between different orders. Taking the Nasdaq platform for example, each stock is traded in a separate LOB with tick size \$0.01, which means all orders must arrive at a price that is integer multiples of \$0.01. Because of the huge difference in share prices between different stocks (from around \$1 to above \$1000), the relative tick size, which is defined by the ratio between the stock price and the tick size, of different stocks also vary considerably. As defined in [12, 30], large-tick stocks are stocks with large relative tick size, in the sense that the spread is almost always equal to the tick size and traders are averse to the order price variations of a single tick.

In this thesis, we restrict our attention to optimal liquidation problems for large-tick stocks. This is mainly because the spread of large-tick stocks is almost always equal to the tick size, so that in most cases traders cannot undercut each other by submitting limit orders inside the spread and therefore have to wait in the queue to get executed. This feature may largely simplify the LOB modelling. More importantly, market conditions and trading strategies for large-tick stocks are deemed to be different from those for small-tick stocks [68]. Therefore, the trading strategies for these two categories of stocks should be studied separately. In Appendix A, we implement some empirical studies on three representative and highly liquid large-tick stocks: Microsoft (MSFT), Intel (INTC) and Yahoo (YHOO), based on the LOBSTER datasets as introduced in the following.

1.4 LOBSTER DATASET

The LOB datasets used in this thesis are provided by LOBSTER, which is short for ‘Limit Order Book System - The Efficient Reconstructor’, and works as an online system that gives researchers access to convenient and high-quality LOB data.

1.4.1 SOURCE AND STRUCTURE

The LOBSTER dataset is derived from the historical Nasdaq TotalView-ITCH data feed, which is the real-time stream of order book events sent to the market participants in the Nasdaq platform. For each Nasdaq traded stock, LOBSTER is working as a translation module that extracts order flow information from the data feed and reconstructs the LOB dynamics from 09:30 to 16:00 EST on each active trading day. In particular, the LOBSTER dataset is limit order oriented, as it is entirely composed of limit order events, i.e. limit order submissions, cancellations and executions, which are recorded in chronological order. In the LOBSTER dataset, information associated with each event includes: timestamp, event type, order ID, size, price and buy/sell indicator, as well as the post-event limit order book state¹ up to the requested number of price levels. See [51] for more introductions to the LOBSTER dataset.

1.4.2 ADVANTAGES AND LIMITATIONS

The LOBSTER dataset has several advantages over other limit order book datasets. For example, the LOBSTER dataset reproduces the order flows and LOB state evolutions directly from the Nasdaq servers. It therefore retains greater information accuracy than the datasets that are recorded by the third-party providers, and possesses higher storage efficiency compared with the datasets that capture snapshots of order book states [45, Chapter 3]. Besides, all events in the LOBSTER dataset are recorded at seconds after midnight with decimal precision of nanoseconds, while most other limit order book datasets are still up to millisecond-timestamped. This improvement in timestamp granularity enables us to observe the extremely subtle dynamics in the order books and analyse the traders' ultra-fast and even intra-millisecond behaviours. Moreover, as a particular feature for the LOBSTER dataset, every visible limit order is assigned with an intraday-unique order ID upon

¹A limit order book state is expressed through the occupied price levels and the associated market depth. A post-event (resp. pre-event) order book state represents the order book state immediately after (resp. before) that event.

submission, in the sense that any subsequent cancellation or execution associated with that limit order is labeled with the same order ID. Apparently, this feature allows us to track the entire life of each (visible) limit order without resorting to any further matching algorithm, which greatly facilitate the analysis of trading behaviours and algorithmic strategies.

However, due to the complexity in modern equity markets and the regulatory requirements to ensure traders' anonymity, the LOBSTER dataset is not able to provide the complete market information, which will inevitably impose some limitations and difficulties on LOB studies. For example, since the LOBSTER dataset originates from the standard Nasdaq data feed, it provides order book activities merely on the Nasdaq platform. Considering the strongly fragmented market structure in recent years [70] and its close relationship with the growth of high frequency trading [63], analyses and studies based solely on the LOBSTER database can not reveal the impact brought by the strategies that span multiple trading venues. Besides, information associated with hidden order execution is censored in order to prevent information leakage. In particular, since July 14, 2014, the information of buy/sell indicator is not included in the messages of hidden order execution, which brings enormous difficulties to the study of hidden order.

1.5 ORGANISATION OF THIS THESIS

From the perspective of agency algorithms combining the first and the second layer, we propose two frameworks in this thesis to study the optimal liquidation strategy of a large-tick stock in the LOB.

In Chapter 2, we consider an agent who trades through sell market orders and displayed/non-displayed sell limit orders pegged at the best ask price, and aims to maximise her utility from the terminal wealth. We transfer the agent's optimal liquidation problem to a Hamilton-Jacobi-Bellman quasi-variational inequality and prove the verification theorem that gives sufficient conditions for the HJBQVI solution being the value function. The optimal strategy is in the form of a stochastic and impulse control, and is solved numerically using finite difference scheme.

In Chapter 3, we consider an agent who aims at maximising her terminal wealth, and trades through sell market and limit orders but only takes actions when there is a price change. We formulate the agent's liquidation process as a semi-Markov decision process, with the semi-Markov kernel calculated using the Laplace method. The optimal strategy is solved using dynamic programming, and illustrated numerically.

*“Markets are constantly in a state of uncertainty
and flux and money is made by discounting the
obvious and betting on the unexpected.”*

— George Soros

2

OPTIMAL LIQUIDATION STRATEGY - FRAMEWORK I

2.1 INTRODUCTION

In this chapter, we consider an agent (or her agency algorithm) who wants to liquidate a fixed amount of a large-tick stock over a finite trading window in a LOB that applies the price-visibility-time priority rule. Along the trading window, the agent needs to slice the parent order into multiple child orders, and select the timing, order type, order size and visibility status for each child order. In terms of order type selection, the agent can submit sell market orders for immediate execution at the best bid price, which is a less favourable price; she can otherwise place sell limit orders that are continuously pegged at the best ask price, but is inevitably subject to the execution risk, as her sell limit orders are executed only when they match counterpart buy market orders. Furthermore, the agent is able to keep any proportion of her sell limit orders invisible to the general market participants¹ in order to avoid

¹In Chapter 2 and Chapter 3, the general market participants refer to all the market participants in the LOB except the agent.

the exposure risk, but at the expense of facing even higher execution risk, as the displayed limit orders always take higher execution priority over the non-displayed ones at the same price level. We also introduce a termination time of the agent's liquidation activities, which arrives as soon as any of the following events occur: (i) the trading window expires; (ii) the ask-side LOB state exits a pre-specified domain; (iii) the agent's remaining inventory position reaches zero. At the termination time, the agent is required to liquidate all the unexecuted inventory position (if any) through a sell market order. The agent's objective is to find an optimal liquidation strategy that maximises her expected utility from the wealth at the termination time.

In order to solve the above problem, we develop a combined stochastic and impulse control model that addresses the trade-offs among order prices, execution probabilities and exposure risks throughout the agent's liquidation process. Specifically, we first construct a stylised underlying LOB model as the agent's trading environment, specifying the dynamics of the ask-side market depth and order flows originated from the general market participants. This framework follows [25, 26], in particular assuming that the spread is constant, equal to the tick size and that the general market participants admit a constant market depth cap at each price level. Under these assumptions, the evolution of the ask-side LOB state in the absence of the agent's participation is modelled by a jump diffusion process, whereby the jumps occur according to three mutually independent point processes with stochastic intensities, representing the arrivals of buy market orders, sell limit orders and cancellations, respectively, originated from the general market participants; the jump sizes associated with the point processes are modelled by independent and identically distributed random variables, representing the sizes of the corresponding order book events; the diffusion part is represented by an arithmetic Brownian motion, indicating the noisy relation between the evolution of the stylised and the actual LOB state. Next, we model the agent's limit order and market order strategy through a combined stochastic and impulse control. The stochastic control continuously specifies the size of a displayed and a non-displayed sell limit order pegged at the best ask price. For modelling convenience, we assume that the agent's displayed limit

orders always hold a fixed relative position in the best ask queue, so that the execution of the agent's limit orders can be explicitly captured based on the price-visibility-time priority rule. We also model the intensities of the general market participants' order flows as deterministic functions of the displayed market depth at the best ask price, reflecting the empirical observations that traders in the market react to the changing of the LOB state. The impulse control, on the other hand, consists of a sequence of decision times and order sizes for sell market order submissions. In this context, we optimise the expected utility from the wealth at the termination time by optimally choosing among sell market orders, displayed and non-displayed sell limit orders.

This chapter is organised as follows. In Section 2.2, we specify the underlying LOB model as well as the agent's set of admissible liquidation strategies and trading objective. In Section 2.3, we formulate the agent's optimal liquidation problem and translate it into solving the associated Hamilton-Jacobi-Bellman quasi-variational inequality (HJBQVI) based on the verification theorem. In Section 2.4, we devote to the model's parameter estimation and the numerical scheme solving the HJBQVI.

2.2 PROBLEM FORMULATION

Throughout this chapter, we fix a probability space $(\Omega, \mathcal{F}, \mathbb{P})$ equipped with a filtration $(\mathcal{F}_t)_{t \geq 0}$ satisfying the usual conditions, and assume that all random variables and stochastic processes are defined on this stochastic basis.

2.2.1 UNDERLYING LOB MODEL

Consider a LOB that admits a constant tick size $\delta > 0$ (that is, all orders must arrive at a price $k\delta$, for some $k \in \mathbb{N}^+$) and \mathbb{R}^+ -valued order sizes. In order to formulate the agent's trading environment, we build up a stylised underlying LOB model specifying the market depth and the order flows originated from the general market participants. In particular, considering that we are dealing with a liquidation problem for a large-tick stock, we focus on modelling the LOB on the ask side.

MARKET DEPTH

Similar to [25, 26], we consider the following framework for the underlying market depth originated from the general market participants at each price level on the ask side of the LOB:

Assumption 2.1 (Market depth).

- (a) the spread of the LOB is equal to the tick size δ ;
- (b) the general market participants admit a constant market depth cap $\bar{d} > 0$, that is, the underlying market depth (in number of shares) takes values in $(0, \bar{d}]$ at the best ask price, and is equal to \bar{d} at each price level above the best ask price;
- (c) buy market order arrivals and sell limit order cancellations from the general market participants occur only at the best ask price: once the underlying market depth declines to zero, both the best bid and ask price will immediately increase by one tick (see Figure 2.1);
- (d) sell limit order submissions from the general market participants occur only at the best ask price: whenever the underlying market depth at the best ask price reaches the cap \bar{d} , any subsequent sell limit order will arrive at the price one tick below, initiating the new best bid and ask price (see Figure 2.2);
- (e) the general market participants never place non-displayed limit orders.

Remark 2.2.

- Due to the fact that order submissions and cancellations are allowed at any price level and the market depth at each price level has a non-trivial distribution, the introduction of the market depth cap \bar{d} is actually a quite strong assumption. However, this restrictive assumption is essential to explicitly and conveniently express the instantaneous effects of all order book events. On top of that, the size of the market depth cap is believed to be positively correlated with the relative tick size,

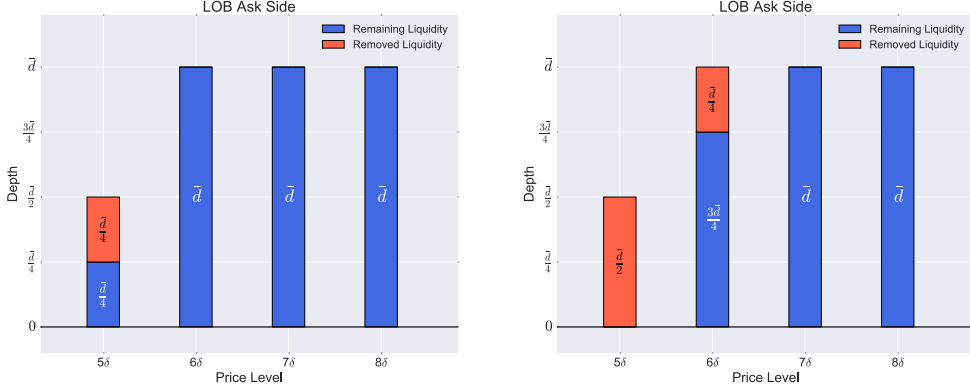


Figure 2.1: examples of buy market order arrival or sell limit order cancellation.

The orange (resp. blue) blocks represent the removed (resp. remaining) underlying liquidity upon the occurrence of a buy market order arrival or a sell limit order cancellation. Immediately before that order book event, the best ask price is equal to 5δ , while the underlying market depth is equal to $\bar{d}/2$ at the best ask price and \bar{d} at each price level above the best ask price. The panel on the left (resp. right) describes the situation where an order of size $\bar{d}/4$ (resp. $3\bar{d}/4$) is removed from the underlying LOB. In the latter situation, the underlying liquidity at the initial best ask price 5δ is depleted, and a new best ask price 6δ is therefore initiated, at which the liquidity consumption or evacuation (of size $\bar{d}/4$) continues.

reflecting traders' trade-off between the execution risk and the order price. Due to the fact that traders consider the tick size for large-tick stocks as non-negligible [30], the market depth cap for large-tick stocks is believed to be larger than that for small-tick stocks: only when the best ask queue becomes long enough, some sell-initiated traders would rather undercut the best ask price by one tick than join in the best ask queue with a unfavourable position.

- Assumption 2.1(d) presumes that the best bid queue becomes sufficiently short when the underlying market depth at the best ask price approaches the cap \bar{d} , so that any subsequent sell limit order submission is able to initiate the new best ask price. In this case, we believe that the buy-initiated traders in the market perceive strong selling pressure when observing a long queue waiting at the best ask price, and thus withdraw their buy limit orders at the best bid price in order to avoid the risk of adverse selection.

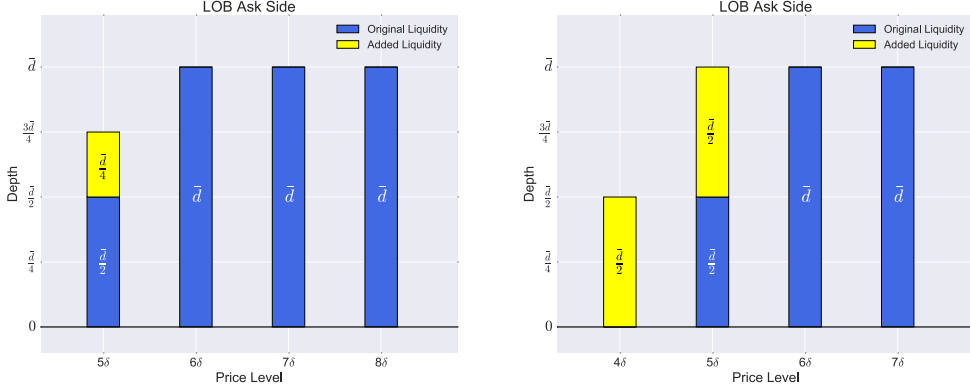


Figure 2.2: examples of sell limit order placement.

The yellow (resp. blue) blocks represent the newly added (resp. previously existing) underlying liquidity upon the placement of a sell limit order. Immediately before that order book event, the best ask price is equal to 5δ , while the underlying market depth is $\bar{d}/2$ at the best ask price and \bar{d} at each price level above the best ask price. The panel on the left (resp. right) describes the situation where an order of size $\bar{d}/4$ (resp. \bar{d}) is placed to the underlying LOB. In the latter situation, the underlying market depth at the previous best ask price 5δ reaches the market depth cap \bar{d} , and the remaining part of that order (of size $\bar{d}/2$) therefore arrives at the new best ask price 4δ .

Based on Assumption 2.1, we model the dynamics of the ask-side LOB state in the absence of the agent's participation as a càdlàg adapted process $(A_t, D_t)_{t \geq 0}$, valued in $\mathbb{N}^+ \setminus \{1\} \times (0, \bar{d}]$, where A_t and D_t represent the best ask price normalised by the tick size² and the underlying market depth at the best ask price, respectively, at time t . We further introduce a càdlàg adapted process $(P_t)_{t \geq 0}$, valued in $[2, +\infty)$, by

$$P_t = A_t + 1 - D_t/\bar{d} \quad \text{for all } t \geq 0, \quad \text{almost surely.} \quad (2.1)$$

The processes P and (A, D) virtually carry the same information describing the evolution of the ask-side LOB state since we have

$$A_t = \lfloor P_t \rfloor \quad \text{and} \quad D_t = d(P_t) \quad \text{for all } t \geq 0, \quad \text{almost surely,} \quad (2.2)$$

²Since the best prices are strictly positive and the LOB admits a fixed tick size, the lowest available best ask price is equal to 2δ and the process A takes values in $\mathbb{N} \setminus \{1\}$.

where the function $d : [2, +\infty) \rightarrow (0, \bar{d}]$ is defined by

$$d(p) := (\lfloor p \rfloor + 1 - p) \bar{d}.$$

Suppose that an order book event changes the aggregate underlying market depth on the ask side of the LOB by $v \in \mathbb{R} \setminus \{0\}$ at time $s > 0$, the process P then evolves as:

$$P_s = P_{s-} + v/\bar{d}. \quad (2.3)$$

Indeed, for $v \in \mathbb{R} \setminus \{0\}$, let $\varkappa := \max\{j \in \mathbb{Z} : D_{s-} + j\bar{d} \leq v\}$, we immediately have

$$(A_s, D_s) = (A_{s-} + \varkappa + 1, (\varkappa + 1)\bar{d} + D_{s-} - v), \quad (2.4)$$

according to the structure of the stylised LOB in Assumption 2.1. Combining (2.4) with (2.1) yields (2.3).

ORDER FLOW

The order flows (that is, the order types, arrival times and sizes of the order book events) originated from the general market participants are modelled according to the ‘zero-intelligence’ approach [26, 28, 75], based on which traders submit orders following rules governed by some specified stochastic processes without strategic or rational considerations. We shall here consider the following setting for the order flows.

Assumption 2.3 (Order flows).

- (a) Buy market order arrivals, sell limit order submissions and cancellations originated from the general market participants occur according to three point processes, denoted by $(N_t^m)_{t \geq 0}$, $(N_t^l)_{t \geq 0}$ and $(N_t^c)_{t \geq 0}$, that admit non-negative predictable intensities λ_t^m , λ_t^l and λ_t^c , respectively³. For $\varpi \in \{m, l, c\}$, we further assume that the intensity λ_t^ϖ is in the form of

$$\lambda_t^\varpi = \lambda^\varpi(D_{t-}), \quad (2.5)$$

³For definition of point process with stochastic intensity, see [13, Chapter II. Definition D7].

where $\lambda^\varpi : \mathbb{R}^+ \rightarrow \mathbb{R}^+$ is a continuous bounded deterministic function.

- (b) For $n \in \mathbb{N}^+$, let M_n, L_n and C_n denote the sizes of the n -th buy market order, sell limit order and sell limit order cancellation, respectively, originated from the general market participants. We further assume that $\{I_n, n \in \mathbb{N}^+\}$ is a sequence of independent and identically distributed \mathcal{F}_0 -measurable random variables, with cumulative distribution function F^ϖ , for $(\varpi, I) \in \{(m, M), (l, L), (c, C)\}$.
- (c) $(N_t^m)_t, (N_t^l)_t, (N_t^c)_t, \{M_n\}, \{L_n\}, \{C_n\}$ are mutually independent.

Remark 2.4.

- Assumption 2.3(a) is made based on the solid empirical evidence that order flows depend on the LOB shape, which can be interpreted as traders digesting and reacting to the changing market conditions [39, Section 3.2]. Particularly, we introduce (2.5) according to [49, 79], in which the intensities of the point processes governing the order flows are modelled as deterministic functions of the (visible) best queue size.
- The time-rescaling theorem [16] indicates that any point process with an integrable conditional intensity function can be simulated from a Poisson process with unit rate by rescaling time with respect to the conditional intensity function. In our model, the jump times $\{u_1^\varpi, u_2^\varpi, \dots\}$ of the processes N^ϖ , for $\varpi \in \{m, l, c\}$, can be generated by the following steps:
 - (a) Draw $\{\tau_i^\varpi, i \in \mathbb{N}^+\}$, for $\varpi \in \{m, l, c\}$, three sequences of mutually independent exponential random variables with mean one;
 - (b) For $\varpi \in \{m, l, c\}$,
 - (i) set $u_0^\varpi = 0$ and $k_\varpi = 1$;
 - (ii) set $u_{k_\varpi}^\varpi = \inf \left\{ t : \int_{u_{k_\varpi-1}^\varpi}^t \lambda_z^\varpi dz \geq \tau_{k_\varpi}^\varpi \right\}$;
 - (iii) $k^\varpi = k^\varpi + 1$ and go to step (ii).

Here, $u_{i_1}^{\varpi_1}$ and $u_{i_2}^{\varpi_2}$ are independent for any $i_1, i_2 \in \mathbb{N}^+$ and $\varpi_1, \varpi_2 \in \{m, l, c\}$ with $\varpi_1 \neq \varpi_2$, since for $t_1 > 0$ and $t_2 > 0$ we have

$$\begin{aligned} \Pr(u_{i_1}^{\varpi_1} \leq t_1, u_{i_2}^{\varpi_2} \leq t_2) &= \Pr\left(\int_0^{t_1} \lambda_z^{\varpi_1} dz \geq \sum_{j=1}^{i_1} \tau_j^{\varpi_1}, \int_0^{t_2} \lambda_z^{\varpi_2} dz \geq \sum_{j=1}^{i_2} \tau_j^{\varpi_2}\right) \\ &= \Pr\left(\int_0^{t_1} \lambda_z^{\varpi_1} dz \geq \sum_{j=1}^{i_1} \tau_j^{\varpi_1}\right) \Pr\left(\int_0^{t_2} \lambda_z^{\varpi_2} dz \geq \sum_{j=1}^{i_2} \tau_j^{\varpi_2}\right) \\ &= \Pr(u_{i_1}^{\varpi_1} \leq t_1) \Pr(u_{i_2}^{\varpi_2} \leq t_2). \end{aligned}$$

Based on (2.3) and Assumption 2.3, suppose that the process $(P_t)_{t \geq 0}$ in (2.1) follows the dynamics:

$$dP_t = \sigma dW_t + \frac{1}{\bar{d}} \left[M_{N_t^m} dN_t^m + C_{N_t^c} dN_t^c - L_{N_t^l} dN_t^l \right], \quad t \geq 0, \quad (2.6)$$

where $\sigma \geq 0$ is a constant and $(W_t)_t$ is a Brownian motion such that $(N_t^m)_t$, $(N_t^l)_t$, $(N_t^c)_t$, $\{M_n\}$, $\{L_n\}$, $\{C_n\}$ and $(W_t)_t$ are mutually independent.

Remark 2.5.

- Similar to [25, Section 1.2], we introduce a diffusion term σdW_t in order to capture the noisy relation between the changes of the ask-side LOB shape and the net order flows at the best ask price for short time intervals. We do so because the order book in reality has extremely complex dynamics: order submissions and cancellations are allowed at any price level, the market depth at each price level has a non-trivial distribution and the market depth cap does not exist.
- The SDE (2.6) does not honour the constraint that P being in $[2, \infty]$. However, we assume that the stock price is far above zero at inception and the trading window is short, so that the process P will not drop below 2 before maturity. Besides, later in this chapter, we introduce a stop loss price $\underline{p} \geq 2$ to the agent's liquidation problem, in the sense that the agent stops trading as soon as the process P touches \underline{p} .

2.2.2 LIQUIDATION STRATEGY

We consider an agent who is allowed to trade via both sell market and limit orders in the underlying LOB model introduced in Section 2.2.1, and thus faces a trade-off between the order price and the execution risk: submitting a market order leads to immediate execution but the price is less favourable, while placing a limit order may result in a better price but the execution cannot be guaranteed. Similar to [42], we model the agent's limit order and market order strategies as continuous-time stochastic and impulse controls, respectively.

LIMIT ORDER STRATEGY

Due to the flexibility of the order-driven trading mechanism, there are enormous amounts of feasible limit order trading methods: the agent can place displayed or non-displayed limit orders of any size at any price and time, and is also free to fully or partially cancel them at any subsequent time, which may result in her limit orders with different sizes, prices, queue positions and visibility status being simultaneously active in the LOB. In this context, it becomes quite difficult to find an optimal strategy. Therefore, we make the following assumptions in order to keep our modelling manageable and tractable.

Assumption 2.6 (Limit order strategies).

- (a) the agent's sell limit orders are always pegged at the best ask price;
- (b) the agent can shield any proportion of her limit orders from public view.

Remark 2.7.

- The reason we introduce Assumption 2.6(a) is twofold: (i) empirical studies on large-tick stocks indicate that a single market order is barely able to consume liquidity beyond the best price [18, 46], which means that limit orders placed deeper than the best price are even more unlikely to get executed; (ii) since the LOB is assumed to admit a constant one-tick spread, the agent is unable to undercut the best ask price

through placing limit orders inside the spread. (2) the LOB is assumed to admit a constant one-tick spread, so the agent cannot undercut the best ask price through posting limit orders inside the spread.

- Assumption 2.6(b) indicates that the agent continuously specifies the size of a displayed and a non-displayed sell limit order pegged at the best ask price and therefore faces a trade-off between the exposure risk and the execution risk: the agent's displayed order always takes higher priority of execution over the non-displayed one according to the price-visibility-time priority rule, but suffers higher exposure risk since the general market participants may adjust their order flows based on their observations on the LOB shape (in particular, size of the visible best queue), in which case the agent may incur higher adverse informational impact.

From Assumption 2.6, together with the fact that limit order submissions and cancellations are at no cost, the agent's limit order strategy is modelled by a continuous-time stochastic control, which is in the form of a predictable process

$$\alpha_t^{\text{lim}} := (Q_t, H_t), \quad t \geq 0, \quad (2.7)$$

valued in $\mathcal{E}_1 := [0, \bar{e}_1]^2$. Here Q_t (resp. H_t) represents the size of a displayed (resp. non-displayed) sell limit order pegged at the best ask price at time t , and the constant $\bar{e}_1 > 0$ represents the maximum size of an active displayed/non-displayed limit order that the agent is allowed to keep in the LOB. Furthermore, we introduce a fixed relative queue position for the agent's displayed sell limit order in the best ask queue.

Assumption 2.8 (Relative queue position). Assume that the agent's displayed sell limit order admits a constant relative queue position $\theta \in [0, 1]$ in the best ask queue, that is, a fraction θ (resp. $(1 - \theta)$) of the underlying market depth at the best ask price has a higher (resp. lower) execution priority than the agent's displayed sell limit order.

Remark 2.9.

- The introduction of the constant relative queue position for the agent's displayed limit order is to some extent for modelling convenience, since it is notoriously intricate to track the complete dynamics of a certain limit order's actual queue position. More importantly, the relative queue position in this model can be intuitively understood as the agent's competence to obtain superior queue positions against the general market participants⁴, in particular when the agent's pegged limit orders automatically adjust their order prices upon the changes of the best ask price. Figure 2.3 gives an example in which a sell limit order submission originated from the general market participants initiates a new best ask price and the agent manages to maintain the relative queue position after the order pegging.
- The agent's displayed limit orders are assumed to be small in the sense that the restriction imposed by the market depth cap \bar{d} in Assumption 2.1(b) does not apply to the agent (see the left panel of Figure 2.3 as an example, where the sum of the underlying market depth and the size of the agent's displayed limit order exceeds the cap \bar{d}).

MARKET ORDER STRATEGIES

On top of the limit order strategy described above, the agent is also allowed to submit sell market orders for immediate execution at marginally lower price levels. We model the agent's market order strategy via an impulse control, which is in the form of a double sequence

$$\alpha^{\text{mar}} := \{(\tau_j, \xi_j) : j \in \mathbb{N}^+\}. \quad (2.8)$$

Here, $\{\tau_j : j \in \mathbb{N}^+\}$ is an increasing sequence of stopping times, representing the agent's decision times to submit sell market orders, and ξ_j , for $j \in \mathbb{N}^+$, is an \mathcal{F}_{τ_j} -measurable random variable taking values in $\mathcal{E}_2 := [0, \bar{e}_2]$, representing

⁴As stated by Moallemi and Yuan [65], a good queue position is quite valuable as it usually means less waiting time as well as lower adverse selection risk. Market participants are therefore making every effort to obtain good queue positions in the LOB.

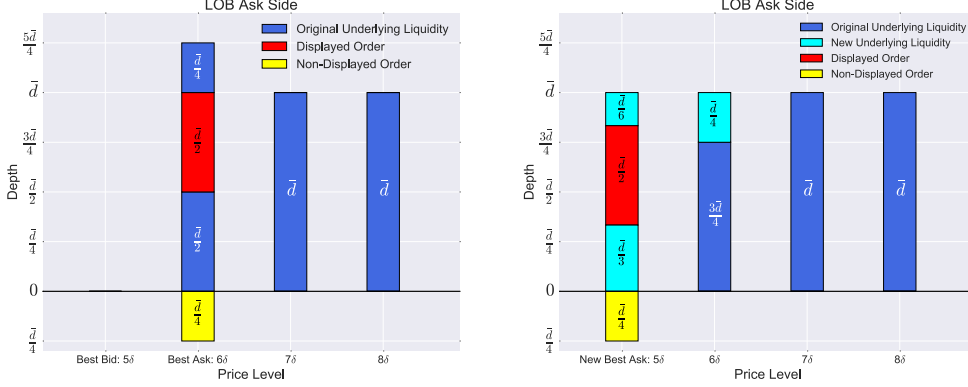


Figure 2.3: example of sell limit order placement in the LOB with the agent's participation.

The blue (resp. cyan) blocks represent the previously existing (resp. newly added) underlying liquidity, and the red (resp. yellow) blocks represent the agent's displayed (resp. non-displayed) sell limit orders. The execution priority of these blocks decreases from top to bottom at each price level. Suppose that the agent adopts a static limit order strategy $(Q_t, H_t) = (\bar{d}/2, \bar{d}/4)$, and her displayed sell limit order admits a relative queue position $\theta = 1/3$. The panel on the left (resp. right) illustrates the ask-side LOB state immediately before (resp. after) a sell limit order submission of size $3\bar{d}/4$ from the general market participants. After this, both the agent's displayed and non-displayed sell limit orders join in the new best ask queue immediately, with the relative queue position θ and the lowest execution priority being maintained, respectively.

the size of a sell market order that the agent decides to submit at τ_j . The constant $\bar{e}_2 > 0$ represents the maximum size of a sell market order that the agent is allowed to submit. The agent's overall liquidation strategy is modelled by a combined control, denoted by

$$\alpha := (\alpha^{\text{lim}}, \alpha^{\text{mar}}), \quad (2.9)$$

with α^{lim} in (2.7) and α^{mar} in (2.8), and we let $\tilde{\mathcal{A}}$ denote the set of all combined controls.

2.2.3 STATE PROCESS

Suppose that the agent wants to liquidate a fixed amount of a large-tick stock in the underlying LOB model introduced in Section 2.2.1 and applies the liquidation strategy illustrated in Section 2.2.2. We introduce the state

process, denoted by

$$Z_t^{(\alpha)} := \left(P_t^{(\alpha)}, Y_t^{(\alpha)}, X_t^{(\alpha)} \right), \quad t \geq 0, \quad (2.10)$$

to describe the dynamic system of the agent's liquidation problem, where $\alpha \in \tilde{\mathcal{A}}$ is the combined control defined in (2.9) and $P^{(\alpha)}, Y^{(\alpha)}, X^{(\alpha)}$ are adapted càdlàg processes tracing the evolution of the ask-side LOB state with the agent's participation⁵, the agent's inventory position and cash amount, respectively. We now illustrate the evolution of the state process in the following assumption.

Assumption 2.10 (State Process). For a given $\alpha \in \tilde{\mathcal{A}}$, the dynamics of the state process $Z^{(\alpha)}$ is given by

$$dP_t^{(\alpha)} = \sigma dW_t + \frac{1}{d} \left[\eta \left(Q_t, H_t, d(P^{(\alpha)})_{t-}, M_{N_t^m} \right) dN_t^m + C_{N_t^c} dN_t^c - L_{N_t^l} dN_t^l \right], \quad (2.11)$$

for $t \geq 0$;

$$dY_t^{(\alpha)} = -\kappa \left(Q_t, H_t, d(P^{(\alpha)})_{t-}, M_{N_t^m} \right) dN_t^m, \quad (2.12)$$

$$dX_t^{(\alpha)} = r \left(\lfloor P^{(\alpha)} \rfloor_{t-} \right) \kappa \left(Q_t, H_t, d(P^{(\alpha)})_{t-}, M_{N_t^m} \right) dN_t^m, \quad (2.13)$$

for $\tau_j < t < \tau_{j+1}$, $j \in \mathbb{N}^+$;

$$Y_{\tau_j}^{(\alpha)} = \check{Y}_{\tau_j-}^{(\alpha)} - \xi_j, \quad (2.14)$$

$$X_{\tau_j}^{(\alpha)} = \check{X}_{\tau_j-}^{(\alpha)} + g \left(\check{P}_{\tau_j-}^{(\alpha)} \right) \xi_j, \quad (2.15)$$

for $j \in \mathbb{N}^+$; where

- $(N_t^\varpi)_{t \geq 0}$ and $\{H_n\}_{n \in \mathbb{N}^+}$, for $\varpi \in \{m, l, c\}$ and $H \in \{M, L, C\}$, are defined as in Assumption 2.3, except that the intensity λ_t^ϖ of $(N_t^\varpi)_{t \geq 0}$ has the form

$$\lambda_t^\varpi = \lambda^\varpi \left(D_{t-}^{(\alpha)} + Q_t \right); \quad (2.16)$$

⁵Similar to (2.1), the process $P^{(\alpha)}$ has an equivalent expression $(A^{(\alpha)}, D^{(\alpha)}) := (\lfloor P^{(\alpha)} \rfloor, d(P^{(\alpha)}))$, and inherits the property (2.3).

- the functions η and κ are defined on $\mathcal{E}_1 \times (0, \bar{d}] \times \mathbb{R}^+$ by:

$$\eta(q, h, d, m) := \begin{cases} m, & \text{if } 0 < m \leq \theta d, \\ \theta d, & \text{if } \theta d < m \leq \theta d + q, \\ m - q, & \text{if } \theta d + q < m \leq d + q, \\ d, & \text{if } d + q < m \leq d + q + h, \\ m - q - h, & \text{if } m > d + q + h; \end{cases} \quad (2.17)$$

$$\kappa(q, h, d, m) := \begin{cases} 0, & \text{if } 0 < m \leq \theta d, \\ m - \theta d, & \text{if } \theta d < m \leq \theta d + q, \\ q, & \text{if } \theta d + q < m \leq d + q, \\ m - d, & \text{if } d + q < m \leq d + q + h, \\ q + h, & \text{if } m > d + q + h; \end{cases} \quad (2.18)$$

- the function r is defined on $\mathbb{N}^+ \setminus \{1\}$ by:

$$r(a) = \delta a + \rho, \quad \text{for some } \rho \geq 0; \quad (2.19)$$

- the function g is defined on $[2, +\infty)$ by:

$$g(p) := \delta(\lfloor p \rfloor - 1) - \epsilon, \quad \text{for some } \epsilon \in [0, \delta); \quad (2.20)$$

- for $j \in \mathbb{N}^+$, let $\check{Z}_{\tau_j^-}^{(\alpha)} := Z_{\tau_j^-}^{(\alpha)} + d_N Z_{\tau_j}^{(\alpha)}$, where

$$d_N Z_t^{(\alpha)} := \left(\begin{array}{c} dP_t^{(\alpha)}, \\ -\kappa \left(Q_t, H_t, d(P^{(\alpha)})_{t-}, M_{N_t^m} \right) dN_t^m, \\ r \left(\lfloor P^{(\alpha)} \rfloor_{t-} \right) \kappa \left(Q_t, H_t, d(P^{(\alpha)})_{t-}, M_{N_t^m} \right) dN_t^m \end{array} \right)', \quad (2.21)$$

for $t \geq 0$.

Remark 2.11.

- The function η in (2.17) (resp. κ in (2.18)) is formulated based on Assumption 2.8 together with the price-visibility-time priority rule: for $(q, h, d, m) \in \mathcal{E}_1 \times (0, \bar{d}] \times \mathbb{R}^+$, the value $\eta(q, h, d, m)$ (resp. $\kappa(q, h, d, m)$)

represents the decrement of the ask-side underlying market depth (resp. the agent's inventory position) upon the arrival of a buy market order of size m , given the agent's limit order strategy (q, h) and the underlying market depth d at the best ask price. For example, taking the left panel of Figure 2.3 as the current LOB state, a buy market order of size $\bar{d}/2$ (resp. $11\bar{d}/8$) will consume the underlying market depth of size $\bar{d}/4$ (resp. $3\bar{d}/4$) and decrease the agent's inventory position by size of $\bar{d}/4$ (resp. $5\bar{d}/8$).

- The function r in (2.19) maps the best ask price in tick size to the cash increment from the execution of one unit of the agent's sell limit order, which is equal to the sum of the best ask price and the (per-unit) rebate ρ for providing liquidity to the market.
- The function g in (2.20) maps the underlying liquidity state to the agent's cash increment from her submission of one unit of sell market order, which is equal to the best bid price minus the (per-unit) fee ϵ for consuming liquidity from the market. Here the agent's sell market orders are assumed to be small in the sense that they never penetrate the entire best bid queue.
- The term $d_N Z_t^{(\alpha)}$ defined in (2.21) represents the jump of the state process $Z^{(\alpha)}$ that stems only from the general market participants (namely, the processes N^ϖ for $\varpi \in \{m, l, c\}$) at $t \geq 0$.

2.2.4 TRADING OBJECTIVE

For some $\underline{p} \geq 2$ and $T > 0$, define the solvency region \mathcal{S} and the trading window \mathbb{T} by

$$\mathcal{S} := (\underline{p}, +\infty) \times \mathbb{R}^+ \times \mathbb{R}_0^+ \quad \text{and} \quad \mathbb{T} := [0, T].$$

Here \underline{p} is interpreted as a stop loss price. For a given initial state $z_0 := (p_0, y_0, x_0) \in \mathcal{S}$ and a combined control $\alpha \in \tilde{\mathcal{A}}$, let the state process $Z^{(\alpha)}$ in (2.10) start with $Z_{0-}^{(\alpha)} = z_0$. Without loss of generality, we assume

that $x_0 = 0$. We further introduce the termination time τ of the agent's liquidation strategy $\alpha \in \tilde{\mathcal{A}}$ by

$$\tau := \inf \left\{ t > 0 : \left(P_t^{(\alpha)}, Y_t^{(\alpha)}, X_t^{(\alpha)} \right) \notin \mathcal{S} \right\} \wedge T, \quad (2.22)$$

at which point the agent is required to liquidate all the unexecuted inventory position (if any) through a sell market order.

Remark 2.12. We introduce the termination time τ to the agent's liquidation problem in the sense that we are only interested in the dynamic system up to any of the following events:

- the trading window \mathbb{T} expires;
- the ask-size LOB state $P^{(\alpha)}$ declines to \underline{p} , that is, the best ask price declines to $\lfloor \underline{p} \rfloor \delta$ with the best ask queue size accumulates to $d(\underline{p})$;
- the remaining inventory position $Y^{(\alpha)}$ reduces to zero.

The agent's objective is to maximise the expected utility from the wealth at the termination time:

$$\sup_{\alpha \in \mathcal{A}} \mathbb{E} \left[u \left(X_\tau^{(\alpha)} + \beta(\tau) g \left(P_\tau^{(\alpha)} \right) Y_\tau^{(\alpha)} \right) \right], \quad (2.23)$$

where

- the set \mathcal{A} of admissible combined controls, assumed non-empty, is defined by

$$\begin{aligned} \mathcal{A} := & \left\{ \alpha = \left((Q_t, H_t)_{t \geq 0}, \{(\tau_j, \xi_j)\}_{j \in \mathbb{N}^+} \right) \in \tilde{\mathcal{A}} : \right. \\ & Q_t + H_t \leq Y_{t-}^{(\alpha)} \text{ for } t \in [0, \tau] \text{ and } (Q_t, H_t) = (0, 0) \text{ for } t > \tau; \\ & \xi_j \leq \check{Y}_{\tau_j-}^{(\alpha)} \text{ for } j \in \mathbb{N}^+ \text{ and } \lim_{j \uparrow \infty} \tau_j = \tau, \text{ a.s.;} \\ & \left. \text{there exists a unique strong solution to (2.11)-(2.15)} \right\}, \quad (2.24) \end{aligned}$$

in the sense that neither short selling nor trading after the termination time is allowed;

- for $\alpha \in \mathcal{A}$, $Z^{(\alpha)}$ is the unique strong solution to (2.11)-(2.15) starting from $Z_{0-} = z_0$;
- the exponential utility function $u : \mathbb{R}_0^+ \rightarrow [0, 1)$ is given by

$$u(x) := -e^{-\gamma x} \quad (2.25)$$

for some constant $\gamma > 0$;

- the function $\beta : \mathbb{T} \rightarrow \{b, 1\}$, which imposes a penalty for the unexecuted inventory at T , is given by

$$\beta(t) := \begin{cases} 1, & \text{if } t \in [0, T), \\ b, & \text{if } t = T, \end{cases} \quad \text{for some constant } b \in (0, 1).$$

2.3 OPTIMAL LIQUIDATION STRATEGY

2.3.1 VALUE FUNCTION

Definition 2.13. Given an initial condition $(t, z) := (t, p, y, x) \in \mathbb{T} \times \mathcal{S}$ and an admissible combined control $\alpha \in \mathcal{A}$, let

$$Z^{t,z,(\alpha)} = (P^{t,z,(\alpha)}, Y^{t,z,(\alpha)}, X^{t,z,(\alpha)})$$

denote the unique strong solution to (2.11)-(2.15) starting from $Z_{t-} = z$. The gain function for the agent's liquidation problem in (2.23) is defined by

$$J(t, z, \alpha) := \mathbb{E} [u(X_\tau^{t,x,(\alpha)}) + \beta(\tau)g(P_\tau^{t,p,(\alpha)})Y_\tau^{t,y,(\alpha)}], \quad (2.26)$$

with associated value function

$$v(t, z) := \sup_{\alpha \in \mathcal{A}} J(t, z, \alpha), \quad (2.27)$$

and we say that $\alpha^* \in \mathcal{A}$ is the optimal admissible combined control if

$$v(\cdot, \cdot) = J(\cdot, \cdot, \alpha^*).$$

2.3.2 DYNAMIC PROGRAMMING EQUATION

Using combined stochastic control and impulse control theory for jump diffusions [71, Chapter 8], we expect that the value function v in (2.27) identifies with a function $w : \mathbb{T} \times \bar{\mathcal{S}} \rightarrow \mathbb{R}$, where $\bar{\mathcal{S}} = [p, +\infty) \times \mathbb{R}_0^+ \times \mathbb{R}_0^+$, that satisfies the dynamic programming equation associated with the optimal liquidation problem (2.23), which is in the form of a Hamilton-Jacobi-Bellman quasi-variational inequality (HJBQVI)

$$\min \left\{ -\frac{\partial w(t, z)}{\partial t} - \frac{\sigma^2}{2} \frac{\partial^2 w(t, z)}{\partial p^2} - \sup_{\substack{(q, h) \in \mathcal{E}_1 \\ \text{s.t. } q+h \leq y}} \mathcal{L}^{q, h} w(t, z), \right. \\ \left. w(t, z) - \sup_{e \in \mathcal{E}_2 \cap [0, y]} \mathcal{M}^e w(t, z) \right\} = 0, \quad (2.28)$$

for $(t, z) := (t, p, y, x) \in [0, T) \times \mathcal{S}$, together with the boundary and terminal condition

$$w(t, z) = u(x + \beta(t)g(p)y), \quad (2.29)$$

for $(t, z) \in \mathcal{B}$, where

$$\mathcal{B} := \left\{ \{T\} \times [p, +\infty) \times \mathbb{R}_0^+ \times \mathbb{R}_0^+ \right\} \\ \cup \left\{ \mathbb{T} \times \{p\} \times \mathbb{R}_0^+ \times \mathbb{R}_0^+ \right\} \cup \left\{ \mathbb{T} \times [p, +\infty) \times \{0\} \times \mathbb{R}_0^+ \right\} \quad (2.30)$$

Here the stochastic control operator $\mathcal{L}^{q, h}$ is defined with $(q, h) \in \mathcal{E}_1$ such that $q + h \leq y$ by

$$\mathcal{L}^{q, h} w(t, z) := \left[\int_{\mathbb{R}^+} w(t, \Gamma(q, h, z, v)) dF^m(v) - w(t, z) \right] \lambda^m(d(p) + q) \\ + \left[\int_{\mathbb{R}^+} w(t, p - v/\bar{d}, y, x) dF^l(v) - w(t, z) \right] \lambda^l(d(p) + q) \\ + \left[\int_{\mathbb{R}^+} w(t, p + v/\bar{d}, y, x) dF^c(v) - w(t, z) \right] \lambda^c(d(p) + q),$$

for $(t, z) \in [0, T) \times \mathcal{S}$, where the functions Γ is defined from $\mathcal{E}_1 \times \mathcal{S} \times \mathbb{R}^+$ by

$$\Gamma(q, h, z, v) := (p + \eta(q, h, d(p), v)/\bar{d}, y - \kappa(q, h, d(p), v), x + r(\lfloor p \rfloor) \kappa(q, h, d(p), v)).$$

The impulse control operator \mathcal{M}^e is defined with $e \in \mathcal{E}_2 \cap [0, y]$ by

$$\mathcal{M}^e w(t, z) = w(t, p, y - e, x + g(p)e), \quad (2.31)$$

for $(t, z) \in [0, T) \times \mathcal{S}$.

2.3.3 VERIFICATION THEOREM

We now give the verification theorem for the value function, proved in Appendix B.1.

Theorem 2.14 (Verification Theorem). *Suppose we can find $w : \mathbb{T} \times \mathcal{S} \rightarrow \mathbb{R}$ such that $w \in C^{1,2}([0, T) \times \mathcal{S}) \cap C_b(\mathbb{T} \times \overline{\mathcal{S}})$ and*

$$\lim_{s \uparrow \tau^-} w(s, Z_s^{t,z,(\alpha)}) = w(\tau, Z_\tau^{t,z,(\alpha)}), \quad \text{almost surely,} \quad (2.32)$$

for all $(t, z) \in [0, T) \times \mathcal{S}$ and $\alpha \in \mathcal{A}$.

(a) Suppose that

$$\min \left(-\frac{\partial w(t, z)}{\partial t} - \frac{\sigma^2}{2} \frac{\partial^2 w(t, z)}{\partial p^2} - \sup_{\substack{(q,h) \in \mathcal{E}_1 \\ \text{s.t. } q+h \leq y}} \mathcal{L}^{q,h} w(t, z), \right. \\ \left. w(t, z) - \sup_{e \in \mathcal{E}_2 \cap [0, y]} \mathcal{M}^e w(t, z) \right) \geq 0, \quad (2.33)$$

for $(t, z) \in [0, T) \times \mathcal{S}$, and

$$w(t, z) \geq u(x + \beta(t)g(p)y), \quad (2.34)$$

for $(t, z) \in \mathcal{B}$, then $w(t, z) \geq v(t, z)$ on $\mathbb{T} \times \overline{\mathcal{S}}$.

(b) Suppose that

$$w(t, z) = u(x + \beta(t)g(p)y), \quad (2.35)$$

for $(t, z) \in \mathcal{B}$, and that there exists a measurable function

$$\widehat{\varphi} : [0, T) \times \mathcal{S} \ni (t, z) \mapsto (q, h) \in \mathcal{E}_1 \text{ with } q + h \leq y$$

satisfying

$$-\frac{\partial w(t, z)}{\partial t} - \frac{\sigma^2}{2} \frac{\partial^2 w(t, z)}{\partial p^2} - \mathcal{L}^{\widehat{\varphi}(t, z)} w(t, z) = 0, \quad (2.36)$$

for all $(t, z) \in \mathcal{D}$, where

$$\mathcal{D} := \left\{ (t, z) \in [0, T) \times \mathcal{S} : w(t, z) - \sup_{e \in \mathcal{E}_2 \cap [0, y]} \mathcal{M}^e w(t, z) > 0 \right\}.$$

Furthermore, suppose that

$$\widehat{\zeta}(t, z) \in \arg \max_{e \in \mathcal{E}_2 \cap [0, y]} \mathcal{M}^e w(t, z)$$

exists for all $(t, z) \in [0, T) \times \mathcal{S}$ and $\widehat{\zeta}(\cdot, \cdot)$ is a Borel measurable selection.

Set $\widehat{\tau}_0 = 0$ and define an impulse control $\{\widehat{\tau}_j, \widehat{\xi}_j\}_{j \in \mathbb{N}^+}$ inductively by

$$\widehat{\tau}_{k+1} := \inf \{s > \widehat{\tau}_k : Z_s^{(\widehat{\alpha}_k)} \notin \mathcal{D}\} \wedge \tau, \quad (2.37)$$

$$\widehat{\xi}_{k+1} := \widehat{\zeta} \left(\widehat{\tau}_{k+1}, \check{Z}_{\widehat{\tau}_{k+1}-}^{(\widehat{\alpha}_k)} \right), \quad (2.38)$$

for $k \in \mathbb{N}$, where $\widehat{\alpha}_k \in \widetilde{\mathcal{A}}$ is a combined control that is in the form of

$$\widehat{\alpha}_k := \left(\left(\widehat{\varphi}(s, Z_s^{(\widehat{\alpha}_k)}) \right)_{s \geq 0}, \left\{ (\widehat{\tau}_j, \widehat{\xi}_j) : j = 1, \dots, k \right\} \right).$$

Suppose that $\widehat{\alpha} := \lim_{k \uparrow \infty} \widehat{\alpha}_k \in \mathcal{A}$, then

$$w(t, z) = v(t, z), \quad \text{for } (t, z) \in \mathbb{T} \times \overline{\mathcal{S}},$$

and $\widehat{\alpha}$ is an optimal admissible combined control.

2.4 PARAMETER ESTIMATIONS AND COMPUTATIONAL RESULTS

Our empirical calculations are based on the LOBSTER data of the top two price levels for a large-tick stock, Yahoo (YHOO), traded on the NASDAQ platform from April 4 to April 22, 2016, recording all market order arrivals,

limit order submissions and cancellations at the first and second best prices between 9.30am and 4pm. This stock is selected based on price, trading volume and market share considerations as in [12, Section 4]. In order to avoid the abnormal trading behaviours shortly after market opening and shortly before market close, we exclude all order book activities during the first and the last twenty minutes of each trading day. We also exclude all hidden order executions, which account for around 12% of the total trading volume. In the following, we first (Section 2.4.1) provide the estimation methods and results for the market depth cap in Assumption 2.1(b), the order size distributions in Assumption 2.3(b) and the order flow intensity functions in (2.16), respectively. We then (Section 2.4.2) give a numerical scheme that solves the HJBQVI in (2.28)-(2.29). We finally (Section 2.4.3) visualise the optimal liquidation strategy under different market conditions.

2.4.1 PARAMETER ESTIMATIONS

MARKET DEPTH CAP

Based on Assumption 2.1, the market depth cap \bar{d} is estimated as in [18, Section 2.2] by averaging the best ask queue sizes (in number of shares) right before the best ask price decreases and those right after the best ask price increases. The estimation result is given in Figure 2.4.

ORDER SIZE

Let \mathfrak{D}^m , \mathfrak{D}^l and \mathfrak{D}^c represent the sets of the sizes (in number of shares) of the buy market orders, sell limit orders and cancellations occurring at the best ask price, respectively. Figure 2.5 displays the empirical distributions of the order sizes in \mathfrak{D}^l and \mathfrak{D}^c , respectively, which are almost the same. Similar to [22], we observe that the order sizes in \mathfrak{D}^l and \mathfrak{D}^c are strongly clustering at integer multiples of 100, in particular at 100 and 200, which account for nearly 60% and around 15% of the entire sample, respectively. Besides, we observe that only about 7% of the order sizes in \mathfrak{D}^l and \mathfrak{D}^c are larger than 600 or less than 100.

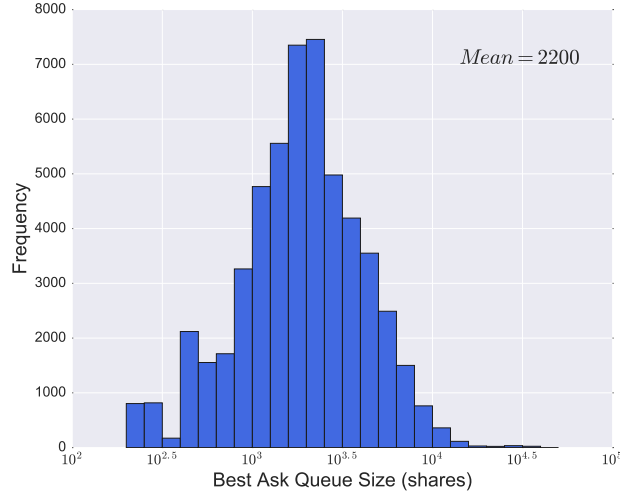


Figure 2.4: histogram of the best ask queue sizes (in number of shares) right before the best ask price decreases and those right after the best ask price increases.

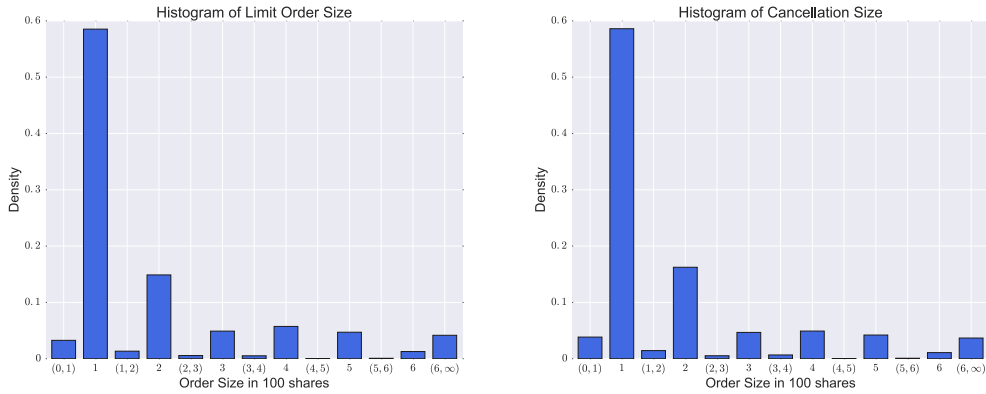


Figure 2.5: YHOO: histograms of order sizes of sell limit order submissions (left) and sell limit order cancellations (right) at the best ask price.

Based on the above empirical findings, let L_1 (resp. C_1) in Assumption 2.3(b) be a discrete random variable defined on $\mathcal{N} := \{100, 200, \dots, 600\}$ with probability mass function f^l (resp. f^c). In Table 2.1, we list the values of f^l (resp. f^c) on \mathcal{N} , which are approximated by the empirical probabilities derived from the truncated sample obtained by rounding the order sizes in \mathfrak{D}_l (resp. \mathfrak{D}_c) to the nearest integer multiples of 100, and discard the results

that are outside \mathcal{N} . In Figure 2.6, we exhibit the histogram of the order

Table 2.1: probability mass functions f^l and f^c on \mathcal{N} .

x	100	200	300	400	500	600
$f^l(x)$	0.64	0.17	0.06	0.07	0.05	0.01
$f^c(x)$	0.65	0.19	0.05	0.05	0.05	0.01

sizes in \mathfrak{D}^m . The order sizes in \mathfrak{D}^m also display a tendency to cluster at integer multiples of 100 (particularly, nearly 35% of the order sizes are equal to 100), but not as strong as that shown in \mathfrak{D}^l and \mathfrak{D}^c . Besides, around 17% of the order sizes in \mathfrak{D}^m are less than 100, compared with 3% to 4% in \mathfrak{D}^l and \mathfrak{D}^c . In Figure 2.7, we exhibit the empirical complementary cumulative

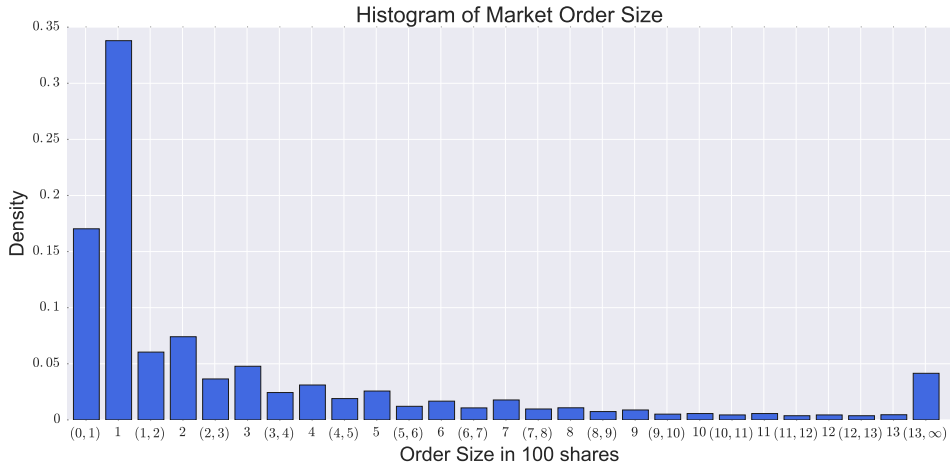


Figure 2.6: histogram of the sizes of buy market order arrivals.

distribution function of the order sizes in \mathfrak{D}^m (line of red circles) on a doubly logarithmic plot. Accordingly, we impose the following assumption on the probability distribution of the random variable M_1 , which is introduced in Assumption 2.3(b) representing the size of a buy market order.

Assumption 2.15 (Distribution of M_1).

Let M_1 be a mixed-type random variable valued in \mathbb{R}^+ , and assume that:

- (a) M_1 has a positive mass at \underline{x} but is continuous elsewhere on \mathbb{R}^+ ;

- (b) M_1 follows uniform distribution given that $0 < M_1 < \underline{x}$;
- (c) M_1 follows exponential distribution with parameter ϑ given that $\underline{x} < M_1 < \bar{x}$;
- (d) M_1 follows power-law distribution with scaling parameter a and lower bound \bar{x} given that $M_1 \geq \bar{x}$.

The cumulative distribution function F^m of M_1 is then written by

$$F^m(x) := \begin{cases} \frac{\mu_1 x}{\underline{x}}, & \text{if } 0 < x < \underline{x}, \\ \mu_1 + \mu_2, & \text{if } x = \underline{x}, \\ \mu_1 + \mu_2 + \mu_3 \frac{e^{-\vartheta x} - e^{-\vartheta \bar{x}}}{e^{-\vartheta \underline{x}} - e^{-\vartheta \bar{x}}}, & \text{if } \underline{x} < x < \bar{x}, \\ 1 - \mu_4 \left(\frac{x}{\bar{x}}\right)^{-a+1}, & \text{if } x \geq \bar{x}, \end{cases} \quad (2.39)$$

where

- $\underline{x} = 100$ reflects the fact that the order sizes in \mathfrak{D}_m are clustering at 100 shares;
- $(\mu_1, \mu_2, \mu_3, \mu_4) = (0.170, 0.338, 0.471, 0.021)$ are the empirical probabilities of the order sizes in \mathfrak{D}_m being less than \underline{x} , equal to \underline{x} , greater than \underline{x} and less than \bar{x} , greater than or equal to \bar{x} , respectively;
- $(\vartheta, a, \bar{x}) = (0.00248, 3.909, 1850)$ are estimated using maximum likelihood method as in [61, 24].

INTENSITY FUNCTIONS

The intensity functions $\lambda^\varpi(\cdot)$ for $\varpi \in \{m, l, c\}$ in (2.16) are formulated as follows. We first round the best ask queue sizes (in number of shares) in our sample data to the nearest integer multiples of 100, and call them the rounded best ask queue sizes. We then estimate the intensities by the maximum



Figure 2.7: YHOO: empirical (line of circles) and the fitted (solid line) complementary cumulative distribution function of buy market order size M_1 on a doubly logarithmic plot.

likelihood method as in [49]:

$$\hat{\lambda}^{\varpi}(d) = \frac{N^{\varpi}(d)}{T(d)}, \quad \text{for } \varpi \in \{m, l, c\} \text{ and } d \in \{100n : n = 0, 1, \dots, 50\},$$

where

- $N^{\varpi}(d)$, $\varpi \in \{m, l, c\}$ represents the total number of buy market order arrivals, sell limit order submissions and cancellations, respectively, at the best ask price when the pre-event rounded best ask queue size is equal to d and the pre-event spread is equal to the tick size δ ;
- $T(d)$ represents the total time (in number of seconds) during which the rounded best ask queue size is equal to d and the spread is equal to the tick size δ .

The estimated intensities are presented in the left panel of Figure 2.8, with the following comments.

Remark 2.16.

- The rate of buy market order arrivals decreases exponentially as the rounded best ask queue size increases, which can be interpreted as traders in the market rushing for liquidity when liquidity becomes scarce while waiting for better price when liquidity is adequate.
- As a function of the rounded best ask queue size, the rate of sell limit order submissions takes its minimum value at 0 (corresponding to the actual best ask queue size being below 50 shares), sees a moderate jump at 100, and declines rapidly until it rebounds at 800 and then increases exponentially. The interpretation of this result is threefold: (i) when the best queue size is below the lot size 100 as a result of the odd-lot trades, most likely initiated by the high frequency or algorithmic traders [69], market participants are reluctant to place limit orders at the best price in order to avoid the risk of adverse selection; (ii) when the best queue size takes values between 100 and 800, the market participants are more motivated to place limit orders at the best price since they can obtain relatively favourable queue positions but avoid being alone in the queue; (iii) when the best queue size exceeds 800, we observe a widespread low-latency market activity at the best price: limit orders are placed and then cancelled almost immediately (within 10^{-4} to 10^{-3} second). This low-latency activity occurs more frequently as the best queue size increases.
- When the best queue size is below 800, the rate of sell limit order cancellations remains a stable and low level, indicating the market participants' reluctance to give up their favourable queue positions. When the best queue size exceeds 800, the rate of sell limit order cancellations increases exponentially at almost the same pace with that of sell limit order submissions, reflecting the prevalence of the low-latency activity mentioned above.

Similar to [79], we propose that the intensity function $\lambda^\varpi(\cdot)$ in (2.16) is in the form of

$$\lambda^\varpi(d) = \exp(\beta_0^\varpi + \beta_1^\varpi d + \beta_2^\varpi d^2), \quad d \in \mathbb{R}^+,$$

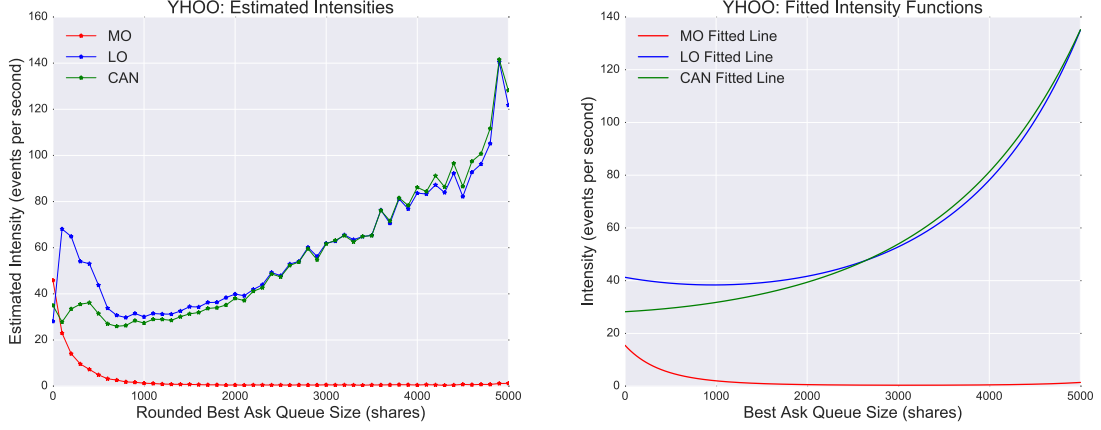


Figure 2.8: left panel: the scatter plot of the set $\left(100\mathfrak{d}, \hat{\lambda}^\varpi(100\mathfrak{d})\right)_{\mathfrak{d}=0,1,\dots,50}$ for $\varpi \in \{m, l, c\}$; right panel: the fitted line $y = \exp\left(\hat{\beta}_0^\varpi + \hat{\beta}_1^\varpi x + \hat{\beta}_2^\varpi x^2\right)$ for $\varpi \in \{m, l, c\}$.

for $\varpi \in \{m, l, c\}$. We then fit a linear regression line

$$y = \beta_0^\varpi + \beta_1^\varpi x + \beta_2^\varpi x^2, \quad (2.40)$$

to the set $\left(100\mathfrak{d}, \log\left(\hat{\lambda}^\varpi(100\mathfrak{d})\right)\right)_{\mathfrak{d}=0,1,\dots,50}$, for each $\varpi \in \{m, l, c\}$. The estimated coefficients $\hat{\beta}_i^\varpi$ for $\varpi \in \{m, l, c\}$ and $i \in \{0, 1, 2\}$ are given in Table 2.2. The fitted curves (2.40) are illustrated in the right panel of Figure 2.8.

Table 2.2: estimated coefficients for the linear regression in (2.40).

Est. Coefficients	Est. Value	Std. Error	t-value	P-value
$\hat{\beta}_0^m$	2.74e+00	1.41e-01	1.95e+01	1.95e-24
$\hat{\beta}_1^m$	-2.43e-03	1.30e-04	-1.86e+01	1.29e-23
$\hat{\beta}_2^m$	3.90e-07	2.52e-08	1.55e+01	2.85e-20
$\hat{\beta}_0^l$	3.72e+00	7.49e-02	4.96e+01	6.66e-43
$\hat{\beta}_1^l$	-1.50e-04	6.93e-05	-2.17e+00	3.53e-02
$\hat{\beta}_2^l$	7.74e-08	1.34e-08	5.77e+00	5.54e-07
$\hat{\beta}_0^c$	3.34e+00	4.55e-02	7.34e+01	5.87e-51
$\hat{\beta}_1^c$	6.92e-05	4.20e-05	1.65e+00	1.06e-01
$\hat{\beta}_2^c$	4.88e-08	8.13e-09	6.00e+00	2.54e-07

2.4.2 NUMERICAL SCHEME

In the case of adopting the exponential utility criterion (2.25) in (2.23), the value function v in (2.27) reduces to the form

$$v(t, z) = v(t, p, y, x) = -u(x)\phi(t, p, y),$$

for $(t, z) \in \mathbb{T} \times \bar{\mathcal{S}}$. The HJBQVI associated with ϕ then reads

$$\min \left(-\frac{\partial \phi(t, p, y)}{\partial t} - \frac{\sigma^2}{2} \frac{\partial^2 \phi(t, p, y)}{\partial p^2} - \sup_{\substack{(q, h) \in \mathcal{E}_1 \\ \text{s.t. } q+h \leq y}} L^{q, h} \phi(t, p, y), \right. \\ \left. \phi(t, p, y) - \sup_{e \in \mathcal{E}_2 \cap [0, y]} M^e \phi(t, p, y) \right) = 0, \quad (2.41)$$

for $(t, p, y) \in [0, T] \times \mathcal{S}_0$, together with the boundary and terminal condition

$$\phi(t, p, y) = u(\beta(t)g(p)y), \quad (2.42)$$

for $(t, p, y) \in \mathcal{B}_0$, where

$$\mathcal{S}_0 := (p, +\infty) \times \mathbb{R}^+, \\ \mathcal{B}_0 := \{ \{T\} \times [p, +\infty) \times \mathbb{R}_0^+ \} \cup \{ \mathbb{T} \times \{p\} \times \mathbb{R}_0^+ \} \cup \{ \mathbb{T} \times [p, +\infty) \times \{0\} \}.$$

The operator $L^{q, h}$ is defined with $(q, h) \in \mathcal{E}_1$ such that $q + h \leq y$ by

$$L^{q, h} \phi(t, p, y) \\ := \left[\int_{\mathbb{R}^+} c(q, h, p, v) \phi(t, \Xi(q, h, p, y, v)) dF^m(v) - \phi(t, p, y) \right] \lambda^m(d(p) + q) \\ + \left[\sum_{v \in \mathcal{N}} \phi(t, p - v/\bar{d}, y) f^l(v) - \phi(t, p, y) \right] \lambda^l(d(p) + q) \\ + \left[\sum_{v \in \mathcal{N}} \phi(t, p + v/\bar{d}, y) f^c(v) - \phi(t, p, y) \right] \lambda^c(d(p) + q), \quad (2.43)$$

for $(t, p, y) \in [0, T) \times \mathcal{S}_0$, where

- the function c is defined on $\mathcal{E}_1 \times \mathcal{S}_0$ by

$$c(q, h, p, v) := -u(r(\lfloor p \rfloor) \kappa(q, h, d(p), v));$$

- the function Ξ is defined on $\mathcal{E}_1 \times \mathcal{S}_0 \times \mathbb{R}^+$ such that $q + h \leq y$ by

$$\Xi(q, h, p, y, v) := \left(p + \frac{\eta(q, h, d(p), v)}{\bar{d}}, y - \kappa(q, h, d(p), v) \right);$$

- the operator M^e is defined with $e \in \mathcal{E}_2 \cap [0, y]$ by

$$M^e \phi(t, p, y) = -u(g(p)e) \phi(t, p, y - e),$$

for $(t, p, y) \in [0, T) \times \mathcal{S}_0$.

We solve the HJBQVI (2.41)-(2.42) numerically using an implicit finite difference scheme as in [52]. We first localise $\overline{\mathcal{S}_0}$ to a bounded domain

$$\mathcal{S}_{\text{loc}} := [\underline{p}, \bar{p}] \times [0, \bar{y}],$$

for fixed $\bar{p} > p$ and $\bar{y} > 0$. The associated localisation error is studied in [29].

We then introduce a regular grid on $\mathbb{T} \times \mathcal{S}_{\text{loc}}$ with uniform spacing:

$$\begin{aligned} o_{j,k}^i &:= (i\delta_T, \underline{p} + j\delta_P, k\delta_Y), & \phi_{j,k}^i &:= \phi(o_{j,k}^i), \\ \delta_T &:= \frac{T}{l}, & \delta_P &:= \frac{\bar{p} - \underline{p}}{m}, & \delta_Y &:= \frac{\bar{y}}{n}, \end{aligned}$$

for $(i, j, k) \in \mathfrak{L} \times \mathfrak{M} \times \mathfrak{N}$, with $\mathfrak{L} := \{0, 1, \dots, l\}$, $\mathfrak{M} := \{0, 1, \dots, m\}$, $\mathfrak{N} := \{0, 1, \dots, n\}$ and $l, m, n \in \mathbb{N}^+$. We further assume that there exists $\nu_1 \in \mathbb{N}^+$ (resp. $\nu_2 \in \mathbb{N}^+$) such that $\bar{e}_1 = \nu_1 \delta_Y$ (resp. $\bar{e}_2 = \nu_2 \delta_Y$), and construct the regular grids on $\mathcal{E}_1 = [0, \bar{e}_1]^2$ (resp. $\mathcal{E}_2 = [0, \bar{e}_2]$) with uniform spacing δ_Y :

$$a_{\mathfrak{q}, \mathfrak{h}} := (\mathfrak{q} \delta_Y, \mathfrak{h} \delta_Y) \quad (\text{resp. } b_{\mathfrak{e}} := \mathfrak{e} \delta_Y),$$

for $(\mathbf{q}, \mathbf{h}) \in \mathfrak{A}_1$ (resp. $\mathbf{c} \in \mathfrak{A}_2$), where $\mathfrak{A}_1 := \{0, 1, \dots, \nu_1\}^2$ (resp. $\mathfrak{A}_2 := \{0, 1, \dots, \nu_2\}$). Next, in order to approximate the Riemann-Stieltjes integral term in (2.43), we truncate the the region of integration \mathbb{R}^+ to a bounded interval $[0, U^b]$, partition the interval into \bar{N} equally spaced subintervals, and apply the trapezoidal rule [33] to each subinterval, that is

$$\int_{\mathbb{R}^+} \mathcal{I}(v) dF^{\mathbf{m}}(v) \approx \sum_{\iota=0}^{\bar{N}-1} \frac{\mathcal{I}(\iota\delta_v) + \mathcal{I}((\iota+1)\delta_v)}{2} [F^{\mathbf{m}}((\iota+1)\delta_v) - F^{\mathbf{m}}(\iota\delta_v)],$$

where $\mathcal{I}(\cdot)$ represents the integrand, $U^b \in \mathbb{R}^+$, $\bar{N} \in \mathbb{N}^+$ are properly chosen, and $\delta_v := U^b/\bar{N}$. Furthermore, for notational convenience, we denote $\phi_{j,k}^i$ the value of $\phi(i\delta_T, j\delta_P, k\delta_Y)$ when $(i, j, k) \in \mathfrak{L} \times \{\mathbb{R} \setminus \mathfrak{M}\} \times \{(-\infty, n] \setminus \mathfrak{N}\}$, and make the following approximations and assumptions:

- for $i \in \mathfrak{L}$, $j \in [0, m] \setminus \mathfrak{M}$ and $k \in [0, n] \setminus \mathfrak{N}$, $\phi_{j,k}^i$ is approximated by the bilinear interpolation of the values of function ϕ at the grid points $o_{i, \underline{J}(j), \underline{K}(k)}$, $o_{i, \underline{J}(j), \bar{K}(k)}$, $o_{i, \bar{J}(j), \underline{K}(k)}$ and $o_{i, \bar{J}(j), \bar{K}(k)}$, that is,

$$\phi_{j,k}^i = \begin{pmatrix} \bar{J}(j) - j & j - \underline{J}(j) \end{pmatrix} \begin{pmatrix} \phi_{\underline{J}(j), \underline{K}(k)}^i & \phi_{\underline{J}(j), \bar{K}(k)}^i \\ \phi_{\bar{J}(j), \underline{K}(k)}^i & \phi_{\bar{J}(j), \bar{K}(k)}^i \end{pmatrix} \begin{pmatrix} \bar{K}(k) - k \\ k - \underline{K}(k) \end{pmatrix},$$

where the functions $\underline{J}, \bar{J}, \underline{K}$ and \bar{K} are defined from \mathbb{R} by

$$\begin{aligned} \underline{J}(j) &:= \max\{j' \in \mathfrak{M} : j' < j\}, & \bar{J}(j) &:= \min\{j' \in \mathfrak{M} : j < j'\}, \\ \underline{K}(k) &:= \max\{k' \in \mathfrak{N} : k' < k\}, & \bar{K}(k) &:= \min\{k' \in \mathfrak{N} : k < k'\}; \end{aligned}$$

- for $i \in \mathfrak{L}$ and $k \in [0, n]$, assume that

$$\begin{aligned} \phi_{j,k}^i &= u(k\delta_Y\beta(i\delta_T)g(\underline{p} + m\delta_P)), & \text{for } j > m, \\ \phi_{j,k}^i &= u(k\delta_Y\beta(i\delta_T)g(\underline{p})), & \text{for } j < 0; \end{aligned}$$

- for $(i, j) \in \mathfrak{L} \times \mathfrak{M}$, assume that $\phi_{j,k}^i = u(0)$ for $k < 0$.

Accordingly, the discretised HJBQVI is written by:

$$\begin{aligned} \max \left(\frac{\phi_{j,k}^{i+1} - \phi_{j,k}^i}{\delta_T} + \frac{\sigma^2}{2} \frac{\phi_{j+1,k}^i - 2\phi_{j,k}^i + \phi_{j-1,k}^i}{\delta_P^2} \right. \\ \left. + \sup_{(\mathbf{q}, \mathbf{h}) \in \mathfrak{A}_1} \left\{ L_\delta^{\mathbf{q}, \mathbf{h}} \phi_{j,k}^{i+1} - \varrho [\max(0, \mathbf{q} + \mathbf{h} - k)]^2 \right\}, \right. \\ \left. \sup_{\mathbf{e} \in \mathfrak{A}_2} \left\{ M_\delta^{\mathbf{e}} \phi_{j,k}^i - \varrho [\max(0, \mathbf{e} - k)]^2 \right\} - \phi_{j,k}^i \right) = 0, \quad (2.44) \end{aligned}$$

when $(i, j, k) \in \{\mathfrak{L} \setminus \{l\}\} \times \{\mathfrak{M} \setminus \{0\}\} \times \{\mathfrak{N} \setminus \{0\}\}$, together with the boundary and terminal condition

$$\phi_{j,k}^i = u(k\delta_Y\beta(i\delta_T)g(\underline{p} + j\delta_P)), \quad (2.45)$$

when $(i, j, k) \in \{\{l\} \times \mathfrak{M} \times \mathfrak{N}\} \cup \{\mathfrak{L} \times \{0\} \times \mathfrak{N}\} \cup \{\mathfrak{L} \times \mathfrak{M} \times \{0\}\}$. Here the constrained maximisers in (2.41) are replaced by the unconstrained ones using the penalty function method [81], where the constant $\varrho > 0$ represents the penalty coefficient; the operator $L_\delta^{\mathbf{q}, \mathbf{h}}$ is defined with $(\mathbf{q}, \mathbf{h}) \in \mathfrak{A}_1$ by

$$\begin{aligned} L_\delta^{\mathbf{q}, \mathbf{h}} \phi_{j,k}^i &:= \lambda^{\mathfrak{m}}(j, \mathbf{q}) \times \\ &\left[\frac{1}{2} \sum_{\ell=0}^{\bar{N}-1} \mathfrak{F}^{\mathfrak{m}}(\ell) \left(\mathbf{c}(\mathbf{q}, \mathbf{h}, j, \ell) \phi_{\Xi_\delta(\mathbf{q}, \mathbf{h}, j, k, \ell)}^i + \mathbf{c}(\mathbf{q}, \mathbf{h}, j, \ell + 1) \phi_{\Xi_\delta(\mathbf{q}, \mathbf{h}, j, k, \ell + 1)}^i \right) - \phi_{j,k}^i \right] \\ &+ \lambda^1(j, \mathbf{q}) \left[\sum_{v \in \mathcal{N}} f^1(v) \phi_{j - \frac{v}{d\delta_P}, k}^i - \phi_{j,k}^i \right] + \lambda^c(j, \mathbf{q}) \left[\sum_{v \in \mathcal{N}} f^c(v) \phi_{j + \frac{v}{d\delta_P}, k}^i - \phi_{j,k}^i \right], \end{aligned}$$

where

- the function Ξ_δ is defined from $\mathfrak{A}_1 \times \mathfrak{M} \times \mathfrak{N} \times \mathbb{N}$ by

$$\Xi_\delta(\mathbf{q}, \mathbf{h}, j, k, \ell) := (j + \Delta_p(\mathbf{q}, \mathbf{h}, j, \ell), k - \Delta_y(\mathbf{q}, \mathbf{h}, j, \ell)),$$

with

$$\begin{aligned}\Delta_p(\mathfrak{q}, \mathfrak{h}, j, \iota) &:= \frac{\eta(\mathfrak{q}\delta_Y, \mathfrak{h}\delta_Y, d(\underline{p} + j\delta_P), \iota\delta_v)}{\bar{d}\delta_P}, \\ \Delta_y(\mathfrak{q}, \mathfrak{h}, j, \iota) &:= \frac{\kappa(\mathfrak{q}\delta_Y, \mathfrak{h}\delta_Y, d(\underline{p} + j\delta_P), \iota\delta_v)}{\delta_Y};\end{aligned}$$

- the function λ^ϖ , for $\varpi \in \{m, l, c\}$, is defined from $\mathfrak{M} \times \{0, \dots, \nu_1\}$ by

$$\lambda^\varpi(j, \mathfrak{q}) := \lambda^\varpi(d(\underline{p} + j\delta_P) + \mathfrak{q}\delta_Y);$$

- the function \mathfrak{c} is defined from $\mathfrak{A}_1 \times \mathfrak{M} \times \mathbb{N}$ by

$$\mathfrak{c}(\mathfrak{q}, \mathfrak{h}, j, \iota) := c(\mathfrak{q}\delta_Y, \mathfrak{h}\delta_Y, \underline{p} + j\delta_P, \iota\delta_v);$$

- the function \mathfrak{F}^m is defined from \mathbb{N} by

$$\mathfrak{F}^m(\iota) := F^m((\iota + 1)\delta_v) - F^m(\iota\delta_v);$$

- the operator $M_\delta^\mathfrak{e}$ is defined with $\mathfrak{e} \in \mathfrak{A}_2$ by

$$M_\delta^\mathfrak{e}\phi_{j,k}^i := -u(\mathfrak{e}\delta_Y g(\underline{p} + j\delta_P))\phi_{j,k-\mathfrak{e}}^i.$$

Before proceeding to the next step, we introduce the following notations:

- for $d \in \mathbb{N}^+$, let \mathbf{I}_d denote the d -dimensional identity matrix; for $d_1, d_2 \in \mathbb{N}^+$, let $\mathbf{J}_{d_1 \times d_2}$ denote the $d_1 \times d_2$ all-one matrix;
- for $d \in \mathbb{N}^+ \setminus \{1\}$ and $b \in \mathbb{N}^+ \cup [1, d]$, let \mathbf{e}_d^b denote the d -dimensional column vector with the b -th element being 1 and the others being 0;
- let Ψ_1 (resp. Ψ_2) denote the space of functions $\psi : \mathbb{N} \rightarrow \mathbb{N}$ (resp. $\mathbb{N} \rightarrow \mathbb{R}$);

- introduce the operators $\mathbb{A}_+, \mathbb{A}_- : \mathbb{N}^+ \times \Psi_1 \ni (d, \psi(\cdot)) \mapsto \mathcal{M}_{d+1}(\mathbb{R})$ by

$$\begin{aligned}\mathbb{A}_+(d, \psi(\cdot)) &:= \begin{bmatrix} \mathbf{e}_{d+1}^{(1+\psi(0)) \wedge (d+1)} & \mathbf{e}_{d+1}^{(2+\psi(1)) \wedge (d+1)} & \cdots & \mathbf{e}_{d+1}^{(d+1+\psi(d)) \wedge (d+1)} \end{bmatrix}, \\ \mathbb{A}_-(d, \psi(\cdot)) &:= \begin{bmatrix} \mathbf{e}_{d+1}^{(1-\psi(0)) \vee 1} & \mathbf{e}_{d+1}^{(2-\psi(1)) \vee 1} & \cdots & \mathbf{e}_{d+1}^{(d+1-\psi(d)) \vee 1} \end{bmatrix};\end{aligned}$$

- introduce the operator $\mathbb{C} : \mathbb{N}^+ \times \Psi_2 \ni (d, \psi(\cdot)) \mapsto \mathcal{M}_{d+1}(\mathbb{R})$ by

$$\mathbb{C}(d, \psi(\cdot)) := \text{Diag}(\psi(0), \dots, \psi(d)).$$

We now write the matrix form of the discretised HJBQVI (2.44) by

$$\max \left(\frac{\Phi^{i+1} - \Phi^i}{\delta_T} + \Upsilon \Phi^i + \sup_{(q,b) \in \mathfrak{A}_1} \mathcal{L}^{q,b} \Phi^{i+1}, \sup_{c \in \mathfrak{A}_2} \mathcal{M}^c \Phi^i - \Phi^i \right) = 0, \quad (2.46)$$

where

- the matrix $\Phi^i \in \mathcal{M}_{(m+1) \times (n+1)}(\mathbb{R})$ is in the form of

$$\Phi^i := \begin{pmatrix} \phi_{0,0}^i & \phi_{0,1}^i & \cdots & \phi_{0,n}^i \\ \phi_{1,0}^i & \phi_{1,1}^i & \cdots & \phi_{1,n}^i \\ \vdots & \vdots & \ddots & \vdots \\ \phi_{m,0}^i & \phi_{m,1}^i & \cdots & \phi_{m,n}^i \end{pmatrix}, \quad \text{for } i \in \mathfrak{L},$$

with its elements satisfying the boundary and terminal condition (2.45);

- the matrix $\Upsilon \in \mathcal{M}_{m+1}(\mathbb{R})$ is defined by

$$\Upsilon := \frac{\sigma^2}{2\delta_P^2} (\mathbb{A}_+^\top(m, 1) - 2\mathbf{I}_{m+1} + \mathbb{A}_-^\top(m, 1));$$

- the operator $\mathcal{L}^{\mathfrak{q}, \mathfrak{h}}$ is defined with $(\mathfrak{q}, \mathfrak{h}) \in \mathfrak{A}_1$ by

$$\begin{aligned} \mathcal{L}^{\mathfrak{q}, \mathfrak{h}} \Phi^i &= \mathbb{E}(m, \lambda^m(\cdot, \mathfrak{q})) \left[\frac{1}{2} \sum_{\iota=0}^{\bar{N}-1} \mathfrak{F}^m(\iota) (\mathcal{C}^{\mathfrak{q}, \mathfrak{h}, \iota} \Phi^i + \mathcal{C}^{\mathfrak{q}, \mathfrak{h}, \iota+1} \Phi^i) - \Phi^i \right] \\ &+ \mathbb{E}(l, \lambda^l(\cdot, \mathfrak{q})) \left[\sum_{v \in \mathcal{N}} f^l(v) \mathcal{D}_-^v \Phi^i - \Phi^i \right] \\ &+ \mathbb{E}(c, \lambda^c(\cdot, \mathfrak{q})) \left[\sum_{v \in \mathcal{N}} f^c(v) \mathcal{D}_+^v \Phi^i - \Phi^i \right] \\ &- \mathbf{J}_{(m+1) \times (n+1)} \mathbb{E}(n, \varrho [\max(0, \mathfrak{q} + \mathfrak{h} - \cdot)]^2); \end{aligned}$$

with the operator $\mathcal{C}^{\mathfrak{q}, \mathfrak{h}, \iota}$ being defined with $(\mathfrak{q}, \mathfrak{h}, \iota) \in \mathfrak{A}_1 \times \mathbb{N}$ by

$$\begin{aligned} \mathcal{C}^{\mathfrak{q}, \mathfrak{h}, \iota} \Phi^i &= \mathbb{E}(m, \mathbf{c}(\mathfrak{q}, \mathfrak{h}, \cdot, \iota)) \begin{bmatrix} \mathbb{E}(m, 1 + \lfloor \Delta_p(\cdot) \rfloor - \Delta_p(\cdot)) \\ \mathbb{E}(m, \Delta_p(\cdot) - \lfloor \Delta_p(\cdot) \rfloor) \end{bmatrix}^\top \times \\ &\begin{bmatrix} \mathbb{A}_+^\top(m, \lfloor \Delta_p(\cdot) \rfloor) \Phi^i \mathbb{A}_-(n, \lceil \Delta_y(\cdot) \rceil) & \mathbb{A}_+^\top(m, \lfloor \Delta_p(\cdot) \rfloor) \Phi^i \mathbb{A}_-(n, \lfloor \Delta_y(\cdot) \rfloor) \\ \mathbb{A}_+^\top(m, \lceil \Delta_p(\cdot) \rceil) \Phi^i \mathbb{A}_-(n, \lceil \Delta_y(\cdot) \rceil) & \mathbb{A}_+^\top(m, \lceil \Delta_p(\cdot) \rceil) \Phi^i \mathbb{A}_-(n, \lfloor \Delta_y(\cdot) \rfloor) \end{bmatrix} \\ &\times \begin{bmatrix} \mathbb{E}(n, \Delta_y(\cdot) - \lfloor \Delta_y(\cdot) \rfloor) \\ \mathbb{E}(n, 1 + \lfloor \Delta_y(\cdot) \rfloor - \Delta_y(\cdot)) \end{bmatrix}, \end{aligned}$$

- the operators \mathcal{D}_\pm^v is defined with $v \in \mathbb{R}^+$ by

$$\begin{aligned} \mathcal{D}_\pm^v \Phi^i &= \left(\frac{v}{\bar{d}\delta_P} - \left\lfloor \frac{v}{\bar{d}\delta_P} \right\rfloor \right) \mathbb{A}_\pm^\top \left(m, \left\lceil \frac{v}{\bar{d}\delta_P} \right\rceil \right) \Phi^i \\ &+ \left(1 - \frac{v}{\bar{d}\delta_P} + \left\lfloor \frac{v}{\bar{d}\delta_P} \right\rfloor \right) \mathbb{A}_\pm^\top \left(m, \left\lfloor \frac{v}{\bar{d}\delta_P} \right\rfloor \right) \Phi^i; \end{aligned}$$

- the operator $\mathcal{M}^\mathfrak{e}$ is defined with $\mathfrak{e} \in \mathfrak{A}_2$ by

$$\begin{aligned} \mathcal{M}^\mathfrak{e} \Phi^i &= \mathbb{E}(m, -u(\mathfrak{e}\delta_Y g(\underline{p} + \cdot \delta_P))) \Phi^i \mathbb{A}_-(n, \mathfrak{e}) \\ &- \mathbf{J}_{(m+1) \times (n+1)} \mathbb{E}(n, \varrho [\max(0, \mathfrak{e} - \cdot)]^2). \end{aligned}$$

According to [29, 52], the discretised HJBQVI in the matrix form in (2.46) is unconditionally stable and can be converted into the fixed point problem:

$$\Phi^i = \max \left(\Upsilon_\varsigma \Phi^i + \sup_{(q,h) \in \mathfrak{A}_1} \mathcal{L}_\varsigma^{q,h} \Phi^{i+1}, \sup_{\epsilon \in \mathfrak{A}_2} \mathcal{M}^\epsilon \Phi^i \right), \quad (2.47)$$

together with the boundary and terminal condition (2.45), where

$$\begin{aligned} \Upsilon_\varsigma &:= \frac{\delta_T}{\delta_T + \varsigma} (\mathbf{I}_{m+1} + \varsigma \Upsilon), \\ \mathcal{L}_\varsigma^{q,h} \Phi^{i+1} &:= \frac{\varsigma}{\delta_T + \varsigma} (\mathbf{I}_{m+1} + \delta_T \mathcal{L}^{q,h}) \Phi^{i+1}, \end{aligned}$$

for $i \in \mathfrak{L} \setminus \{l\}$ and $\varsigma > 0$. For a given tolerance level $\text{tol} > 0$, the implicit finite difference scheme solving the HJBQVI (2.41)-(2.42) is illustrated as follows:

Step 1. let $\phi_{j,k}^l = u(kb\delta_Y g(\underline{p} + j\delta_P))$, for $(j, k) \in \mathfrak{M} \times \mathfrak{N}$;

Step 2. suppose that Φ^{i+1} , for $i \in \mathfrak{L} \setminus \{l\}$ is already known:

Step 2.1. choose arbitrary $\Psi \in \mathcal{M}_{(m+1) \times (n+1)}(\mathbb{R})$;

Step 2.2. calculate

$$\Psi' := (\psi'_{j,k}) = \max \left(\Upsilon_\varsigma \Psi + \sup_{(q,h) \in \mathfrak{A}_1} \mathcal{L}_\varsigma^{q,h} \Phi^{i+1}, \sup_{\epsilon \in \mathfrak{A}_2} \mathcal{M}^\epsilon \Psi \right);$$

Step 2.3. let $\psi'_{j,k} = u(k\delta_Y g(\underline{p} + j\delta_P))$ for $(j, k) \in \{\mathfrak{M} \times \{0\}\} \cup \{\{0\} \times \mathfrak{N}\}$;

Step 2.4. if $\|\Psi' - \Psi\| < \text{tol}$, go to Step 3; otherwise, set $\Psi = \Psi'$ and go to Step 2.2;

Step 3. set $\Phi^i = \Psi'$; if $i = 0$, the scheme is over; otherwise, set $i = i - 1$ and go to Step 2.

Suppose that we have obtained Φ^i , for all $i \in \mathfrak{L}$ based on the above numerical scheme. Now, for $i \in \mathfrak{L} \setminus \{l\}$ (i.e. at time $i\delta_T$), $j \in \mathfrak{M} \setminus \{0, m\}$ (i.e. when the liquidity state is equal to $j\delta_P$) and $k \in \mathfrak{N} \setminus \{0, n\}$ (i.e. when the remaining inventory position is equal to $k\delta_Y$), the corresponding optimal strategy,

denoted by $OS(i, j, k)$, is given by:

$$OS(i, j, k) = \begin{cases} \arg \max_{(q, h) \in \mathfrak{A}_1} \mathcal{L}_\zeta^{q, h} \Phi^i, & \text{if } (j, k) \notin \mathfrak{C}, \\ \arg \max_{\epsilon \in \mathfrak{A}_2} \mathcal{M}^\epsilon \Phi^i, & \text{if } (j, k) \in \mathfrak{C}, \end{cases} \quad (2.48)$$

where

$$\mathfrak{C} := \left\{ (j, k) \in \mathfrak{M} \setminus \{0, m\} \times \mathfrak{N} \setminus \{0, n\} : \Upsilon_\zeta \Phi^i(j, k) + \sup_{(q, h) \in \mathfrak{A}_1} \mathcal{L}_\zeta^{q, h} \Phi^i(j, k) < \sup_{\epsilon \in \mathfrak{A}_2} \mathcal{M}^\epsilon \Phi^i(j, k) \right\}.$$

2.4.3 OPTIMAL STRATEGY

In this section, we provide the optimal strategy computed through the finite difference scheme illustrated in Section 2.4.2. The parameters used are shown in Table 2.3.

In Figure 2.9, we visualise the map $OS(\cdot, \cdot, \cdot)$ in (2.48), illustrating how different market conditions (namely, time to maturity, best ask queue size and remaining inventory position) can affect the agent's optimal action. We observe the following:

- The optimal strategy is more aggressive when there is less time to maturity. In such case, the agent will place limit orders only when both the best ask queue size and the remaining inventory position are small. This is mainly because the execution risk of limit orders decreases as the time to maturity increases and the best ask queue size and the remaining inventory position decreases.
- Compared with placing displayed limit orders, placing non-displayed ones is more profitable when the best ask queue size is smaller. This is mainly because the execution risk of non-displayed limit orders decreases as the best ask queue size decreases.

Table 2.3: parameter settings.

Parameter	Description	Value
Market		
δ	tick size (¢)	1
\bar{d}	market depth cap (share)	2200
ρ	per share rebate for limit order execution (¢)	0.27
ϵ	per share fee for market order execution (¢)	0.27
Agent		
T	length of trading window (second)	100
\bar{e}_1	upper bound of limit order (share)	300
\bar{e}_2	upper bound of market order (share)	300
θ	relative queue position	0.5
γ	exponential utility parameter	1e-5
b	terminal penalty parameter	0.95
Localisation		
\bar{y}	upper bound of inventory (share)	1000
\underline{p}	lower bound of liquidity (cent)	3500
\bar{p}	upper bound of liquidity state	3501
U^b	upper bound of integration	10000
Discretisation		
δ_T	step size of time (second)	0.1
δ_Y	step size of inventory (share)	100
δ_Y	step size of liquidity	1/22
δ_v	step size when approximating integral	50

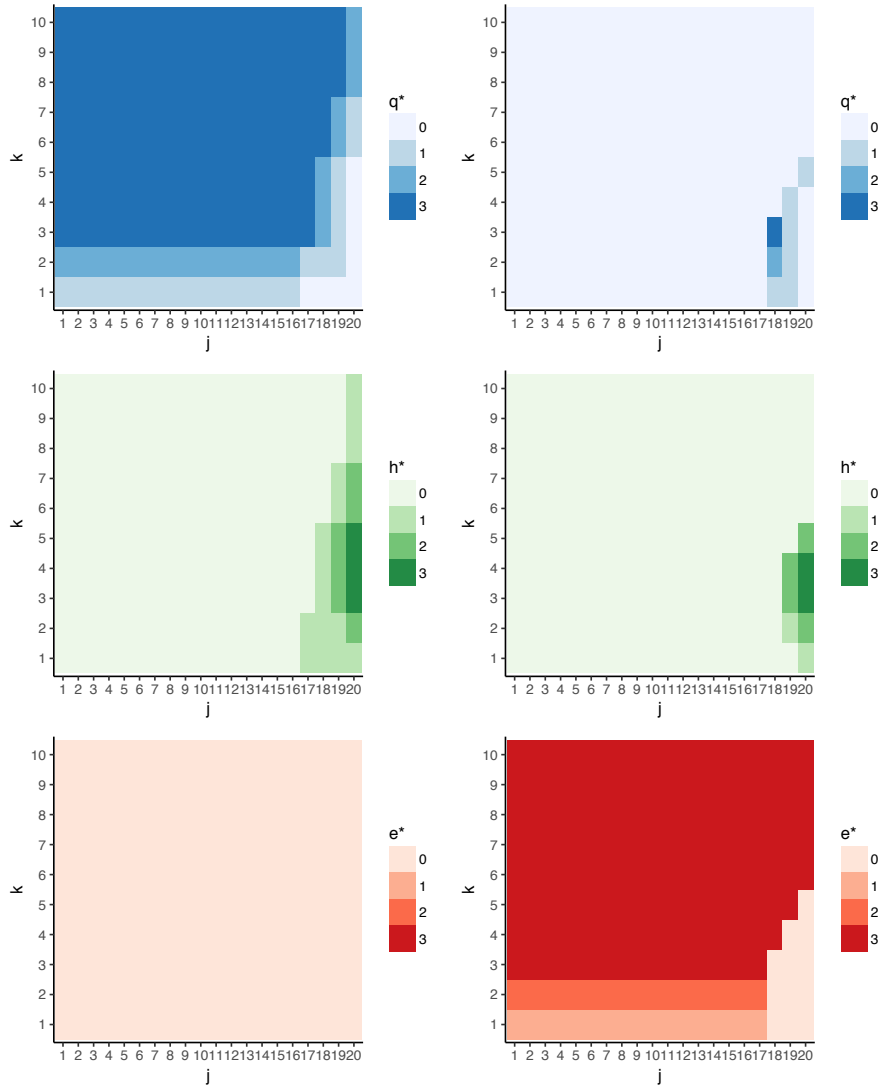


Figure 2.9: optimal strategy (q^*, h^*, e^*) , namely, the optimal size of displayed limit order, non-displayed limit order and market order, as a function $QS(\cdot, \cdot, \cdot)$ of the best ask queue size (x-axis: $j = 1, 2, \dots, 20$, corresponding to 2100, 2000, \dots , 200 shares), the remaining inventory position (y-axis: $k = 1, 2, \dots, 10$, corresponding to 100, 200, \dots , 1000 shares) and the time to maturity (panels on the left (resp. right): $i = 500$ (resp. 50), corresponding to 500 (resp. 50) seconds.)

*“Rule No. 1: Never lose money.
Rule No. 2: Never forget rule No.1.”*

— Warren Buffett

3

OPTIMAL LIQUIDATION STRATEGY - FRAMEWORK II

3.1 INTRODUCTION

In this chapter, we consider an agent (or her agency algorithm) who wants to sell an order of a pre-specified (small) quantity over a fixed (short) trading window in a LOB for a large-tick stock, where the price-time priority mechanism¹ is applied. Following [26, Section 2.1], information available to this agent contains historical order flows and depths at the best prices of this LOB (‘Level-I’ data). In particular, we are mostly interested in how different trading conditions (i.e. LOB state, inventory position, time to maturity) affect the agent’s trading decisions when liquidating the order. In order to achieve this, we first build up a ‘Level-I’ LOB model describing the trading environment whose dynamics are driven by the general market participants’ order flows and exogenous information. Realistic simplifying assumptions for this LOB follow those in [26, 28], including unit order size, constant one-tick

¹In this chapter, we are only interested in the displayed part of the LOB and do not consider the activities of the non-displayed limit orders.

spread, Poisson order flows, depletion of the best bid (resp. ask) queue moving the price one tick downward (resp. upward) and volumes at best prices after a price move being regarded as stationary variables drawn from a joint distribution. We further develop this model by allowing the Poisson rates of the order flows and the joint distribution determining the depths at the best prices after a price move to depend on the most recent price move direction. Under these assumptions, the evolution of this LOB can be modelled as a Markov renewal process as in [34], whose transition mechanism is intuitively described as a queueing race between the volumes at the best prices. We then assume the agent to be risk-neutral, trying to maximise her expected terminal wealth by selling a fixed-amount of order within a fixed finite time horizon in this LOB. In order to model the price-time priority rule and capture the execution of the agent's limit orders, we assume that the agent is slow and only reacts immediately after the price moves using both limit and market orders: at each price-change time, the agent can chose to post a limit order at the best ask price with the least time priority and/or submit a market order that never consumes up the entire volumes at the best bid price. Through combining the assumptions for the LOB and the liquidation strategy, the agent's trading process is then formulated by a (stationary) semi-Markov decision process within a finite horizon [50], among a certain class of horizon-related Markov deterministic policies. In general, at each price-change time, the optimal policy is a deterministic function which tells the agent the size of the market and limit order to trade based on the current LOB state (i.e. price move direction, depths at the best prices), the agent's inventory position and time to maturity in order to achieve terminal wealth maximisation.

This chapter is organised as follows. In Section 3.2, we set the basic assumptions for the LOB model, illustrate the evolutionary dynamics of a 'Level-I' LOB and define the objective together with the admissible trading strategy set for the agent. In Section 3.3, a semi-Markov decision process with a horizon-related Markov deterministic policy is introduced to model the agent's trading process and an optimal policy is defined. In Section 3.4, we provide an expression for the semi-Markov kernel, which works as the

transition mechanism of the semi-Markov decision process. Existence of a stationary optimal policy is proved in Section 3.5, and empirical studies show our numerical results in Section 3.6.

3.2 LOB AND TRADING STRATEGY

3.2.1 ‘LEVEL-I’ LOB MODEL

We consider a limit order book characterised by two resolution parameters as in [39, Section 2.1]: the tick size $\delta > 0$ represents the smallest interval (assumed constant) between price levels, and the lot size, $\sigma > 0$, specifies the smallest amount of the asset that can be traded. All buy and sell orders thus must arrive at a price $k_1\delta$ and with a size $k_2\sigma$, for some $k_1, k_2 \in \mathbb{N}^+$. Throughout this chapter we shall work with the following modelling assumptions for the LOB:

Assumption 3.1 (Order book settings).

- (a) orders from general market participants are of lot size σ ;
- (b) the spread of the LOB is equal to the tick size δ .

The LOB model is formulated based on a ‘Level-I’ data, that is, the order flows and depths at the best bid and ask prices. As illustrated in [26, Section 2.1], this reduced-form modelling approach is motivated by the empirical findings showing that large amounts of order flows occur at the best price levels for large-tick stocks [35], the imbalance between the order flows at the best prices is shown to be a good predictor of the order book dynamics [18, 25], together with the fact that data at the best prices are more obtainable than the ‘Level-II’ market data. In the following, we impose the assumption for the evolution of the LOB:

Assumption 3.2 (Evolution of the LOB).

- (a) whenever the depths at the best bid (resp. ask) price are depleted, both the best bid and ask prices decrease (resp. increase) by one tick;

- (b) immediately after each price increase (resp. decrease), volumes at the best price levels are treated as random variables with joint distribution f_{+1} (resp. f_{-1}) : $(\mathbb{N}^+)^2 \rightarrow [0, 1]$; for any $v^b, v^a \in \mathbb{N}^+$, $f_{+1}(v^b, v^a)$ (resp. $f_{-1}(v^b, v^a)$) represents the probability that the best bid and ask queue contain v^b and v^a unit limit orders (of actual size $v^b\sigma$ and $v^a\sigma$), right after a price increase (resp. decrease).

Remark 3.3. Assumption 3.2(a) presumes that the LOB contains no empty level near the mid price so that price changes are restricted to one tick. Assumption 3.2(b) presumes that price changes are entirely due to exogenous information, in which case market participants swiftly readjust their order flows at the new best prices, as if a new state of the LOB is drawn from an invariant distribution [49]. In other words, we rule out the possibility that depletion of the best bid (resp. ask) queue is followed by the insertion of a buy (resp. sell) limit order inside the spread, keeping the best bid and ask prices unchanged. See Section 3.6.1 for some related empirical analysis.

Order flows from the general market participants are modelled according to the ‘zero-intelligence’ approach. See [26, 28, 75] for related literature. Generally speaking, the ‘zero-intelligence’ approach introduces some specific stochastic processes, with rate parameters depending on variables such as the LOB state, to describe the aggregated order flows, making the assumption that general market participants blindly follow a set of rules without strategic considerations [39, Section 3.1].

Assumption 3.4 (Poisson order flows).

Order book events (i.e. market orders, limit orders and cancellations) from the general market participants occur according to independent Poisson processes, with parameters depending on the most recent price move direction. To be more specific, taking order flows at the best ask price for example, during any period between a price increase (resp. decrease) and the next price change, the following mutually independent events happen:

- (a) buy market orders arrive at independent, exponential times with rate $\mu_{+1}^a > 0$ (resp. $\mu_{-1}^a > 0$);

- (b) sell limit orders arrive at independent, exponential times with rate $\kappa_{+1}^a > 0$ (resp. $\kappa_{-1}^a > 0$);
- (c) cancellations of limit orders occur at independent, exponential times with rate $\theta_{+1}^a > 0$ (resp. $\theta_{-1}^a > 0$) multiplied by the amount (in unit size) of the outstanding sell limit orders.

Furthermore, we assume an analogous framework for the order flows at the best bid price, with parameters $\mu_{+1}^b, \mu_{-1}^b, \kappa_{+1}^b, \kappa_{-1}^b, \theta_{+1}^b, \theta_{-1}^b > 0$.

Remark 3.5.

- Despite the fact that the ‘zero-intelligence’ model is not exactly compatible with empirical observations [82], it still retains the major statistical features of LOBs while remaining computationally manageable [75]. Under the ‘zero-intelligence’ hypothesis, the agent can easily characterise the dynamical properties of the LOB from historical data without assuming behavioural assumptions for other market participants or resorting to auxiliary assumptions to quantify unobservable parameters.
- Assumption 3.4(c) means that if there are v limit orders at the best ask (resp. bid) price, each of which can be cancelled at an exponential time with rate θ^a (resp. θ^b) independently, and the overall cancellation rate is then $\theta^a v$ (resp. $\theta^b v$). Here, this linear cancellation rate assumption, as proposed in [28], is made for modelling convenience, but it is virtually in contradiction with empirical data. For example, Huang, Lehalle and Rosenbaum [49] find that the cancellation rate at the best prices is an increasing concave function for small best queue sizes, and becomes flat or even slightly decreasing for large best queue sizes. Such observation is interpreted by the fact that the priority value increases as the queue size increases and orders with higher priority value are less likely to be cancelled.

3.2.2 OBJECTIVE AND ADMISSIBLE TRADING STRATEGIES

In the LOB model introduced in Section 3.2.1, we assume that the agent is risk-neutral and her goal is to maximise the expected wealth obtained through selling an order of $\chi \in \mathbb{N}^+$ unit size ($\chi\sigma$ actual size) within the trading horizon $\mathbb{T} := [0, T]$, where $T > 0$ is a fixed finite terminal time. The following assumption describes the set of admissible trading strategies:

Assumption 3.6 (Admissible trading strategies).

- (a) the agent can only take actions immediately after a price change; let τ_n denote her n -th decision epoch, namely the time of the n -th price change; $\tau_0 = 0$ and the last decision epoch before or at maturity is $\tau_{\mathbf{n}}$, where $\mathbf{n} := \sup\{n \in \mathbb{N} : \tau_n \leq T\}$;
- (b) at maturity T , the agent is required to sell all the unexecuted stocks through a market order;
- (c) at each decision epoch τ_n , the agent observes the bid and ask queues, with volumes of v^b and v^a unit size; she can then post a sell limit order of l unit size at the best ask price and submit a sell market order of m unit size at the best bid price; we assume that the best bid queue is never depleted by the agent, and that the agent is slow, meaning that her limit order (of l unit size) has less time priority upon submission than the limit orders from other market participants (of v^a unit size);
- (d) the agent follows a ‘no cancellation’ rule: she will not cancel her limit order unless the price goes down;
- (e) short selling is not allowed.

Remark 3.7.

- Restricting the agent’s trading actions at price changes (Assumption 3.6(a)) might sound relatively strong, but is necessary to capture the time-priority rule and the executions of the agent’s limit orders.

- The ‘no cancellation’ rule (Assumption 3.6(d)) is introduced mainly for modelling convenience, and it can be interpreted as the agent applying a strategy with limit orders continuously pegged to the best ask price after being placed. For literature that study optimal liquidation strategy considering both order placement and cancellation, See [32] for example.

3.3 TRADING PROCESS MODELLED BY SEMI-MARKOV DECISION PROCESSES

A semi-Markov decision model [78, Chapter 7] is a dynamic system whose states are observed at random epochs, each of when an action is taken and a payoff incurs (either as a lump sum at that epoch or at a rate continuously until the next epoch) as a result of the action. It satisfies the following two Markovian properties:

- (M1) given the current state and the action at a given epoch, the time until the next epoch and the next state only depend on the current state and action;
- (M2) the payoff incurred at any epoch depends only on the state and the action at that epoch.

The semi-Markov decision model well describes the agent’s liquidation problem within our stylised LOB: the LOB with the agent’s participation is a dynamic system, and the agent’s selling action at each decision epoch may lead to a payoff. Indeed, Assumption 3.6(a) enables us to track the state of this system merely at the decision epochs, and Assumptions 3.2, 3.4 and 3.6(c) ensure that the transition mechanism of the system is stationary and satisfies (M1)-(M2). Moreover, according to Assumption 3.10, each payoff from the agent’s matched limit order is allocated to the nearest incoming decision epoch in order to make the payoff as a lump sum. In Section 3.3.1, we define a (stationary) semi-Markov decision model with lump-sum payoffs for the agent’s liquidation process. In Section 3.3.2, we define a horizon-related

Markov deterministic policy and illustrate the evolution of the semi-Markov decision process. In Section 3.3.3, we give the definition of the expected reward function, the value function and the optimal policy for the agent's liquidation problem.

3.3.1 SEMI-MARKOV DECISION MODEL

The semi-Markov decision model with lump-sum payoffs and the finite-horizon constraint is defined as a six-tuple $\{\mathcal{E}, (\mathcal{A}(e))_{e \in \mathcal{E}}, Q(\cdot, \cdot), P(\cdot | \cdot), r(\cdot, \cdot), w(\cdot, \cdot)\}$, where each element is defined below.

STATE SPACE

Fix $N \in \mathbb{N}^+$ large enough. The state space $\mathcal{E} := \{-1, +1\} \times \{1, \dots, N\}^3 \times \{0, \dots, N\}^2$ is the set of all pre-decision conditions of the system (i.e. the LOB with the agent's participation) observed at each decision epoch. Specifically, the system being in state $e := (j, v^b, v^a, p, z, y) \in \mathcal{E}$ means that:

- the ask/bid price change is equal to j tick;
- the best bid (resp. ask) queue contains v^b (resp. v^a) unit orders;
- the ask price² is equal to $p\delta$;
- the executed part of the limit order posted by the agent at the previous decision epoch is of z unit size;
- the agent's remaining inventory position is of y unit size.

ACTION SPACE

The action space $\mathcal{A} := \{0, \dots, \bar{m}\} \times \{0, \dots, \bar{l}\}$, with $\bar{m}, \bar{l} \in \mathbb{N}^+$, represents the set of trading strategies, that is, the amount (in unit size) of the market

²The stylised LOB model does not implement a positive restriction on the stock price. But we assume that the stock price is far above zero at inception and the liquidation horizon \mathbb{T} is short, so that the stock price will never become negative.

and limit order that the agent chooses to submit and post at the best bid and ask price respectively. The constant \bar{m} (resp. \bar{l}) represents the maximum amount (in unit size) of a single market (resp. limit) order that the agent is allowed to trade. From Assumption 3.6(c)(e), the agent's admissible action space in state $e \in \mathcal{E}$ is defined by

$$\mathcal{A}(e) := \{(m, l) \in \mathcal{A} : m < v^b, m + l \leq y\}, \quad (3.1)$$

so that the agent will never consume up the entire best bid queue nor short sell. The set of all feasible state-action pairs is denoted by $\mathcal{K} := \{(e, \alpha) | e \in \mathcal{E}, \alpha \in \mathcal{A}(e)\}$.

SEMI-MARKOV KERNEL

Before introducing our next concept, recall the following definition.

Definition 3.8 (sub-/semi-Markov kernel). Let $(\Omega_1, \mathcal{F}_1)$ and $(\Omega_2, \mathcal{F}_2)$ be real measurable spaces. A map $p(\cdot|\cdot) : \mathcal{F}_2 \times \Omega_1 \rightarrow [0, 1]$ is called a sub-Markov kernel on Ω_2 given Ω_1 if:

- for any $\omega_1 \in \Omega_1$, $p(\cdot|\omega_1)$ is a measure on $(\Omega_2, \mathcal{F}_2)$ with $p(\Omega_2|\omega_1) \leq 1$;
- for any $F_2 \in \mathcal{F}_2$, $p(F_2|\cdot)$ is a Borel measurable function.

In particular, if $p(\Omega_2|\omega_1) = 1$ for all $\omega_1 \in \Omega_1$, then $p(\cdot|\cdot)$ is a Markov kernel on Ω_2 given Ω_1 . Furthermore, a map $q(\cdot, \cdot|\cdot) : \mathbb{R}_0^+ \times \mathcal{F}_2 \times \Omega_1 \rightarrow [0, 1]$ is a semi-Markov kernel on $\mathbb{R}_0^+ \times \Omega_2$ given Ω_1 if:

- for $(F_2, \omega_1) \in \mathcal{F}_2 \times \Omega_1$, $q(\cdot, F_2|\omega_1)$ is non-decreasing, right-continuous and $q(0, F_2|\omega_1) = 0$;
- for $t \geq 0$, $q(t, \cdot|\cdot)$ is a sub-Markov kernel on Ω_2 given Ω_1 ;
- the limit $\lim_{t \uparrow \infty} q(t, \cdot|\cdot)$ is a Markov kernel on Ω_2 given Ω_1 .

In our model, let $Q(\cdot, \cdot|\cdot)$ be a semi-Markov kernel on $\mathbb{R}_0^+ \times \mathcal{E}$ given \mathcal{K} , determining the (stationary) transition mechanism of the semi-Markov decision

process: for any $t \geq 0$ and $\tilde{e} \in \mathcal{E}$, given the state-action pair $(e, \alpha) \in \mathcal{K}$ at some decision epoch, the quantity³ $Q(t, \tilde{e}|(e, \alpha))$ represents the (joint) probability that the time until the next decision epoch is less than or equal to t and the next system state is \tilde{e} . Detailed computations are given in Section 3.4.

TERMINAL KERNEL

The terminal kernel $P(\cdot|\cdot)$ is a sub-Markov kernel on \mathbb{N} given $\mathcal{K} \times \mathbb{T}_-$, where we introduce $\mathbb{T}_- := \mathbb{R}^- \cup \mathbb{T}$. Specifically, $P(\cdot|\cdot)$ describes the execution dynamics between the last decision epoch and the maturity: for any $\mathfrak{z} \in \mathbb{N}$, given the state-action pair $(e, \alpha) \in \mathcal{K}$ and the time to maturity $\lambda \in \mathbb{T}_-$ at some decision epoch⁴, the quantity⁵ $P(\mathfrak{z}|(e, \alpha), \lambda)$ represents the (joint) probability that the time until the next decision epoch is strictly larger than λ and the executed part of the limit order up to the maturity is of \mathfrak{z} unit size. Detailed computations are given in Section 3.4.

Remark 3.9. According to our modelling framework, the terminal kernel satisfies the following properties:

- $P(0|(e, \alpha), \lambda) = 1$ when $\lambda \leq 0$;
- $\sum_{\mathfrak{z} \geq 0} P(\mathfrak{z}|(e, \alpha), \lambda) = 1 - Q(\lambda, \mathcal{E}|(e, \alpha))$ when $\lambda > 0$;
- $P(\mathfrak{z}|(e, \alpha), \lambda) = 0$ when $\mathfrak{z} > l$;

for any $(e, \alpha) \in \mathcal{K}$.

PERIODICAL REWARD FUNCTION

The periodical reward function $r : \mathcal{K} \rightarrow \mathbb{R}_0^+$ is defined as

$$r(e, \alpha) := \rho [m(p-1) + z(p-j)], \quad (3.2)$$

³By abuse of language, we write $Q(t, \{\tilde{e}\}|(e, \alpha))$ as $Q(t, \tilde{e}|(e, \alpha))$.

⁴A decision epoch with time to maturity $\lambda < 0$ means that it happens a period of time $|\lambda|$ after the maturity.

⁵By abuse of language, we write $P(\{\mathfrak{z}\}|((e, \alpha), \lambda))$ as $P(\mathfrak{z}|(e, \alpha), \lambda)$.

for all $(e, \alpha) \in \mathcal{K}$, where $\rho := \delta\sigma$, and represents the lump-sum payoff associated with a decision epoch given the state-action pair (e, α) . Specifically, the definition (3.2) is given based on the following assumption that assigns the payoff from the matched part of the agent's limit order to the nearest incoming decision epoch.

Assumption 3.10 (Periodic reward function).

For $n \in \mathbb{N}^+$, the payoff from any limit order that is executed within the interval $[\tau_{n-1}, \tau_n)$ is allocated at τ_n .

Suppose that the system is in state $e \in \mathcal{E}$ and the agent takes action $\alpha \in \mathcal{A}(e)$ at some decision epoch. She then earns an immediate payoff worth $m(p-1)\rho$ from submitting the market order of m unit size at the best bid price $(p-1)\delta$. On top of that, the matched limit order of z unit size at the previous best ask price $(p-j)\delta$ entails a payoff worth $z(p-j)\rho$, which is allocated at the current decision epoch according to Assumption 3.10.

TERMINAL REWARD FUNCTION

The terminal reward function $w : \mathcal{K} \times \mathbb{N} \rightarrow \mathbb{R}_0^+$ is defined by

$$w(e, \alpha, \mathfrak{z}) := \rho [(p-1)(y-m) + \mathfrak{z}] - g(y-m-\mathfrak{z}), \quad (3.3)$$

for all $(e, \alpha) \in \mathcal{K}$ and $\mathfrak{z} \in \mathbb{N}$, where the market impact function $g : \mathbb{N} \rightarrow \mathbb{R}_0^+$ is in the form of

$$g(x) := \rho \frac{x}{\bar{v}}, \quad (3.4)$$

for a constant $\bar{v} \in \mathbb{N}^+$. For any $(e, \alpha) \in \mathcal{K}$ and $\mathfrak{z} \in \mathbb{N}$, the quantity $w(e, \alpha, \mathfrak{z})$ represents the lump-sum payoff associated with the maturity T , given the state-action pair (e, α) at the last decision epoch, and the matched part of the agent's limit order between the last decision epoch and the maturity being of \mathfrak{z} unit size. Particularly, the identity (3.3) is given based on the following assumption:

Assumption 3.11 (Terminal reward function).

- (a) the payoff from the matched limit order obtained within the interval $[\tau_n, T)$ is allocated at T ;
- (b) when depicting the market impact brought by the market order at maturity, we assume that the impact is linear with \bar{v} representing the average depth (in unit size) on the bid side of the LOB;
- (c) the unexecuted shares at maturity cannot sweep all the liquidity on the bid side of the LOB, so that the terminal reward function is \mathbb{R}_0^+ -valued.

Assumption 3.11(b) yields the market impact function g in Formula (3.4). Furthermore, based on Assumption 3.11(a)(b), the terminal reward $w(e, \alpha, \mathfrak{z})$ consists of the payoff from the matched limit order (of amount $\rho p \mathfrak{z}$) and the market order at maturity (of amount $\rho(p-1)(y-m-\mathfrak{z})$), deducted by the corresponding market impact (of amount $g(y-m-\mathfrak{z})$).

3.3.2 DYNAMICS OF THE FINITE-HORIZON SEMI-MARKOV DECISION PROCESS

Assume that the agent applies a horizon-related Markov deterministic policy defined below, specifying a decision rule for her action at each epoch based on the current state and time to maturity.

Definition 3.12. A decision rule is a measurable function

$$\phi : \mathcal{E} \times \mathbb{T}_- \ni (e, \lambda) \mapsto \alpha \in \mathcal{A}(e),$$

such that $\phi(e, \lambda) = (0, 0)$ for any $(e, \lambda) \in \mathcal{E} \times \mathbb{R}^-$. Let Φ represent the set of decision rules. A horizon-related Markov deterministic policy is a sequence of decision rules

$$\pi := \{\phi_0, \phi_1, \phi_2, \dots\}, \tag{3.5}$$

with $\phi_n \in \Phi$ for any $n \in \mathbb{N}$. We denote by Π the set of horizon-related Markov deterministic policies. A policy $\pi \in \Pi$ is said to be stationary if there exists $\phi \in \Phi$ such that $\phi_n = \phi$ for any $n \in \mathbb{N}$ and we write $\pi = \{\phi, \phi, \dots\} := \pi^\phi$. We denote Π^S the set of stationary horizon-related Markov deterministic policies.

Remark 3.13. At the n -th decision epoch with system state e_n and time to maturity $\lambda_n := T - \tau_n$, an action $a_n = \phi_n(e_n, \lambda_n)$ is given by the decision rule ϕ_n when the policy $\pi \in \Pi$ in (3.5) is applied. In particular, the agent stops trading at any decision epoch τ_n with $n > \mathbf{n}$ (namely $\lambda_n < 0$) as $\alpha_n = (0, 0)$ by Definition 3.12, fulfilling Assumption 3.6(b).

Table 3.1 summarises the evolution of the semi-Markov decision model when implementing a policy $\pi \in \Pi$. Suppose that the system is in state e_0 at inception τ_0 , and the agent has a planned trading horizon λ_0 . According to the policy π , she chooses the action $\alpha_0 = \phi_0(e_0, \lambda_0)$ at the initial decision epoch. It then takes a period of time t_1 to reach the next decision epoch $\tau_1 = \tau_0 + t_1$, at which point the system state changes to e_1 and the time to maturity for the agent becomes $\lambda_1 = \lambda_0 - t_1$. She then chooses the action $\alpha_1 = \phi_1(e_1, \lambda_1)$, and so on. At the n -th decision epoch, a periodic payoff of amount $r(e_n, \alpha_n)$ incurs. At maturity T , a terminal payoff $w(e_n, \alpha_n, \mathfrak{z})$ is obtained. In particular, the agent takes no action after T according to Remark 3.13, and correspondingly no payoff is paid.

Table 3.1: evolution of the semi-Markov decision process under a horizon-related Markov deterministic policy $\pi \in \Pi$.

Index	Time	State	Time to Maturity	Action	Payoff
Initial	τ_0	e_0	$\lambda_0 \geq 0$	$\alpha_0 = \phi_0(e_0, \lambda_0)$	$r(e_0, \alpha_0)$
1 st	$\tau_1 = \tau_0 + t_1$	e_1	$\lambda_1 = \lambda_0 - t_1 \geq 0$	$\alpha_1 = \phi_1(e_1, \lambda_1)$	$r(e_1, \alpha_1)$
2 nd	$\tau_2 = \tau_1 + t_2$	e_2	$\lambda_2 = \lambda_1 - t_2 \geq 0$	$\alpha_2 = \phi_2(e_2, \lambda_2)$	$r(e_2, \alpha_2)$
\vdots	\vdots	\vdots	\vdots	\vdots	\vdots
$(\mathbf{n} - 1)$ -th	$\tau_{\mathbf{n}-1} = \tau_{\mathbf{n}-2} + t_{\mathbf{n}-1}$	$e_{\mathbf{n}-1}$	$\lambda_{\mathbf{n}-1} = \lambda_{\mathbf{n}-2} - t_{\mathbf{n}-1} \geq 0$	$\alpha_{\mathbf{n}-1} = \phi_{\mathbf{n}-1}(e_{\mathbf{n}-1}, \lambda_{\mathbf{n}-1})$	$r(e_{\mathbf{n}-1}, \alpha_{\mathbf{n}-1})$
\mathbf{n} -th	$\tau_{\mathbf{n}} = \tau_{\mathbf{n}-1} + t_{\mathbf{n}}$	$e_{\mathbf{n}}$	$\lambda_{\mathbf{n}} = \lambda_{\mathbf{n}-1} - t_{\mathbf{n}} \geq 0$	$\alpha_{\mathbf{n}} = \phi_{\mathbf{n}}(e_{\mathbf{n}}, \lambda_{\mathbf{n}})$	$r(e_{\mathbf{n}}, \alpha_{\mathbf{n}})$
	Terminal T				$w(e_{\mathbf{n}}, \alpha_{\mathbf{n}}, \mathfrak{z})$
$(\mathbf{n} + 1)$ -th	$\tau_{\mathbf{n}+1} = \tau_{\mathbf{n}} + t_{\mathbf{n}+1}$	$e_{\mathbf{n}+1}$	$\lambda_{\mathbf{n}+1} = \lambda_{\mathbf{n}} - t_{\mathbf{n}+1} < 0$	$\alpha_{\mathbf{n}+1} = (0, 0)$	0
\vdots	\vdots	\vdots	\vdots	\vdots	\vdots

In the following, we construct the semi-Markov decision process in a probability space based on the Ionescu Tulcea's Theorem.

Definition 3.14. Let (Ω, \mathcal{F}) be a measurable space consisting of the sample space Ω , defined by

$$\Omega := \left\{ \mathbf{n} \in \mathbb{N}, \mathfrak{z} \in \mathbb{N}, \left(\{t_n, e_n, \lambda_n, \alpha_n\} \in \mathbb{R}_0^+ \times \mathcal{E} \times \mathbb{T}_- \times \mathcal{A}(e_n) \right)_{n \in \mathbb{N}} \right\},$$

and the corresponding Borel σ -algebra \mathcal{F} . Define the random variables \mathfrak{N} , \mathfrak{Z} , X_n , E_n , Λ_n , A_n on (Ω, \mathcal{F}) as:

$$\begin{aligned} \mathfrak{N}(\omega) &= \mathfrak{n}, & \mathfrak{Z}(\omega) &= \mathfrak{z}, \\ X_n(\omega) &= t_n, & E_n(\omega) &:= (J_n, V_n^b, V_n^a, P_n, Z_n, Y_n)(\omega) = e_n, \\ \Lambda_n(\omega) &= \lambda_n, & A_n(\omega) &:= (M_n, L_n)(\omega) = \alpha_n, \end{aligned}$$

for any $\omega \in \Omega$ and $n \in \mathbb{N}$, where

- X_n is the time between the $(n - 1)$ -th and the n -th decision epoch ($X_0 = 0$ almost surely);
- E_n, Λ_n, A_n represent the system state, time to maturity and agent's action at the n -th decision epoch;
- \mathfrak{N} is the index of the last decision epoch;
- \mathfrak{Z} is the amount (in unit size) of the agent's limit order executed between the \mathfrak{N} -th decision epoch and the maturity.

Remark 3.15. Based on this modelling framework, the following properties hold almost surely for $n \in \mathbb{N}$

- $\Lambda_{n+1} = \Lambda_n - X_{n+1}$: evolution of the time to maturity;
- $P_{n+1} = P_n + J_{n+1}$: evolution of the ask price (in tick size);
- $Y_{n+1} = Y_n - M_n - Z_{n+1}$: evolution of the inventory position (in unit size);
- $Z_{n+1} \leq L_n$: the amount of the matched limit order cannot exceed that of the limit order posted by the agent in each queueing race;
- $\mathfrak{N} = \sup\{n \in \mathbb{N} : \Lambda_n \geq 0\}$: index of the last decision epoch;
- $\mathfrak{Z} \leq Z_{\mathfrak{N}+1}$: the amount of the matched limit order between the last decision epoch and the maturity cannot exceed that of limit order executed when there is no finite-horizon restriction.

Theorem 3.16. [Ionescu Tulcea's Theorem [7, Section 2.7.2]] For any $(e, \lambda) \in \mathcal{E} \times \mathbb{T}$ and $\pi \in \Pi$, there exists a unique probability measure $\mathbb{P}_{(e, \lambda)}^\pi$ on (Ω, \mathcal{F}) such that, for any $t \geq 0$, $\tilde{e} \in \mathcal{E}$, $\alpha \in \mathcal{A}$, $\mathfrak{z} \in \mathbb{N}$ and $n \in \mathbb{N}$,

$$\begin{aligned} \mathbb{P}_{(e, \lambda)}^\pi(X_0 = 0, E_0 = e, \Lambda_0 = \lambda) &= 1, \\ \mathbb{P}_{(e, \lambda)}^\pi(A_n = \alpha | H_n = h_n) &= \mathbf{1}_{\{\phi_n(e_n, \lambda_n) = \alpha\}}, \\ \mathbb{P}_{(e, \lambda)}^\pi(X_{n+1} \leq t, E_{n+1} = \tilde{e} | H_n = h_n, A_n = \alpha_n) &= Q(t, \tilde{e} | (e_n, \alpha_n)), \\ \mathbb{P}_{(e, \lambda)}^\pi(X_{n+1} > \lambda_n, \mathfrak{Z} = \mathfrak{z} | H_n = h_n, A_n = \alpha_n) &= P(\mathfrak{z} | (e_n, \alpha_n), \lambda_n), \end{aligned}$$

where

$$H_n := \begin{cases} (\{X_0, E_0, \Lambda_0\}), & \text{if } n = 0, \\ (\{X_i, E_i, \Lambda_i, A_i\}_{i=0, \dots, n-1}, \{X_n, E_n, \Lambda_n\}), & \text{if } n \in \mathbb{N}^+, \end{cases}$$

is the sequence of random variables describing the history up to the n -th decision epoch. In particular, realisations of the random variables (or sequences of random variables) are denoted by the corresponding lower case letters.

3.3.3 VALUE FUNCTION AND OPTIMAL POLICY

Consider an agent with the objective and trading strategies as described in Section 3.2.2, introduce the following definition.

Definition 3.17. Define the finite-horizon expected reward function under a policy $\pi \in \Pi$ by

$$V^\pi(e, \lambda) := \mathbb{E}_{(e, \lambda)}^\pi \left(\sum_{n=0}^{\mathfrak{N}} r(E_n, A_n) + w(E_{\mathfrak{N}}, A_{\mathfrak{N}}, \mathfrak{Z}) \right), \quad \text{for any } (e, \lambda) \in \mathcal{E} \times \mathbb{T}, \quad (3.6)$$

as well as the value function

$$V^*(e, \lambda) := \sup \{V^\pi(e, \lambda), \pi \in \Pi\}. \quad (3.7)$$

A policy $\pi^* \in \Pi$ is called \mathbb{T} -optimal if the equality

$$V^{\pi^*}(e, \lambda) = V^*(e, \lambda) \quad (3.8)$$

holds for all $(e, \lambda) \in \mathcal{E} \times \mathbb{T}$.

Remark 3.18. For any $(e, \lambda) \in \mathcal{E} \times \mathbb{T}$, we can rewrite the quantity $V^\pi(e, \lambda)$ in (3.6) as

$$\begin{aligned} V^\pi(e, \lambda) &= \mathbb{E}_{(e, \lambda)}^\pi \left(\sum_{n=0}^{\infty} (r(E_n, A_n) \mathbb{1}_{\{\mathfrak{N} \geq n\}}) + w(E_n, A_n, \mathfrak{Z}) \mathbb{1}_{\{\mathfrak{N} = n\}} \right) \\ &= \mathbb{E}_{(e, \lambda)}^\pi \left(\sum_{n=0}^{\infty} (r(E_n, A_n) \mathbb{1}_{\{\Lambda_n \geq 0\}} + w(E_n, A_n, \mathfrak{Z}) \mathbb{1}_{\{0 \leq \Lambda_n < X_{n+1}\}}) \right) \\ &= \sum_{n=0}^{\infty} \mathbb{E}_{(e, \lambda)}^\pi \left(r(E_n, A_n) \mathbb{1}_{\{\Lambda_n \geq 0\}} + w(E_n, A_n, \mathfrak{Z}) \mathbb{1}_{\{0 \leq \Lambda_n < X_{n+1}\}} \right), \end{aligned}$$

where the second equality follows by writing

$$\begin{aligned} \{\mathfrak{N} \geq n\} &= \{\Lambda_0 \geq 0, \dots, \Lambda_n \geq 0\} = \{\Lambda_n \geq 0\}, \text{ and} \\ \{\mathfrak{N} = n\} &= \{\Lambda_0 \geq 0, \dots, \Lambda_n \geq 0, \Lambda_{n+1} < 0\} = \{\Lambda_n \geq 0, \Lambda_{n+1} < 0\} = \{0 \leq \Lambda_n < X_{n+1}\}, \end{aligned}$$

since the sequence $\{\Lambda_n\}_{n \in \mathbb{N}}$ is non-increasing, and the third equality is due to the non-negativity of the periodic/terminal reward function and the monotone convergence theorem.

3.4 SEMI-MARKOV KERNEL

We now provide the expressions for the semi-Markov kernel $Q(\cdot, \cdot|\cdot)$ and the terminal kernel $P(\cdot|\cdot)$ defined in Section 3.3.1 using the language of queueing theory. We first (Section 3.4.1) model the dynamics of the best queues with the agent's participation as generalised birth-death processes, and derive the closed-form expressions for the semi-Markov kernel and the terminal kernel in all possible scenarios in terms of the distributions of the first-passage time of the generalised birth-death processes to zero. We then (Section 3.4.2) compute these distributions by using Laplace method.

3.4.1 CLOSED-FORM EXPRESSIONS

For notational convenience, we shall fix an element (\mathbf{e}, λ) in $\mathcal{E} \times \mathbb{T}$ together with a Markov deterministic policy $\pi \in \Pi$ and denote $\mathbb{P}_{(\mathbf{e}, \lambda)}^\pi$ by \mathbb{P} throughout this section.

SEMI-MARKOV KERNEL

According to Theorem 3.16 and the Markovian property (M1), we can express the semi-Markov kernel as a (stationary) distribution of the duration and outcome of a queueing race given its initial condition and the agent's action:

$$Q(t, \tilde{e} | (e, \alpha)) = \mathbb{P}(X_{n+1} \leq t, E_{n+1} = \tilde{e} | E_n = e, A_n = \alpha), \quad (3.9)$$

for any $t \geq 0, \tilde{e} \in \mathcal{E}, (e, \alpha) \in \mathcal{K}, n \in \mathbb{N}$. In order to simplify further calculations, we now factorise the conditional probability in (3.9).

Proposition 3.19. *For any $\tilde{e} := (\tilde{j}, \tilde{v}^b, \tilde{v}^a, \tilde{p}, \tilde{z}, \tilde{y}) \in \mathcal{E}, e := (j, v^b, v^a, p, z, y), \alpha := (m, l),$ s.t. $(e, \alpha) \in \mathcal{K},$ we have*

$$Q(t, \tilde{e} | (e, \alpha)) = \mathcal{Q}_{j, v, \alpha}(t, \tilde{j}, \tilde{z}) f_{\tilde{j}}(\tilde{v}^b, \tilde{v}^a) \mathbf{1}_{\{\tilde{p} = p + \tilde{j}\}} \mathbf{1}_{\{\tilde{y} = y - m - \tilde{z}\}}, \quad (3.10)$$

for all $t \geq 0,$ where⁶ for any $n \in \mathbb{N},$

$$\begin{aligned} & \mathcal{Q}_{j, v, \alpha}(t, \tilde{j}, \tilde{z}) \\ & := \mathbb{P}\left(X_{n+1} \leq t, J_{n+1} = \tilde{j}, Z_{n+1} = \tilde{z} \mid J_n = j, (V_n^b, V_n^a) = (v^b, v^a), A_n = \alpha\right). \end{aligned}$$

⁶ \mathbb{P} (short for $\mathbb{P}_{(\mathbf{e}, \lambda)}^\pi$ in this section) is the probability measure introduced in Theorem 3.16, and we use the short-hand notation $\mathbb{P}\left(X_{n+1} \leq t, J_{n+1} = \tilde{j}, Z_{n+1} = \tilde{z}, \dots\right) = \mathbb{P}\left(X_{n+1} \leq t, J_{n+1} = \tilde{j}, Z_{n+1} = \tilde{z}, V_{n+1}^b \in \mathbb{N}^+, V_{n+1}^a \in \mathbb{N}^+, P_{n+1} \in \mathbb{N}^+, Y_{n+1} \in \mathbb{N} \mid \dots\right)$

Proof. According to Assumption 3.2 and Remark 3.15, we can write

$$\begin{aligned}
Q(t, \tilde{e} | (e, \alpha)) &= \mathbb{P}(X_{n+1} \leq t, J_{n+1} = \tilde{j}, Z_{n+1} = \tilde{z} | E_n = e, A_n = \alpha) \\
&\times \mathbb{P}((V_{n+1}^b, V_{n+1}^a) = (\tilde{v}^b, \tilde{v}^a), P_{n+1} = \tilde{p}, Y_{n+1} = \tilde{y} | \\
&\quad X_{n+1} \leq t, J_{n+1} = \tilde{j}, Z_{n+1} = \tilde{z}, E_n = e, A_n = \alpha) \\
&= \mathcal{Q}_{j,v,\alpha}(t, \tilde{j}, \tilde{z}) \mathbb{P}((V_{n+1}^b, V_{n+1}^a) = (\tilde{v}^b, \tilde{v}^a) | J_{n+1} = \tilde{j}) \times \\
&\quad \mathbb{P}(P_{n+1} = \tilde{p} | J_{n+1} = \tilde{j}, P_n = p) \mathbb{P}(Y_{n+1} = \tilde{y} | Y_n = y, M_n = m, Z_{n+1} = \tilde{z}) \\
&= \mathcal{Q}_{j,v,\alpha}(t, \tilde{j}, \tilde{z}) f_{\tilde{j}}(\tilde{v}^b, \tilde{v}^a) \mathbb{1}_{\{\tilde{p}=p+\tilde{j}\}} \mathbb{1}_{\{\tilde{y}=y-m-\tilde{z}\}}.
\end{aligned}$$

□

Remark 3.20. The function \mathcal{Q} is a semi-Markov kernel on $\mathbb{R}_0^+ \times \mathcal{E}'$ given \mathcal{K}' , where

$$\begin{aligned}
\mathcal{E}' &:= \{-1, +1\} \times \{0, 1, \dots, N\}; \\
\mathcal{K}' &:= \{(j, v^b, v^a, \alpha) : j \in \{+1, -1\}, (v^b, v^a) \in \{1, \dots, N\}^2, \alpha \in \mathcal{A}, m < v^b\}.
\end{aligned}$$

Indeed, for any $(j, v^b, v^a, \alpha) \in \mathcal{K}'$, the probability $\mathcal{Q}_{j,v,\alpha}(t, \{+1, -1\}, \{0, \dots, l\})$ converges to 1 for large t , indicating the amount of the matched limit order cannot exceed that of the limit order posted by the agent.

According to Assumptions 3.2, 3.4 and 3.6, the semi-Markov kernel \mathcal{Q} describes the dynamical mechanism of a queueing race between the volumes sitting at the best bid and ask prices. Intuitively, fix $(j, v^b, v^a, \alpha) \in \mathcal{K}'$, and consider a queueing race starting with v^b and v^a units limit orders (from the general market participants) at the best bid and ask prices at a certain decision epoch. The agent subsequently submits a sell market order of m unit size, which decreases the best bid volume to $(v^b - m)$ unit size, and posts a sell limit order of l unit size, which has less time priority than the pre-existing v^a units limit orders at the best ask price. After the agent's action, mutually independent order book events happen at exponential times with the rates depending on the price move direction j and therefore change the volumes of the best bid and ask queues. The queueing race terminates whenever the volume of either the best bid or ask queue reaches zero, and we denote the result of a queueing race by $+1$ (resp. -1) if the best ask (resp.

bid) queue is depleted first. For $(t, \tilde{j}, \tilde{z}) \in \mathbb{R}_0^+ \times \mathcal{E}'$, the quantity $\mathcal{Q}_{j,v,\alpha}(t, \tilde{j}, \tilde{z})$ is the probability that the duration of the race is less than or equal to t , the result is \tilde{j} , and \tilde{z} unit size of the agent's limit order gets executed. In the following, we model the dynamics of the volumes at the best bid and ask prices as generalised birth-death processes, and therefore build a connection between the semi-Markov kernel and the queueing theory.

Before proceeding to the next definition, we introduce the following notations: for any continuous-time process $(L_s)_{s \geq 0}$, denote by τ_L its first passage time to the origin, and f_L (resp. F_L) the probability density function (resp. cumulative distribution function) of τ_L .

Definition 3.21. Let $(\overline{\Omega}, \overline{\mathcal{F}}, \overline{\mathbb{P}})$ be a new filtered probability space. For $v \in \mathbb{N}^+$, $l \in \mathbb{N}$ and $\kappa, \mu, \theta, \eta > 0$, define the following processes on this space:

- $(B[v, \kappa, \mu, \theta]_s)_{s \geq 0}$ is a birth and death process with state space \mathbb{N} and absorbing state 0, given the initial state v ; κ is the birth rate and $\mu + i\theta$ the death rate when in state $i \in \mathbb{N}^+$;
- $(C[v, l, \mu, \theta]_s)_{s \geq 0}$ is a pure death process with state space \mathbb{N} and absorbing state 0 given initial state $l + v$; the death rate equals to $\mu + \max(0, i - l)\theta$ when in state $i \in \mathbb{N}^+$;
- $(G[\kappa, \mu, \theta, \eta]_s)_{s \geq 0}$ is a process with state space \mathbb{N} given initial state 0. Strictly before time η , it is a birth and death process with birth rate κ and death rate $i\theta$ when in state $i \in \mathbb{N}$. After η , the birth and death rate of this process change to κ and $\mu + i\theta$ when in state $i \in \mathbb{N}^+$ and 0 becomes the absorbing state.
- $(A[v, l, \kappa, \mu, \theta]_s)_{s \geq 0}$ is a process with state space \mathbb{N}^2 defined by

$$A[v, l, \kappa, \mu, \theta]_s := (C[v, l, \mu, \theta]_s, G[\kappa, \mu, \theta, \tau_{C[v, l, \mu, \theta]}]_s), \quad \text{for } s \geq 0.$$

Lemma 3.22. [28, Lemma 3] Fix $(j, v^b, v^a, \alpha) \in \mathcal{K}'$. Suppose that, at the n -th decision epoch, the queueing race starts with v^b and v^a units limit orders at the best bid and ask prices after the price moves by j tick, and the agent takes an action $\alpha = (m, l)$. On $[\tau_n, \tau_{n+1})$, define the following processes:

- \tilde{B} : size of the orders sitting at the best bid price;
- \tilde{C} : size of the agent's limit order together with the orders with higher time priority at the best ask price;
- \tilde{G} : size of the orders with lower time priority than the agent's limit order at the best ask price.

Then there exist two independent processes $B[v^b - m, \kappa_j^b, \mu_j^b, \theta_j^b]$, $A[v^a, l, \kappa_j^a, \mu_j^a, \theta_j^a]$ such that

$$B[v^b - m, \kappa_j^b, \mu_j^b, \theta_j^b]_s = \tilde{B}_{s+\tau_n} \quad \text{and} \quad A[v^a, l, \kappa_j^a, \mu_j^a, \theta_j^a]_s = (\tilde{C}_{s+\tau_n}, \tilde{G}_{s+\tau_n}),$$

for all $s \in [0, \tau_{n+1} - \tau_n)$. According to Lemma 3.22, we provide an expression for \mathcal{Q} in the following, and defer its proof to Appendix C.1.

Proposition 3.23. Fix $(j, v^b, v^a, \alpha) \in \mathcal{K}'$, introduce the following short-hand notations:

$$\begin{aligned} B^b &:= B[v^b - m, \kappa_j^b, \mu_j^b, \theta_j^b], & B^a &:= B[v^a, \kappa_j^a, \mu_j^a, \theta_j^a], \\ A^l &:= A[v^a, l, \kappa_j^a, \mu_j^a, \theta_j^a], & C^l &:= C[v^a, l, \mu_j^a, \theta_j^a], \end{aligned}$$

as well as the scenarios:

S1	S2±	S3	S4	S5	S6
$l \geq 1$	$l = 0$	$l \geq 1$	$l = 1$	$l > 1$	$l > 1$
$\tilde{j} = +1$	$\tilde{j} = \pm 1$	$\tilde{j} = -1$	$\tilde{j} = -1$	$\tilde{j} = -1$	$\tilde{j} = -1$
		$\tilde{z} = 0$	$\tilde{z} = 1$	$\tilde{z} \in \{1, \dots, l-1\}$	$\tilde{z} = l$

Then the following holds for $(t, \tilde{j}, \tilde{z}) \in \mathbb{R}_0^+ \times \mathcal{E}'$:

$$\mathcal{Q}_{j,v,\alpha}(t, \tilde{j}, \tilde{z}) = \begin{cases} \left[F_{A^l}(t) - \int_0^t f_{A^l}(u) F_{B^b}(u) du \right] \mathbb{1}_{\{\tilde{z}=l\}}, & [S1], \\ \left[F_{B^a}(t) - \int_0^t f_{B^a}(u) F_{B^b}(u) du \right] \mathbb{1}_{\{\tilde{z}=0\}}, & [S2+], \\ \left[F_{B^b}(t) - \int_0^t f_{B^b}(u) F_{B^a}(u) du \right] \mathbb{1}_{\{\tilde{z}=0\}}, & [S2-], \\ F_{B^b}(t) - \int_0^t f_{B^b}(u) F_{C^1}(u) du, & [S3], \\ \int_0^t f_{B^b}(u) [F_{C^1}(u) - F_{A^l}(u)] du, & [S4], \\ \int_0^t f_{B^b}^*(\epsilon) \int_0^\epsilon f_{C^{\tilde{z}}}^*(u) du d\epsilon, & [S5], \\ \int_0^t f_{B^b}(u) [F_{C^1}(u) - F_{A^l}(u)] du \\ \quad - \sum_{z=1}^{l-1} \int_0^t f_{B^b}^*(\epsilon) \int_0^\epsilon f_{C^z}^*(u) du d\epsilon, & [S6], \\ 0, & \text{otherwise,} \end{cases}$$

where $f_{C^z}^*(\xi) := e^{\mu_j^a \xi} f_{C^z}(\xi)$ and $f_{B^b}^*(\xi) := e^{-\mu_j^a \xi} f_{B^b}(\xi)$ for $\xi \geq 0$ and $z \in \mathbb{N}^+$.

TERMINAL KERNEL

According to Theorem 3.16 and the Markovian property (M1), we can express the terminal kernel as

$$P(\mathfrak{z}|(e, \alpha), \lambda) = \mathbb{P}(X_{n+1} > \lambda, \mathfrak{Z} = \mathfrak{z} | E_n = e, A_n = \alpha), \quad (3.11)$$

for any $(e, \alpha) \in \mathcal{K}$, $\lambda \in \mathbb{R}$, $\mathfrak{z} \in \mathbb{N}$. Remark 3.9 implies that only the cases when $\lambda > 0$ and $\mathfrak{z} \in \{0, \dots, l\}$ need to be considered. According to Lemma 3.22, we now provide an expression for \mathcal{Q} , proved in Appendix C.2.

Proposition 3.24. *For any $\lambda > 0$, $(e, \gamma) \in \mathcal{K}$ (with corresponding $(j, v^b, v^a, m, l) \in \mathcal{K}'$), introduce the processes B^b, B^a, A^l, C^l as in Proposition 3.23. Then the*

following equality holds:

$$P(\mathfrak{z}|(e, \gamma), \lambda) = \begin{cases} \bar{F}_{B^b}(\lambda)\bar{F}_{B^a}(\lambda), & \text{if } l = 0, \mathfrak{z} = 0, \\ \bar{F}_{B^b}(\lambda)\bar{F}_{C^1}(\lambda), & \text{if } l \geq 1, \mathfrak{z} = 0, \\ \bar{F}_{B^b}(\lambda) [F_{C^3}(\lambda) - (F_{C^3} * F_{\Xi})(\lambda)], & \text{if } l > 1, \mathfrak{z} \in \{1, \dots, l-1\}, \\ \bar{F}_{B^b}(\lambda) [F_{C^l}(\lambda) - F_{A^l}(\lambda)], & \text{if } l \geq 1, \mathfrak{z} = l, \\ 0, & \text{otherwise,} \end{cases}$$

where Ξ is an exponentially distributed random variable with parameter μ_j^a , $*$ is the convolution operator and $\bar{F}_L := 1 - F_L$.

3.4.2 LAPLACE METHOD

Not surprisingly, the distributions of the first-passage time of the generalised birth-death processes A, B, C in Definition 3.21 do not admit closed-form expressions. To compute them, we first determine their Laplace transforms, and invert them numerically. We keep here the notations of Proposition 3.23.

Definition 3.25. Let $f : \mathbb{R}_0^+ \rightarrow \mathbb{R}$ be a function absolutely integrable on $[0, \omega]$ for any $\omega > 0$. Its (one-sided) Laplace transform is defined by

$$\hat{f}(s) := \lim_{\omega \uparrow \infty} \int_0^\omega e^{-st} f(t) dt,$$

for all $s \in \mathbb{C}$ such that the right-hand side converges.

The standard (albeit simplified) inversion formula for the Laplace transform is the Bromwich contour integral, or Mellin inversion [1, Chapter 1]: for an absolutely integrable continuous function f , the identity

$$f(t) = \frac{1}{2\pi \mathbf{i}} \int_{x-i\infty}^{x+i\infty} e^{ts} \hat{f}(s) ds$$

holds for any $x > 0$, and, by symmetry arguments, can be simplified to

$$f(t) = \frac{2e^{xt}}{\pi} \int_0^\infty \Re \left[\hat{f}(x + \mathbf{i}u) \right] \cos(ut) du, \quad \text{for all } t > 0. \quad (3.12)$$

We then apply the Euler algorithm in [3, Section 1] that exploits the specific structure of the integrand in (3.12). We now consider the general case of a birth-death process X^b with initial state $b \in \mathbb{N}^+$, and with birth rate $\lambda_n \geq 0$ and death rate $\mu_n > 0$ in state $n \in \mathbb{N}^+$. The following lemma, derived in [28, Equation (14)] following Abate-Whitt methodology [2, Section 4], expresses the Laplace transforms of the density and cumulative distribution function of τ_{X^b} .

Lemma 3.26. *The equality $\hat{F}_{X^b}(s) = s^{-1} \hat{f}_{X^b}(s)$ holds on $\{s \in \mathbb{C} : \Re(s) > 0\}$, and*

$$\hat{f}_{X^b}(s) = \prod_{n=1}^b \left[-\frac{1}{\lambda_{n-1}} \Phi_{k \geq 0} \left(\frac{-\lambda_{k+n-1} \mu_{k+n}}{\lambda_{k+n} + \mu_{k+n} + s} \right) \right], \quad \text{for all } s \in \mathbb{C} \text{ s.t. } \Re(s) > 0, \quad (3.13)$$

where $\Phi_{k \geq 0} \frac{a_k}{b_k} := \lim_{k \uparrow \infty} t_0 \circ t_1 \circ \dots \circ t_k(0)$ and $t_k(u) := \frac{a_k}{b_k + u}$ for $u \geq 0$.

Proposition 3.27. *Fix $v \in \mathbb{N}^+$, $l \in \mathbb{N}$ and $\kappa, \mu, \theta > 0$, and denote the processes $A[v, l, \kappa, \mu, \theta]$, $B[v, \kappa, \mu, \theta]$, $C[v, l, \mu, \theta]$ (as in Definition 3.21) by A , B and C , respectively. In particular, we denote the process $B[j, \kappa, \mu, \theta]$ by B^j for any $j \in \mathbb{N}^+$. Assume that f_A , f_B and f_C are continuous on \mathbb{R}^+ . Then*

$$\begin{aligned} \hat{f}_B(s) &= \frac{1}{(-\kappa)^v} \prod_{n=1}^v \Phi_{k \geq 0} \left[\frac{-\kappa \mu - \kappa(k+n)\theta}{\kappa + \mu + (k+n)\theta + s} \right], \quad \text{and} \\ \hat{f}_C(s) &= \left(\frac{\mu}{\mu + s} \right)^l \prod_{n=l+1}^{l+v} \frac{\mu + (n-l)\theta}{\mu + (n-l)\theta + s}, \quad \text{for all } \Re(s) > 0. \end{aligned}$$

Besides, given $R_j(u) := \frac{1}{j!} \exp\left(-\frac{\kappa}{\theta}(1 - e^{-\theta u})\right) \left[\frac{\kappa}{\theta}(1 - e^{-\theta u})\right]^j$ for $u \geq 0$, $j \in \mathbb{N}$, we have

$$f_A(t) = f_C(t)R_0(t) + \int_0^t \sum_{j=1}^{\infty} f_{B^j}(t-u) f_C(u) R_j(u) du. \quad (3.14)$$

Proof. The formulae for \hat{f}_B and \hat{f}_C are derived directly from Lemma 3.26, and we therefore focus on (3.14). Let $\tau_\Delta := \tau_A - \tau_C$. Before time τ_C , the process $(G_u) := (G[\kappa, \mu, \theta, \tau_C]_u)$ can be regarded as an initial empty $M/M/\infty$

queue with arrival rate κ and service rate θ . Let $R_j(u)$ denote the probability of G_u being in state $j \in \mathbb{N}$ when $u < \tau_C$. Then, by [77, p. 160], we have

$$R_j(u) = \overline{\mathbb{P}}\left(G_u = j \mid \tau_C = u\right) = \frac{1}{j!} \exp\left\{-\frac{\kappa}{\theta}(1 - e^{-\theta u})\right\} \left[\frac{\kappa}{\theta}(1 - e^{-\theta u})\right]^j.$$

Given $\tau_C = u, G_u = j \in \mathbb{N}^+$, the probability density function of τ_Δ is f_{B^j} . Indeed, in the case when $\tau_C = u$ and $G_u = G_{\tau_C} = j$, the time spent on depleting the agent's order and the orders with higher time priority is u and at that time the volume remaining in the queue is of j unit size. The remaining queue can be described by the process B^j , and the depletion time τ_Δ is thus τ_{B^j} (with density f_{B^j}). And given $\tau_C = u, G_u = 0$, we have $\tau_\Delta = 0$ almost surely. Therefore, the mixture density $\delta(\cdot)R_0(u) + \sum_{j=1}^{\infty} f_{B^j}(\cdot)R_j(u)$, with $\delta(\cdot)$ being the Dirac mass, provides the density of τ_Δ given $\tau_C = u$. Furthermore, the function $\delta(\cdot - u)R_0(u) + \sum_{j=1}^{\infty} f_{B^j}(\cdot - u)R_j(u)$ is the density of $\tau_A = \tau_\Delta + \tau_C$ given $\tau_C = u$. Consequently, we obtain (3.14). \square

3.5 EXISTENCE OF OPTIMAL POLICY

We now illustrate our main result, namely the existence and uniqueness of the value function, and the existence of a stationary optimal policy, as in the following theorem.

Theorem 3.28. *The value function V^* in (3.7) exists and is unique, and there exists a stationary \mathbb{T} -optimal policy $\pi^{\phi^*} := \{\phi^*, \phi^*, \dots\} \in \Pi^S$ in (3.8), with*

$$\phi^*(e, \lambda) = \arg \max_{\alpha \in \mathcal{A}(e)} \left\{ r(e, \alpha) + \sum_{\mathfrak{z}=0}^{\infty} w(e, \alpha, \mathfrak{z})P(\mathfrak{z} | (e, \alpha), \lambda) + \sum_{\tilde{e} \in \mathcal{E}} \int_0^\lambda V^*(\tilde{e}, \lambda - t)Q(dt, \tilde{e} | (e, \alpha)) \right\}, \quad (3.15)$$

for any $(e, \lambda) \in \mathcal{E} \times \mathbb{T}$.

The proof of Theorem 3.28 relies on several ingredients. In the first place, to make a finite-horizon semi-Markov decision model sensible, it is essential to have a (almost surely) finite number of decision epochs before maturity. In our setting, this is equivalent to the following lemma.

Lemma 3.29. *For any $(\mathfrak{e}, \lambda) \in \mathcal{E} \times \mathbb{T}$, $\pi \in \Pi$, the limit $\lim_{n \uparrow \infty} \mathbb{P}_{(\mathfrak{e}, \lambda)}^\pi(\mathfrak{N} < n) = 1$ holds for \mathfrak{N} as in Definition 3.14.*

Proof. According to [50, Proposition 2.1], it suffices to prove that there exist $\zeta, v > 0$ such that

$$Q(\zeta, \mathcal{E} | (e, \alpha)) \leq 1 - v, \quad (3.16)$$

for any $(e, \alpha) \in \mathcal{K}$. According to (3.9) and Lemma 3.22, we can write, for any $\zeta > 0$ and $(e, \alpha) \in \mathcal{K}$,

$$\begin{aligned} Q(\zeta, \mathcal{E} | (e, \alpha)) &= \mathbb{P}_{(\mathfrak{e}, \lambda)}^\pi(X_{n+1} \leq \zeta | E_n = e, A_n = \alpha) \\ &= \bar{\mathbb{P}}(\tau_{B^b} \wedge \tau_{A^l} \leq \zeta) = 1 - \bar{\mathbb{P}}(\tau_{B^b} > \zeta) \bar{\mathbb{P}}(\tau_{A^l} > \zeta). \end{aligned}$$

By Assumption 3.6(c), the agent never consumes up all the volumes at the best bid price through submitting market orders, so that there is at least one unit size order left at the best bid and ask price after the agent's action. Then according to stochastic ordering for the birth and death processes [53, Section 3], the inequalities

$$\bar{\mathbb{P}}(\tau_{B^b} > \zeta) \geq \bar{\mathbb{P}}\left(\tau_{B[1,0,\mu_j^b,\theta_j^b]} > \zeta\right) \geq e^{-\iota\zeta},$$

and

$$\bar{\mathbb{P}}(\tau_{A^l} > \zeta) \geq \bar{\mathbb{P}}(\tau_{C^l} > \zeta) \geq \bar{\mathbb{P}}\left(\tau_{C[1,0,\mu_j^a,\theta_j^a]} > \zeta\right) \geq e^{-\iota\zeta},$$

hold with $\iota := \max\{\mu_j^s + \theta_j^s : (s, j) \in \{a, b\} \times \{+1, -1\}\}$, and (3.16) therefore holds for $\zeta > 0$ and $v = e^{-2\iota\zeta}$. \square

Next, let \mathcal{U} denote the Banach space of non-negative valued functions on $\mathcal{E} \times \mathbb{T}$ with a finite supremum norm:

$$\mathcal{U} := \left\{ u : \mathcal{E} \times \mathbb{T} \rightarrow \mathbb{R}_0^+ \mid \|u\| := \sup_{(e, \lambda) \in \mathcal{E} \times \mathbb{T}} |u(e, \lambda)| < \infty \right\}.$$

and, for any decision rule $\phi \in \Phi$, introduce the dynamic programming operator \mathcal{T}^ϕ acting on \mathcal{U} as

$$\begin{aligned} \mathcal{T}^\phi u(e, \lambda) := & r(e, \phi(e, \lambda)) + \sum_{\mathfrak{z}=0}^{\infty} w(e, \phi(e, \lambda), \mathfrak{z}) P(\mathfrak{z}|(e, \phi(e, \lambda)), \lambda) \\ & + \sum_{\tilde{e} \in \mathcal{E}} \int_0^\lambda u(\tilde{e}, \lambda - t) Q(dt, \tilde{e}|(e, \phi(e, \lambda))), \end{aligned}$$

for any $u \in \mathcal{U}$ and $(e, \lambda) \in \mathcal{E} \times \mathbb{T}$. The following proposition, as proved in Appendix C.3, gives properties of \mathcal{T}^ϕ .

Proposition 3.30. *For any $\phi \in \Phi$ and $\pi := \{\phi_0, \phi_1, \phi_2, \dots\} \in \Pi$, we have*

- (a) \mathcal{T}^ϕ is a monotone contraction on \mathcal{U} with codomain \mathcal{U} ;
- (b) the identity $V^\pi = \mathcal{T}^{\phi_0} V^{\pi_-}$ holds on $\mathcal{E} \times \mathbb{T}$, where $\pi_- := \{\phi_1, \phi_2, \dots\} \in \Pi$.

By Proposition 3.30(b), the identity $V^{\pi^\phi} = \mathcal{T}^\phi V^{\pi^\phi}$ holds for any $\phi \in \Phi$ and the corresponding stationary policy $\pi^\phi := \{\phi, \phi, \dots\} \in \Pi^S$. For any $\pi \in \Pi$, the finiteness of the state space and the action space together with Lemma 3.29 yield that $V^\pi \in \mathcal{U}$. Therefore, the Banach Fixed-Point's Theorem [40], together with Proposition 3.30(a), guarantees the existence and uniqueness of V^{π^ϕ} and yields that

$$\lim_{n \uparrow \infty} (\mathcal{T}^\phi)^n u = V^{\pi^\phi}, \quad \text{for any } u \in \mathcal{U}. \quad (3.17)$$

Introduce now the iteration operator \mathcal{V} acting on \mathcal{U} as, for any $u \in \mathcal{U}$, $(e, \lambda) \in \mathcal{E} \times \mathbb{T}$,

$$\begin{aligned} \mathcal{V}u(e, \lambda) := & \sup_{\alpha \in \mathcal{A}(e)} \left\{ r(e, \alpha) + \sum_{\mathfrak{z}=0}^{\infty} w(e, \alpha, \mathfrak{z}) P(\mathfrak{z}|(e, \alpha), \lambda) \right. \\ & \left. + \sum_{\tilde{e} \in \mathcal{E}} \int_0^\lambda u(\tilde{e}, \lambda - t) Q(dt, \tilde{e}|(e, \alpha)) \right\}, \end{aligned} \quad (3.18)$$

which is also a contraction with codomain \mathcal{U} . Indeed, $\mathcal{V}(\mathcal{U}) \subset \mathcal{U}$ is immediate since the action space is finite, and the contraction property is inherited from

that of \mathcal{T}^ϕ by [31, Theorem 2]. The Banach Fixed-Point's Theorem [40] then ensures that $\mathcal{V}u = u$ has a unique solution, denoted by u^* . By [60, Section 1], the fixed point u^* admits a maximiser ϕ^* such that $u^* = \mathcal{T}^{\phi^*}u^*$, with

$$\phi^*(e, \lambda) := \arg \max_{\alpha \in \mathcal{A}(e)} \left\{ r(e, \alpha) + \sum_{\mathfrak{z}=0}^{\infty} w(e, \alpha, \mathfrak{z}) P(\mathfrak{z}|(e, \alpha), \lambda) + \sum_{\tilde{e} \in \mathcal{E}} \int_0^\lambda u^*(\tilde{e}, \lambda - t) Q(dt, \tilde{e}|(e, \alpha)) \right\}, \quad (3.19)$$

for any $(e, \lambda) \in \mathcal{E} \times \mathbb{T}$.

Finally, Theorem 3.28 follows by proving $V^* = u^* = V^{\pi^{\phi^*}}$. Suppose that a policy $\pi^* := \{\phi_0^*, \phi_1^*, \phi_2^*, \dots\} \in \Pi$ is \mathbb{T} -optimal in (3.8). Proposition 3.30, together with (3.17), yields that

$$V^* = V^{\pi^*} = \mathcal{T}^{\phi_0^*} V^{\pi^*} \leq \mathcal{T}^{\phi_0^*} V^{\pi^*} \leq \lim_{n \uparrow \infty} (\mathcal{T}^{\phi_0^*})^n V^{\pi^*} = V^{\pi^{\phi_0^*}}. \quad (3.20)$$

Combining this with $V^{\pi^{\phi_0^*}} \leq V^*$ by Definition 3.17 indicates that the stationary policy $\pi^{\phi_0^*} := \{\phi_0^*, \phi_0^*, \dots\} \in \Pi^S$ is also \mathbb{T} -optimal. Since $u^* = \mathcal{T}^{\phi^*}u^* \geq \mathcal{T}^{\phi_0^*}u^*$, applying Proposition 3.30 and (3.17) we obtain

$$V^* = V^{\pi^{\phi_0^*}} = \lim_{n \uparrow \infty} (\mathcal{T}^{\phi_0^*})^n u^* \leq \mathcal{T}^{\phi_0^*} u^* \leq u^* = \mathcal{T}^{\phi^*} u^* = \lim_{n \uparrow \infty} (\mathcal{T}^{\phi^*})^n u^* = V^{\pi^{\phi^*}} \leq V^*,$$

Theorem 3.28 therefore follows.

3.6 EMPIRICAL STUDIES AND COMPUTATIONAL RESULTS

Our empirical calculations are based on the ‘Level-I’ LOBSTER data for three large-tick stocks: Microsoft (MSFT), Intel (INTC) and Yahoo (YHOO), that are traded on the Nasdaq platform from 11 April 2016 to 15 April 2016, recording all market order arrivals, limit order arrivals and cancellations at the best prices between 9:30 am and 4 pm. These three large-tick stocks are selected due to price, trading volume and market share considerations as in [12, Section 4]. In order to avoid the impact from the abnormal trading

behaviours shortly after market opening or shortly before market closing, we exclude market activities during the first and the last twenty minutes of each trading day. We also exclude all the executions of hidden orders which account for around 12% of the entire trading volume. In the following, we first (Section 3.6.1) show some descriptive statistics for the selected large-ticks stocks. We then (Section 3.6.2) illustrate the estimation methodology of the Poisson parameters in Assumption 3.4, as well as the joint distribution of the best volumes after a price change in Assumption 3.2(b). We next (Section 3.6.3) give a numerical scheme that approximates the value function (3.7). We finally (Section 3.6.4) visualise the optimal decision rule in (3.15) for liquidating the stock YHOO under different trading conditions.

3.6.1 DESCRIPTIVE STATISTICS

Table 3.2 presents the percentage of time during which the LOB is with a given spread. For the three selected stocks, the spread is equal to one tick for around 98% of time and is barely over two ticks. Next, we introduce

Table 3.2: percentage of time with a given spread

Spread	1 tick	2 ticks	> 2 ticks
MSFT	98.14	1.86	0.00
INTC	98.33	1.67	0.00
YHOO	97.70	2.30	0.00

the definitions of forward and backward insertion. Suppose that the spread is equal to one tick in the initial stage and then becomes two ticks when either of the best bid or ask queue is depleted. Once the spread increases to two ticks, a new limit order is quickly placed inside the spread, driving the spread back to one tick. If the mid price after the insertion of that limit order is the same as (resp. one tick higher or lower than) the mid price in the initial stage, we call the insertion a backward (resp. forward) insertion. Table 3.3 gives the probability of backward insertions being around 25% and Figure 3.1 shows that the distribution of the queueing race duration after a backward insertion is bimodal, with nearly 30% of the queueing races being shorter than one millisecond, indicating the instability of the LOB state after

a backward insertion. In sum, the above empirical observations enable us to make Assumption 3.1(b) that omits the time when the spread is over one tick and Assumption 3.2(a) that excludes the possibility of backward insertions.

Table 3.3: percentage of forward and backward insertions.

Insertion	Forward	Backward
MSFT	77.54	22.46
INTC	76.76	23.24
YHOO	73.95	26.05

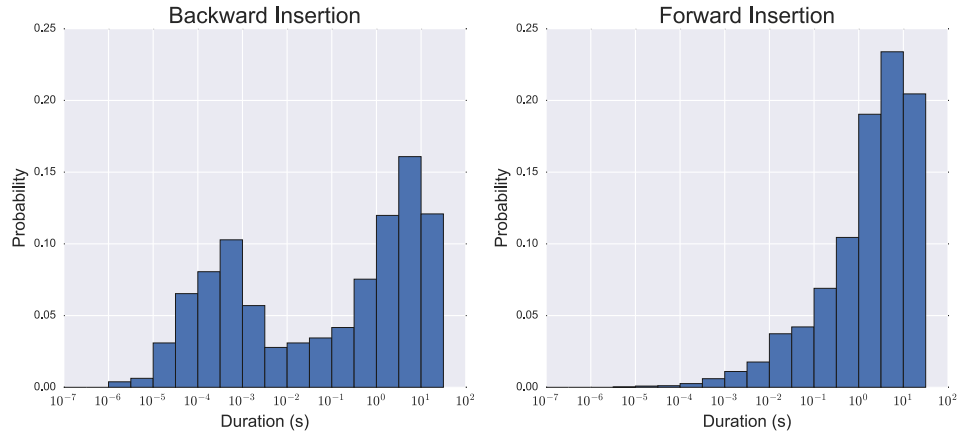


Figure 3.1: YHOO: histogram of the queuing race duration after a backward Insertion (left panel) and a forward insertion (right panel).

3.6.2 PARAMETER ESTIMATION

POISSON PARAMETERS

As in Assumption 3.1(a), orders from the general market participants are of unit size. We first compute the average size of the limit orders, market orders and cancellations at the best prices, denoted by S^l , S^m and S^c respectively, and choose the unit size to be S^l . Estimation results are given in Table 3.4.

We then estimate the Poisson parameters as follows. From our sample data, we formulate a set Ω_{+1} (resp. Ω_{-1}) consisting of the queuing races happening immediately after a price increase (resp. decrease): if the spread

Table 3.4: average order size (in shares).

	MSFT	INTC	YHOO
S^l	176	317	209
S^m	332	565	334
S^c	163	309	201

is currently one tick, a queueing race $\mathbf{q}_{+1} \in \mathfrak{Q}_{+1}$ (resp. $\mathbf{q}_{-1} \in \mathfrak{Q}_{-1}$) starts when the best bid (resp. ask) price increases (resp. decreases) by one tick after the best ask (resp. bid) queue depletes, and ends whenever either the new best ask or bid queue depletes. By maximum likelihood estimation (see Appendix C.5), we have

$$\hat{\mu}_j^{\mathfrak{s}} = \frac{N_{\mathfrak{s},j}^m S^m}{D_j S^l}, \quad \hat{\kappa}_j^{\mathfrak{s}} = \frac{N_{\mathfrak{s},j}^l}{D_j}, \quad \hat{\theta}_j^{\mathfrak{s}} = \frac{N_{\mathfrak{s},j}^c S^c}{V_{\mathfrak{s},j} S^l}, \quad (3.21)$$

for $\mathfrak{s} \in \{a, b\}$ and $j \in \{+1, -1\}$, where

- $N_{\mathfrak{s},j}^m, N_{\mathfrak{s},j}^l$ and $N_{\mathfrak{s},j}^c$ represent the total number of market orders, limit orders and cancellations at \mathfrak{s} price⁷ for the queueing races in set \mathfrak{Q}_j ;
- D_j represents the sum of the length of the queueing races in \mathfrak{Q}_j ;
- $V_{\mathfrak{s},j} := \sum_{i=1}^{\#\mathfrak{Q}_j} \int_{\mathfrak{T}_i} \text{Vol}_i^{\mathfrak{s}}(t) dt$, where $\text{Vol}_i^{\mathfrak{s}}(t)$ (resp. \mathfrak{T}_i) denotes the volume in unit size at \mathfrak{s} price at time t (resp. the time interval) of the i -th queueing race in \mathfrak{Q}_j .

Table 3.5 gives the Poisson parameter estimation where the agent's action at each decision epoch has no latency. For the three stocks, we find that:

- the rates of market order arrivals are indifferent to the side of the best price and the price move direction;
- immediately after a price increase (resp. decrease), there is a surge of limit order arrivals and cancellations at the best bid (resp. ask) price;

⁷By abuse of language, 'at a (resp. b price)' means 'at the best ask (resp. bid) price'.

- from an estimation (of the Poisson parameters) point of view, an increase of the price on the bid (resp. ask) side is symmetric to a decrease of price on the ask (resp. bid) side.

Table 3.6 gives the Poisson parameter estimation where the agent’s action at each decision epoch has a one-millisecond latency⁸. By comparing it with Table 3.5, we observe that:

- the rates of market order arrivals barely change;
- the rates of limit order arrivals and cancellations see a decrease, especially on the bid side after a price increase and on the ask side after a price decrease;
- the symmetry remains unaffected.

Table 3.5: Poisson parameter estimation with no latency.

		MSFT			INTC			YHOO		
s	j	μ	κ	θ	μ	κ	θ	μ	κ	θ
a	+1	0.32	3.07	0.31	0.16	2.45	0.16	0.14	1.97	0.26
b	+1	0.34	5.97	0.50	0.17	3.59	0.21	0.17	3.54	0.32
a	-1	0.35	5.97	0.51	0.18	3.87	0.22	0.15	3.29	0.33
b	-1	0.34	3.06	0.32	0.18	2.22	0.16	0.15	1.92	0.21

Table 3.6: Poisson parameter estimation with 1ms latency.

		MSFT			INTC			YHOO		
s	j	μ	κ	θ	μ	κ	θ	μ	κ	θ
a	+1	0.31	2.89	0.27	0.15	2.36	0.15	0.13	1.87	0.23
b	+1	0.33	3.31	0.40	0.19	2.46	0.17	0.16	2.07	0.26
a	-1	0.34	3.22	0.41	0.18	2.49	0.18	0.14	2.02	0.27
b	-1	0.34	2.87	0.27	0.19	2.36	0.17	0.15	1.83	0.18

⁸When estimating the Poisson parameters in this case, market activities at the first one millisecond of each queueing race are excluded, and the queueing races with duration shorter than one millisecond are excluded.

VOLUME DISTRIBUTION AFTER A PRICE CHANGE

The best volumes in unit size are approximated by rounding the division of the volume in shares by S^l up to the nearest integer. Figure 3.2 compares the volume distribution immediately after a price change and one millisecond later for YHOO⁹. We observe that:

- the volume at the best bid (resp. ask) price is quite thin immediately after a price increase (decrease), but see a dramatic increase one millisecond later;
- the volume at the best ask (resp. bid) price keeps the distribution almost unchanged within the first millisecond of the queueing race starting with a price increase (resp. decrease).

We believe that this observation is mainly due to the existence of National Best Bid Offer (NBBO) pegged orders: whenever a limit order initiates a new price inside the spread and is not cancelled immediately, all the limit orders pegged to the NBBO price will move in less than a millisecond to the new price level correspondingly [26].

3.6.3 NUMERICAL SCHEME

Dynamic programming techniques usually suffer from the ‘curse of dimensionality’ [72] to compute the value function through the iteration operator \mathcal{A} in (3.18). The next proposition, proved in Appendix C.4, allows us to reduce the dimension of the problem, and hence to accelerate the implementation.

Proposition 3.31. *Given $e := (j, v^b, v^a, p, z, y) \in \mathcal{E}$, $\bar{e} := (j, v^b, v^a, \bar{p}, \bar{z}, y) \in \mathcal{E}$ and $\lambda \in \mathbb{T}$, we have*

$$V^*(e, \lambda) = V^*(\bar{e}, \lambda) + \rho(p - \bar{p})(y + z) + \rho(z - \bar{z})(\bar{p} - j).$$

⁹In order to implement the numerical calculations later, we introduce the truncation by assuming $f_{\pm 1}(v^b, v^a) = 0$ for any $v^b, v^a > 25$ since $\sum_{v^b=1}^{25} \sum_{v^a=1}^{25} f_{\pm 1}(v^b, v^a) \geq 95\%$ holds right after a price change and one millisecond later for YHOO.

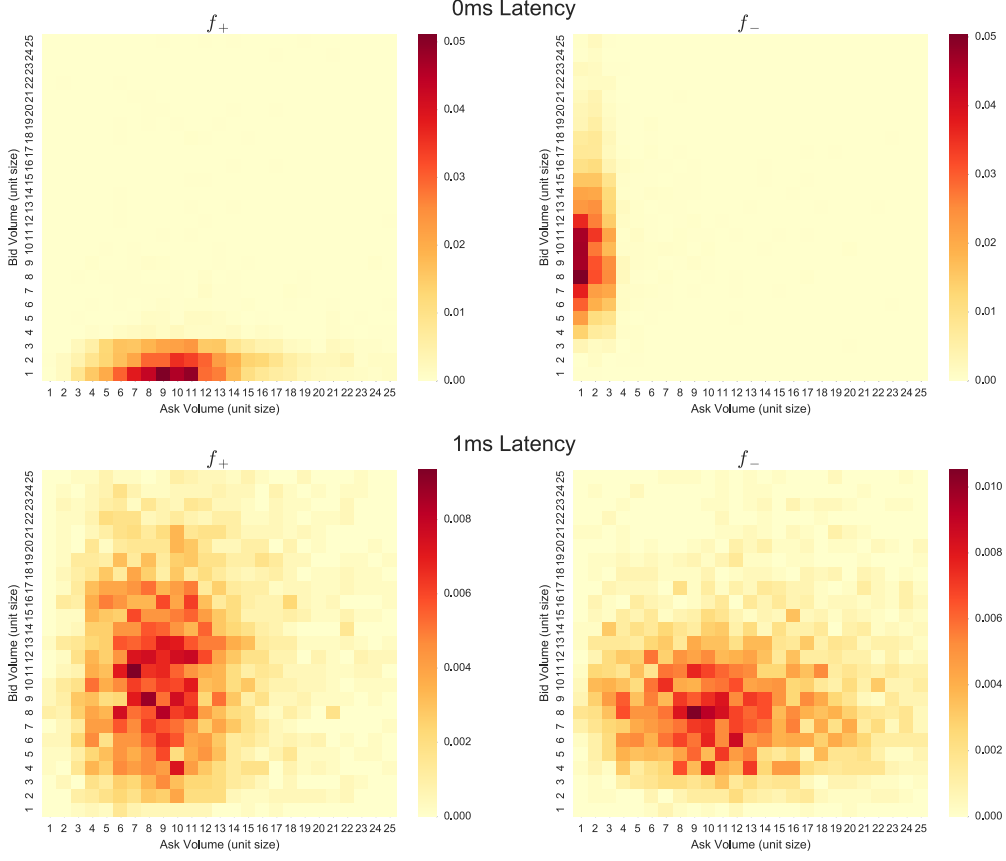


Figure 3.2: YHOO: f_{+1} (left) and f_{-1} (right) with no latency (top) and with one-millisecond latency (bottom).

Besides, the value function V^* is monotone with respect to time to maturity. Indeed, let $\pi^* := \{\phi^*, \phi^*, \dots\}$ be \mathbb{T} -optimal and construct a policy $\pi^\varepsilon := \{\phi^\varepsilon, \phi^\varepsilon, \dots\}$, for fixed $\varepsilon \in (0, T)$, as

$$\phi^\varepsilon(e, \lambda) := \begin{cases} \phi^*(e, \lambda - \varepsilon), & \text{if } \varepsilon \leq \lambda \leq T, \\ (0, 0), & \text{if } 0 \leq \lambda < \varepsilon. \end{cases}$$

Definition 3.17 immediately implies that $V^{\pi^\varepsilon}(e, \lambda) \leq V^*(e, \lambda)$ for any $(e, \lambda) \in \mathcal{E} \times \mathbb{T}$ and $V^{\pi^\varepsilon}(e, \lambda) = V^*(e, \lambda - \varepsilon)$ for any $(e, \lambda) \in \mathcal{E} \times [\varepsilon, T]$. The monotonicity in time to maturity therefore follows since ε is arbitrary. As in [54, 66], we can take advantage of the monotonicity of the value function to get a faster

convergence rate. The implementation procedure proceeds as follows, for a given tolerance level \mathbf{tol} :

Step 1. (initialization): let $n = 0$ and $V_0(e, \lambda) = \rho(p - 1)y + \lambda\rho y/T$ for every $(e, \lambda) \in \mathcal{E} \times \mathbb{T}$;

Step 2. (iteration): choose a random pair $(e_n, \lambda_n) \in \mathcal{E} \times \mathbb{T}$ and compute $\widehat{V}_n := \mathcal{A}V_n(e_n, \lambda_n)$;

Step 3. (correction): with $\widehat{U}_n := \gamma\widehat{V}_n + (1 - \gamma)V_n(e_n, \lambda_n)$ for $\gamma \in (0, 1)$, define the monotonicity projection as:

$$V_{n+1}(e, \lambda) = \begin{cases} \widehat{U}_n, & \text{if } e = e_n, \lambda = \lambda_n, \\ \widehat{U}_n \vee V_n(e, \lambda), & \text{if } e = e_n, \lambda > \lambda_n, \\ \widehat{U}_n \wedge V_n(e, \lambda), & \text{if } e = e_n, \lambda < \lambda_n, \\ V_n(e, \lambda), & \text{if } e \neq e_n; \end{cases}$$

Step 4. (accuracy control): if $\|V_{n+1} - V_n\| \leq \mathbf{tol}$, end the scheme; otherwise go to Step 2 incrementing n to $n + 1$.

3.6.4 OPTIMAL STRATEGY

In this section, we visualise the results of the optimal decision rule computed in (3.15) in which the value function is approximated through the numerical scheme in Section 3.6.3. To begin with, we set the size of the order $\chi = 2$ and the maturity $T = 10$ (throughout this section, order size is measured in numbers of unit size and time is measured in seconds), both of which are relatively small. Furthermore, we apply the parameters for the stylised LOB model estimated in Section 3.6.2 together with the market parameters $\rho = 1$ and $\bar{v} = 9$ (see (3.2) and (3.4) for the definitions) and the tolerance level $\mathbf{tol} = 0.001$ in the numerical scheme. Indeed, Proposition 3.31 together with (3.15) indicates that the optimal decision rule depends on the price move direction j , the volumes at the best prices v^b and v^a , remaining inventory y and time to maturity λ , and is irrelevant to the ask price in tick size p and the executed limit order volume in the previous queueing race z . Moreover, the parameter

estimation results in Table 3.5 and 3.6, together with those in Figure 3.2, indicate that the agent's latency (denoted by \mathbf{lat}) also affect her optimal trading strategy.

Figure 3.3 illustrates the optimal decision rule as a function of v^b , v^a , j and \mathbf{lat} when fixing $y = 2$ and $\lambda = 10$, where the agent's admissible trading strategies are give by (3.1) as:

$$(m, l) \in \begin{cases} \{(2, 0), (1, 0), (1, 1), (0, 0), (0, 1), (0, 2)\}, & \text{if } v^b > 1, \\ \{(0, 0), (0, 1), (0, 2)\}, & \text{if } v^b = 1. \end{cases}$$

Comparing the subfigures horizontally and vertically, we observe the following:

- The trading strategy that executes part of the order, either through placing a limit order $(m, l) = (0, 1)$ or submitting a market order $(m, l) = (1, 0)$, or doing nothing $(m, l) = (0, 0)$ is never optimal in all scenarios. Generally speaking, in the situations where the best ask volume is low and the best bid volume is high (corresponding to the top-left part of the subfigures), it is expected that the price will soon increase and the agent will choose to wait or to trade partially as her best choice. However, since the trading horizon is quite short and the intensity rate for the incoming market orders is relatively low, it seems that the agent would rather post limit orders in order to increase the execution probability than wait for better opportunities. On top of that, this model does not consider the risk of adverse selection, so that posing limit orders is basically at no additional cost.
- The queue imbalance of the best prices, defined as $I := (v^b - v^a)/(v^b + v^a)$, is regarded as a powerful and effective predictor of the short-term price movements [11, 80] and is incorporated into the optimal market making strategy [18]. However, we observe no clear relationship between the queue imbalance and the choice of the optimal strategy in all scenarios, which may imply that queue imbalance should not be the only consideration in building the optimal execution strategy. Reason

for this result may come from Assumption 3.6(d) that the agent sticks to a ‘no cancellation’ rule, so that the best bid and ask queue follow different dynamics. On the contrary, the volume at the best ask price individually plays the most decisive part in the selection of the optimal strategy: the larger the best ask volume, the more aggressive trading strategy the agent will employ. In particular, when the best ask volume $v^a \leq 6$, the optimal strategy is always $(m, l) = (0, 2)$, indicating the value of queue position for limit orders [65]. Besides, volume at the best bid price also contributes to determining the optimal strategy, in particular when the best ask volume is high and the best bid volume is low (corresponding to the bottom-right part of the subfigures). In such situations, the optimal decision rule normally chooses to take all the available liquidity through market orders in case the price soon moves against the agent’s favour. However, when the best bid volume $v^b \geq 10$, the pattern of the optimal strategy is unchanged in all scenarios.

- The optimal strategy is no more aggressive after a price decline than after a price increase. This is mainly because the cancellation rate of each limit order from the general market participants is lower at the best ask price after a price increase, which increases the execution risk of the agent’s limit order, so the the agent prefers to use a market order in this case.
- The optimal policy is no more aggressive when the agent has no latency than one-millisecond latency. On the one hand, this result comes as the cancellation rate of each limit order from the general market participants is higher at the best ask price when there is no latency, which increases the execution probability of the agent’s limit order. On the other hand, suppose the liquidation process enters into the next round of queueing race, in which the volumes at the best prices change dramatically within the first one millisecond, an agent with zero latency can take most advantage of the speed to occupy a good queue position in the new queueing race. By contrast, an agent with one-millisecond latency is less likely to get a high time priority in the new queue, and therefore prefers to react more aggressively in order to terminate the

trade as soon as possible.

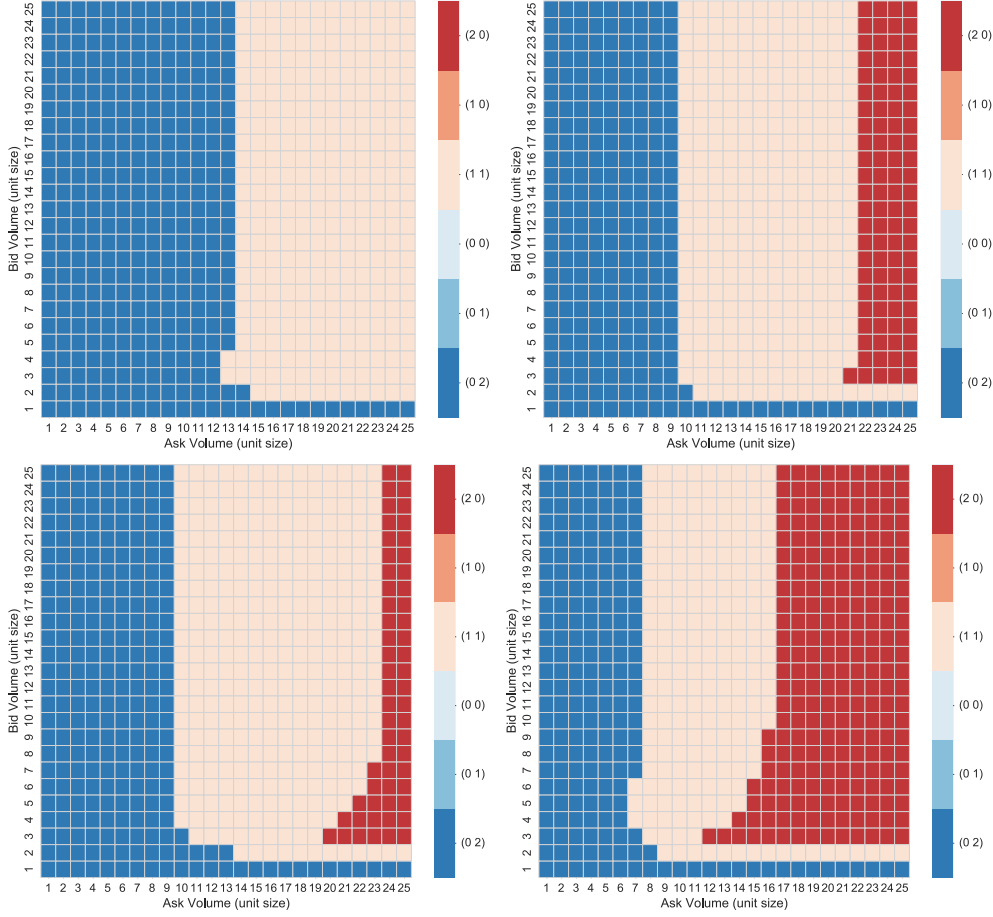


Figure 3.3: optimal policy as a function of best ask volume (x-axis: $v^a = 1, \dots, 25$), best bid volume (y-axis: $v^b = 1, \dots, 25$), latency (top: $\text{lat} = 0\text{ms}$; bottom: $\text{lat} = 1\text{ms}$) and price move direction (left: $j = -1$; right: $j = 1$) when fixing inventory $y = 2$ and time to maturity $\lambda = 10$.

Figure 3.4 shows the optimal decision rule as a function of v^b , v^a , j and λ (valued in 3 and 10 seconds) by fixing $y = 1$ and $\text{lat} = 1\text{ms}$, where the agent's admissible trading strategies are given by

$$(m, l) \in \begin{cases} \{(1, 0), (0, 0), (0, 1)\}, & \text{if } v^b > 1, \\ \{(0, 0), (0, 1)\}, & \text{if } v^b = 1. \end{cases}$$

In addition to the previous results, we find the agent to be more aggressive when there is less time to maturity.

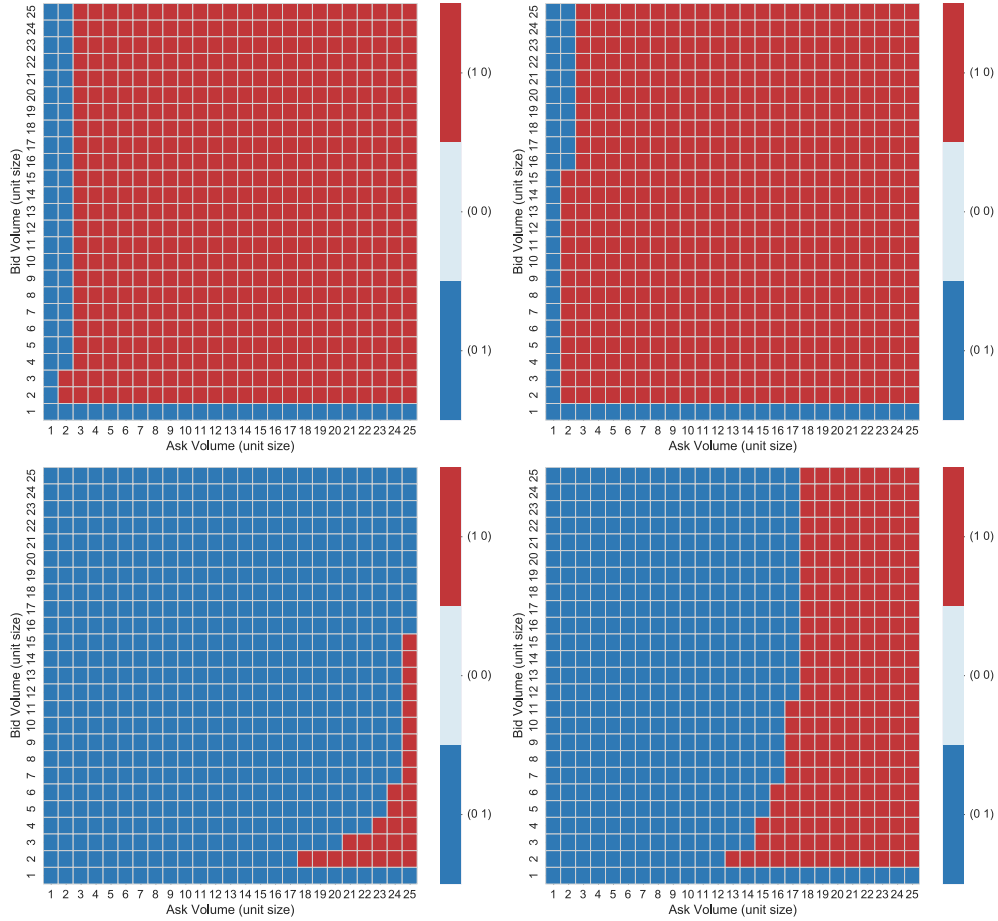


Figure 3.4: optimal policy as a function of best ask volume (x-axis: $v^a = 1, \dots, 25$), best bid volume (y-axis: $v^b = 1, \dots, 25$), time to maturity (top: $\lambda = 3$; bottom: $\lambda = 10$) and price move direction (left: $j = -1$; right: $j = 1$) when fixing inventory $y = 1$ and latency $\text{lat} = 1\text{ms}$.



EMPIRICAL STUDIES FOR LARGE-TICK STOCKS

In this section, we conduct some empirical studies based on the LOBSTER dataset (introduced in Section 1.4) for three highly liquid large-tick stocks: Microsoft (MSFT), Intel (INTC) and Yahoo (YHOO), that are traded on the Nasdaq platform in 2016 (corresponds to 252 trading days). These three large-tick stocks are selected according to price, trading volume and market share considerations, see [12, Section 4] for the detailed selection rule. On top of that, the sample data we request contain information up to the second best price level on both sides of the market. Our focus on the top two price levels is motivated by the empirical findings indicating that orders placed deeper into the order book virtually have no price impact on the market [47]. We also exclude events that occur during the first and last ten minutes of each active trading day in order to avoid the erratic effects shortly after market opening and shortly before market closure.

A.1 CONCURRENCY

A key feature of a LOB dataset is its timestamp granularity, that is, the smallest time interval between different event timestamps. Currently, almost all LOB literatures are based on datasets with timestamp granularity up to one millisecond, which means, events that arrive within the same millisecond are displayed at the same timestamp in such dataset. However, empirical evidence shows that sub-millisecond algorithmic trading behaviours indeed exist. For example, Menkveld [64] shows that twenty percent of the trades occur within the same millisecond and proposes that these clustered market order arrivals increase the adverse selection cost for non-HFT traders. Thanks to the nanosecond granularity provided in the LOBSTER dataset, we are able to observe the most subtle LOB dynamics and study the ultra-fast activities in the market.

For each of the selected stocks over the entire sample period, we categorise the timestamps in the raw dataset into three categories based on the number of order book events being recorded at that timestamp, namely, one event, two events and more than two events. To be more specific, if exactly one event is recorded at a timestamp, we call it an isolated event; if exactly two (resp. more than two) events are recorded at a timestamp, we treat these events as a whole and call it an event pair (resp. event bundle). In particular, events recorded at the same timestamp are listed in a logical sequence reflecting the price-visibility-time priority. Table A.1 presents the descriptive statistics on the isolated events, event pairs and event bundles, respectively. We are particularly interested in the composition and structure of the event pairs and event bundles.

In general, we observe that the timestamps and the associated events in the datasets of the three selected stocks have similar characteristics, which are summarised in the following:

- over 93% of the timestamps have only one event being recorded: slightly more than half (resp. nearly half) of these isolated events are of type submission (resp. cancellation), while only around 1% of the isolated

Table A.1: descriptive statistics on timestamps and recorded events in 2016.

Panel A gives the total number of timestamps (# Timestamp) and the percentage of timestamps at which an isolated event (1 Event %), an event pair (2 Events %) and an event bundle (> 2 Event %) is recorded.

Panel B gives the percentage of isolated events belonging to event type submission (SUB %), full cancellation (Full CAN %), partial cancellation (Partial CAN %) and execution (EXE %).

Panel C gives the percentage of event pairs being in the form of a full cancellation followed by a submission of the same size and on the same side (CAN-SUB %), two executions on the same side (TWO-EXE %) and other paired combinations (Others %).

Panel D gives the percentage of event bundles being in the form of all executions on the same side (All-EXE %) and other serial combinations (Other %).

Particularly, all means and standard deviations (displayed in the brackets) in this table are reported across trading days.

Panel A: Overall

Ticker	# Timestamp	1 Event %	2 Events %	> 2 Events %
MSFT	684,000 (315,721)	93.11 (2.31)	6.39 (2.31)	0.50 (0.11)
INTC	398,523 (171,709)	94.24 (0.99)	5.32 (1.00)	0.44 (0.08)
YHOO	423,360 (206,285)	93.84 (0.79)	5.79 (0.80)	0.37 (0.09)

Panel B: Isolated events

Ticker	SUB %	Full CAN %	Partial CAN %	EXE %
MSFT	50.51 (0.52)	47.37 (0.59)	1.12 (0.34)	1.00 (0.23)
INTC	50.61 (0.40)	47.58 (0.67)	0.97 (0.63)	0.84 (0.21)
YHOO	50.16 (0.39)	47.89 (0.63)	0.90 (0.34)	1.05 (0.28)

Panel C: Event pairs

Ticker	CAN-SUB %	TWO-EXE %	Others %
MSFT	94.66 (1.53)	4.80 (1.38)	0.54 (0.26)
INTC	93.65 (2.37)	4.60 (1.53)	1.75 (1.45)
YHOO	94.28 (1.66)	5.35 (1.58)	0.37 (0.15)

Panel D: Event bundles

Ticker	ALL-EXE %	Others %
MSFT	94.95 (2.62)	5.05 (2.62)
INTC	93.87 (2.20)	6.13 (2.20)
YHOO	94.70 (1.73)	5.30 (1.73)

events are of type execution;

- around 6% of the timestamps have two events being recorded: nearly 95% of these event pairs are in the form of ‘a full cancellation followed by a submission of an order with the same size and on the same side’, and nearly 5% of those event pairs are in the form of ‘executions of two orders on the same side’;
- around 0.5% of the timestamps have more than two events being recorded, and nearly 95% of those event bundles are in the form of ‘executions of multiple orders on the same side’.

Remark A.1. A timestamp is the time at which an event is recorded by a computer, which is different from the time of the event itself [9]. Intuitively, the greater the timestamp granularity, the less likely different events are recorded at the same timestamp. However, we observe that approximately 12.6% of the events are non-isolated in a nanosecond-timestamped environment. Furthermore, Nasdaq has a platform latency of around 10^{-6} second [12], which arises due to the time it takes to process and route messages¹ inside the automated trading platform [57]. Therefore, we propose that events recorded at the same timestamp are processed concurrently and are extremely likely triggered by a single message. Based on our empirical results in Table A.1, most event pairs are in the form of ‘same-size, same-side full cancellation and submission’. Together with Figure A.1 indicating the direction of the order price modification, we believe that this pattern is interpreted as a pegged order adjusting its price to the newly generated best price inside the spread. Furthermore, most event bundles are in the form of ‘same-side executions’. We believe that this pattern indicates a single market order matching with several different limit orders.

Based on Remark A.1, we convert the limit order oriented raw dataset into a message oriented dataset through the following rules:

(R1) if two events, first (resp. second) of which is of type full cancellation

¹A message is a standardised packet of data that enables a trader and a trading platform to communicate with each other.

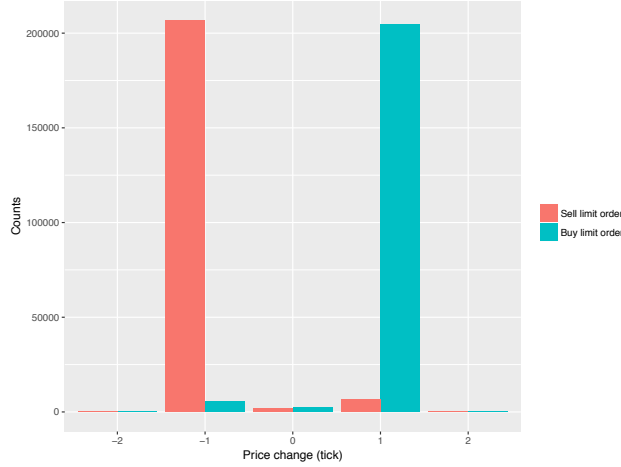


Figure A.1: YHOO: direction of order price modification for event pairs in the form of 'same-size, same-side full cancellation and submission'.

The red (resp. green) bars represent the counts of the event pairs on the sell (resp. buy) side of the market. On the horizontal axis, 0 represents that the cancellation and submission of an order occur at the same price level; 1 (resp. -1) represents that the submission price is one tick higher (resp. lower) than the cancellation price.

(resp. submission), have the same timestamp, same size, same direction, they will be combined into a single message of type modification;

(R2) if more than one event, all of which are of type execution, have the same timestamp, they will be combined into a single message of type market order;

(R3) in other cases, each event of type submission, full/partial cancellation and execution is treated as a message of type limit order, full/partial cancellation and market order, respectively².

We call the dataset generated through the above procedures the message dataset. Clearly, the message dataset describes the market participants' behaviours in a more efficient and convenient way, as each message represents a single trading directive sent to the platform.

²Event pairs or event bundles with a pattern that is not included in **(R1)** and **(R2)** barely appear and we therefore regard them as collections of isolated events for simplicity.

A.2 CLOCK-TIME PERIODICITY

In this section, we study the periodicity of the messages arriving to the market by processing the timestamps in the message datasets. In the first place, we introduce the following definition for nanosecond timestamps.

Definition A.2. For a nanosecond timestamp t (in seconds after midnight), we define its millisecond remainder (resp. microsecond remainder) by

$$\lfloor 1000(t - \lfloor t \rfloor) \rfloor \quad (\text{resp. } \lfloor 1000(1000t - \lfloor 1000t \rfloor) \rfloor),$$

which is interpreted as the number of the millisecond (resp. microsecond) past the most recent one-second (resp. one-millisecond) boundary.

Under the premiss that message arrivals have no clock-time periodicity, the millisecond and the microsecond remainders are expected to be uniformly distributed over the integer set $\{0, 1, \dots, 999\}$. However, this is not true for millisecond remainders based on a previous empirical study by Hasbrouck and Saar [44]. The authors employ a millisecond-timestamped Nasdaq sample data in October 2007 and June 2008, and find that the empirical distributions of the millisecond remainders in both sample periods distinctively departure from uniformity: large peaks occur at roughly 10 to 30 millisecond and around 150 millisecond after the one-second mark. They propose that this periodic pattern is mainly driven by the employments of agency algorithms that examine and respond to market conditions every second. They also argue that the peak positions shown in the empirical distributions reflect the levels of algorithm latency caused by computation and information transmission.

In Figure A.2, we exhibit the empirical distributions of both the millisecond and microsecond remainders together with the null distribution depicted by the horizontal line at 0.001.

In terms of the empirical distribution of the millisecond remainders, the results obtained from our sample data (we call them new distributions) are similar to those from Hasbrouck and Saar's experiment (we call them old

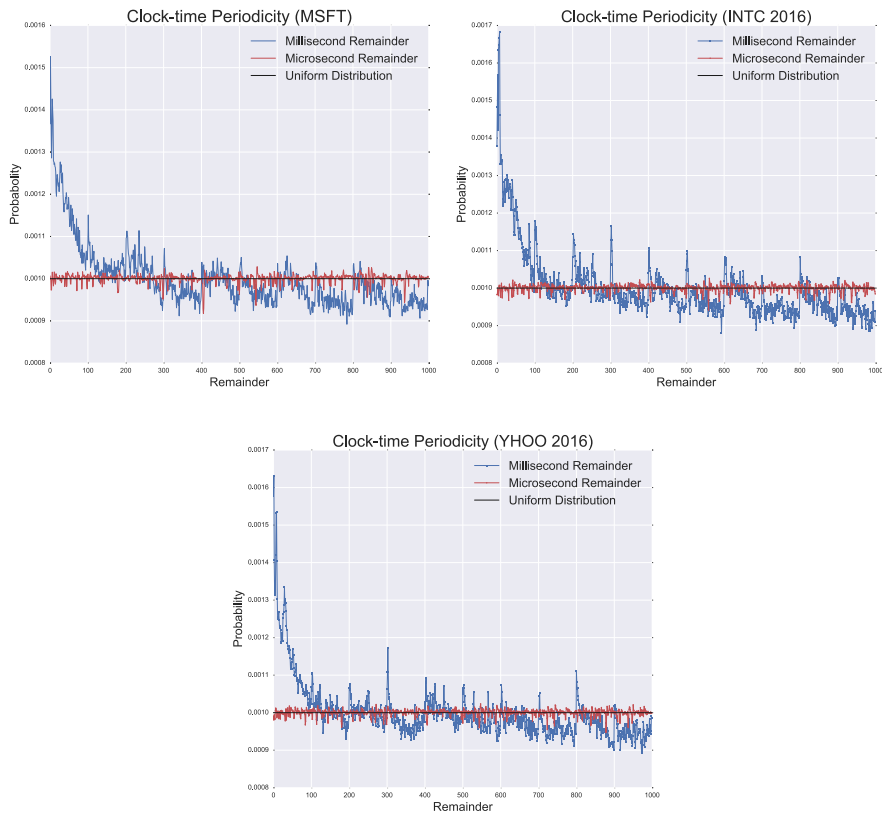


Figure A.2: MSFT (top-left), INTC (top-right) and YHOO (bottom): empirical distributions of the millisecond and microsecond remainders in 2016.

This figure exhibits the empirical distributions of the millisecond remainders (blue lines) and the microsecond remainders (red lines) of the timestamps in the message datasets for three stocks, MSFT, INTC and YHOO, in 2016. For a certain timestamp, the millisecond (resp. microsecond) remainder is the number (rounded down to the nearest integer) of millisecond (resp. microsecond) past the most recent one-second (one-millisecond) boundary. The horizontal black solid line in each subgraph represents the position of the uniform distribution (the null hypothesis).

distributions): large peaks occur shortly after the one-second boundary. In general, we agree with Hasbrouck and Saar’s viewpoint proposing that such pattern is indicative of the periodic behaviour by the agency algorithms. Furthermore, the new distributions are more positively skewed than the old ones and the peak positions observed in the new distributions are located at around 0 to 5 millisecond and roughly 20 to 30 millisecond, which are closer to the one-second boundary than those in the old distributions. These differences may indicate a general decline of algorithm latency in recent years because of wider applications of co-location services and developments in information technology. Besides, moderate elevations in probability are observed at and shortly after integer multiples of one hundred millisecond in the new distributions. This may suggest that some agency algorithms are implementing the check-and-react strategies at a higher frequency, from every second to every one hundred millisecond.

The empirical distributions of the microsecond remainders are much closer to the uniform distribution than those of the millisecond remainders. This direct comparison suggests that market participants have more control over the message arrivals to the market within each one-second interval than those within each one-millisecond interval. In order to measure the clock-time periodicity at the microsecond level, we propose the following hypothesis test for the sample data consisting of the microsecond remainders in the message datasets for each of the selected stocks over the entire sample period.

\mathcal{H}_0 : The sample data of the microsecond remainders are consistent with the discrete uniform distribution over the set $\{0, 1, \dots, 999\}$;

\mathcal{H}_A : The sample data of the microsecond remainders are not consistent with the discrete uniform distribution over the set $\{0, 1, \dots, 999\}$

We use the Cramér-von Mises statistics for discrete distributions [23] in our hypothesis test, namely, W^2 , U^2 and A^2 . As shown in Panel A of Table A.2, we reject the null hypotheses at a significance level of 5% for all the selected stocks when using any of the test statistic. We further implement the same hypothesis test on a daily basis, and Panel B of Table A.2 indicates that the null hypotheses is rejected at a significance level of 5% in 222

Table A.2: Cramér-von Mises test for discrete uniform distribution

This table presents the Cramér-von Mises goodness-of-fit tests of the sample distributions of the microsecond remainders compared with the discrete uniform distribution over the integer set $\{0, 1, \dots, 999\}$. The null and alternative hypotheses are:

\mathcal{H}_0 : The sample data of the microsecond remainders are consistent with the discrete uniform distribution over the set $\{0, 1, \dots, 999\}$;

\mathcal{H}_A : The sample data of the microsecond remainders are not consistent with the discrete uniform distribution over the set $\{0, 1, \dots, 999\}$

In **Panel A**, we illustrate the test results (that is, the name of the statistics, the critical value at a significance level of 5% and the value of the test statistics for each selected stock) for microsecond remainders in the message datasets over the entire sample period (January to August, 2016). We then apply the same goodness-of-fit test on a daily basis. **Panel B** presents the percentages of trading days in which the null hypotheses is rejected at a significance level of 5% for each selected stocks. **Panel C** presents the same percentages after the probability anomalies are manually removed.

Panel A: Microsecond remainders over the entire sample period

Statistic	$CV(\alpha = 0.05)$	MSFT	INTC	YHOO
W^2	0.461	3.203	0.931	2.500
U^2	0.187	2.949	0.648	2.427
A^2	2.492	16.356	8.439	15.614

Panel B: Microsecond remainders on a daily basis

Statistic	MSFT (%)	INTC (%)	YHOO (%)
W^2	88.62	89.22	90.42
U^2	97.60	95.21	95.21
A^2	95.21	90.42	93.41

Panel C: Microsecond remainders on a daily basis (after removing anomalies)

Statistic	MSFT (%)	INTC (%)	YHOO (%)
W^2	3.9	4.8	4.4
U^2	6.0	5.6	6.7
A^2	4.8	4.4	4.4

to 245 out of the total 252 trading days, depending on the selection of the stocks and the test statistic. We therefore draw the preliminary conclusion that the microsecond remainders are not uniformly distributed. In order to verify the rationality and robustness of this conclusion, we visualise all the daily empirical distributions of the microsecond remainders for each of the selected stocks. Surprisingly, we observe a strange but widespread pattern: the empirical probability for each microsecond remainder is in general closely located around the level of 0.001, except for one or several short-lived but significant ‘probability anomalies’, each of which is composed of a slump immediately followed by a spike. We then repeat the hypothesis test to the sample microsecond remainders on a daily basis after manually removing the probability anomalies. Panel C of Table A.2 shows that the null hypotheses is rejected at the significance level of 5% in only 10 to 17 out of 252 trading days, depending on the selection of the stocks and the test statistics. Furthermore, the probability anomalies basically appear in the same positions within the same week across all the selected stocks. For example, for each selected stock and trading day in the first week in 2016 (Jan 4th to Jan 8th, 2016), we observe one probability anomaly, which is composed of a slump in probability at 936 to 938 microsecond followed by a spike in probability at 939 to 941 microsecond (See Figure A.3). We believe that this weekly periodic pattern across all selected stocks is unlikely to be driven by certain algorithm strategies in the market. Instead, this phenomenon is probably caused by the system latency in the platform.

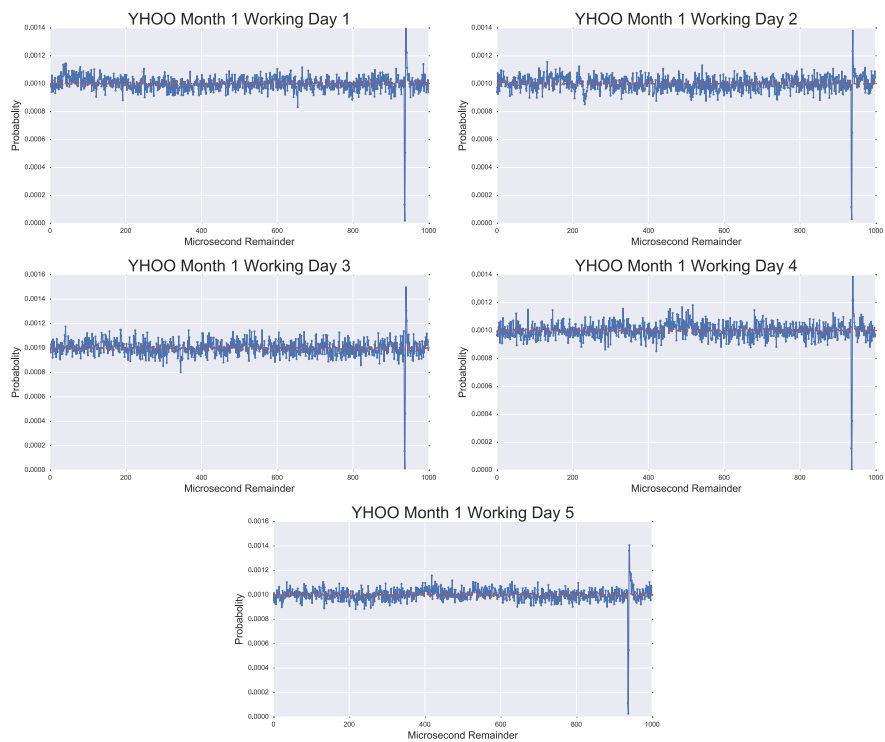


Figure A.3: YHOO: example of probability anomalies in the daily empirical distributions of microsecond remainders.

For each working day in the first week in 2016, we observe one probability anomaly, which is composed of a slump in probability at 936 to 938 microsecond followed by a spike in probability at 939 to 941 microsecond.

B

APPENDIX FOR CHAPTER 2

B.1 PROOF OF THEOREM 2.14

(a) Consider an initial condition $(t, z) := (t, p, y, x) \in \mathcal{B}$. Based on the definition of the termination time τ in (2.22), we immediately have

$$Z_\tau^{t,z,(\alpha)} = Z_t^{t,z,(\alpha)} = z \quad \text{almost surely, for all } \alpha \in \mathcal{A}. \quad (\text{B.1})$$

Combining (B.1) and (2.34) yields

$$\begin{aligned} w(t, z) &\geq u(x + \beta g(p)y) = \mathbb{E} [u(X_\tau^{t,x,(\alpha)} + \beta g(P_\tau^{t,p,(\alpha)})Y_\tau^{t,y,(\alpha)})] \\ &= J(t, z, \alpha), \end{aligned} \quad (\text{B.2})$$

for all $\alpha \in \mathcal{A}$ and then $w(t, z) \geq v(t, z)$ on \mathcal{B} .

Now consider an initial condition $(t, z) \in [0, T) \times \mathcal{S}$. Choose an admissible liquidation strategy $\alpha = \left((Q_t, H_t)_{t \geq 0}, (\tau_j \cdot \xi_j)_{j \in \mathbb{N}^+} \right) \in \mathcal{A}$ and $n < m \in \mathbb{N}^+$ such that $\tau_{n-1} < t < \tau_n < \tau_{n+1} < \dots < \tau_m$. Without loss of generality,

we set $\tau_0 = 0$. Since $w \in C^{1,2}([0, T] \times \mathcal{S})$, applying Itô formula yields

$$\begin{aligned}
& w\left(\tau_{i+1}^R, \check{Z}_{\tau_{i+1}^R-}^{t,z,(\alpha)}\right) = w\left(\tau_i^R, Z_{\tau_i^R}^{t,z,(\alpha)}\right) \\
& + \int_{\tau_i^R}^{\tau_{i+1}^R} \left(\frac{\partial w}{\partial t}(s, Z_s^{t,z,(\alpha)}) + \frac{1}{2} \sigma^2 \frac{\partial^2 w}{\partial p^2}(s, Z_s^{t,z,(\alpha)}) \right) ds + \int_{\tau_i^R}^{\tau_{i+1}^R} \sigma \frac{\partial w}{\partial p}(s, Z_s^{t,z,(\alpha)}) dW_s \\
& + \sum_{\substack{(\varpi, \Pi) = \\ \{(m, M), (l, L), (c, C)\}}} \int_{\tau_i^R}^{\tau_{i+1}^R} \left[w\left(s, \Gamma^\varpi\left(Q_s, H_s, Z_{s-}^{t,z,(\alpha)}, \Pi_{N_s^\varpi}\right)\right) - w\left(s, Z_{s-}^{t,z,(\alpha)}\right) \right] \\
& \qquad \qquad \qquad \times \left(\lambda_s^\varpi ds + d\tilde{N}_s^\varpi \right), \quad (\text{B.3})
\end{aligned}$$

for $i = n-1, n, \dots, m-1$ and $R > 0$, where

- $\tilde{N}_s^\varpi := N_s^\varpi - \int_0^s \lambda_v^\varpi dv$ for $s \geq 0$;
- $\lambda_s^\varpi = \lambda^\varpi \left(d\left(P_{s-}^{t,p,(\alpha)}\right) + Q_s \right)$ for $\varpi \in \{m, l, c\}$ and $s \geq 0$ as in (2.16);
- $\check{Z}_{\tau_j-}^{t,z,(\alpha)} := Z_{\tau_j-}^{t,z,(\alpha)} + d_N Z_{\tau_j}^{t,z,(\alpha)}$ for $j \in \mathbb{N}^+$ as in (2.21);
- $\tau_j^R := \tau_j' \wedge T_R$, where

$$\begin{aligned}
T_R &:= \inf \{s > 0 : \|Z_s^{t,z,(\alpha)} - z\| \geq R\}, \quad \text{and} \\
\tau_j' &:= \begin{cases} t, & \text{if } j = n-1, \\ \tau_j, & \text{if } j \in \{n, n+1, \dots, m\}. \end{cases}
\end{aligned}$$

For each $\varpi \in \{m, l, c\}$, the process Δ^ϖ defined by

$$\Delta_t^\varpi := w\left(t, \Gamma^\varpi(Q_t, H_t, Z_{t-}, \Pi_{N_t^\varpi})\right) - w\left(t, Z_{t-}\right), \quad \text{for } t \geq 0,$$

is predictable. Therefore, $\mathbb{E} \left[\int_0^t |\Delta_s^\varpi| \lambda_s^\varpi ds \right]$ is finite for all $t \geq 0$ since w and λ^ϖ are bounded, and $\int_0^\cdot \Delta_s^\varpi d\tilde{N}_s^\varpi$ is a martingale by [13, Chapter II, Theorem T8]. Taking expectation on both sides of (B.3) and letting R

tends to infinity, we obtain

$$\begin{aligned}
& \mathbb{E} \left[w \left(\tau'_{i+1}, \check{Z}_{\tau'_{i+1}-}^{t,z,(\alpha)} \right) \right] = \mathbb{E} \left[w \left(\tau'_i, Z_{\tau'_i}^{t,z,(\alpha)} \right) \right] \\
& \quad + \mathbb{E} \left[\int_{\tau'_i}^{\tau'_{i+1}} \left(\frac{\partial w}{\partial t} (s, Z_s^{t,z,(\alpha)}) + \frac{1}{2} \sigma^2 \frac{\partial^2 w}{\partial p^2} (s, Z_s^{t,z,(\alpha)}) \right) ds \right] \\
& + \sum_{\substack{(\varpi, \Pi) = \\ \{(m, M), (l, L), (c, C)\}}} \mathbb{E} \left[\int_{\tau'_i}^{\tau'_{i+1}} \left(\int_{\mathbb{R}^+} w(s, \Gamma^\varpi (Q_s, H_s, Z_{s-}^{t,z,(\alpha)}, \nu)) dF^\varpi(\nu) \right. \right. \\
& \quad \left. \left. - w \left(s, Z_{s-}^{t,z,(\alpha)} \right) \right) \lambda^\varpi (d(P)_{s-} + Q_s) ds \right], \quad (\text{B.4})
\end{aligned}$$

for $i = n - 1, n, \dots, m - 1$. We then translate (2.33) into

$$-\frac{\partial w(t, z)}{\partial t} - \frac{\sigma^2}{2} \frac{\partial^2 w(t, z)}{\partial p^2} - \sup_{\substack{(q, h) \in [0, \bar{v}]^2 \\ \text{s.t. } q+h \leq y}} \mathcal{L}^{q, h} w(t, z) \geq 0, \quad (\text{B.5})$$

$$w(t, z) - \sup_{e \in [0, \bar{e} \wedge y]} \mathcal{M}^e w(t, z) \geq 0, \quad (\text{B.6})$$

for $(t, z) \in [0, T) \times \mathcal{S}$. Summing up (B.4) from $i = n$ to $i = m - 1$, together with (B.5), yields

$$\begin{aligned}
& w(t, z) + \sum_{i=n}^{m-1} \mathbb{E} \left[w \left(\tau_i, Z_{\tau_i}^{t,z,(\alpha)} \right) - w \left(\tau_i, \check{Z}_{\tau_i-}^{t,z,(\alpha)} \right) \right] - \mathbb{E} \left[w \left(\tau_m, \check{Z}_{\tau_m-}^{t,z,(\alpha)} \right) \right] \\
& = -\mathbb{E} \left[\int_t^{\tau_m} \frac{\partial w}{\partial t} (s, Z_s^{t,z,(\alpha)}) + \frac{\sigma^2}{2} \frac{\partial^2 w}{\partial p^2} (s, Z_s^{t,z,(\alpha)}) + \mathcal{L}^{Q_s, H_s} w \left(s, Z_{s-}^{t,z,(\alpha)} \right) ds \right] \\
& \geq 0. \quad (\text{B.7})
\end{aligned}$$

Besides, combining (B.6) with (2.14) and (2.15) yields

$$\begin{aligned}
w \left(\tau_i, Z_{\tau_i}^{t,z,(\alpha)} \right) & = w \left(\tau_i, \check{P}_{\tau_j-}^{t,p,(\alpha)}, \check{Y}_{\tau_j-}^{t,y,(\alpha)} - \xi_i, \check{X}_{\tau_j-}^{t,x,(\alpha)} + g \left(\check{P}_{\tau_j-}^{t,p,(\alpha)} \right) \xi_i \right) \\
& = \mathcal{M}^{\xi_i} w \left(\tau_i, \check{Z}_{\tau_i-}^{t,z,(\alpha)} \right) \leq \sup_{e \in [0, \bar{e} \wedge \check{Y}_{\tau_j-}^{t,y,(\alpha)}]} \mathcal{M}^e w \left(\tau_i, \check{Z}_{\tau_i-}^{t,z,(\alpha)} \right) \\
& \leq w \left(\tau_i, \check{Z}_{\tau_i-}^{t,z,(\alpha)} \right). \quad (\text{B.8})
\end{aligned}$$

Next, combining (B.8) with (B.7) gives

$$w(t, z) \geq \mathbb{E} \left[w(\tau_m, \check{Z}_{\tau_m^-}^{t, z, (\alpha)}) \right].$$

Based on (2.32) and (2.34), together with $\lim_{m \uparrow \infty} \tau_m = \tau$ as in (2.24), letting $m \rightarrow \infty$ yields

$$w(t, z) \geq J(t, z, \alpha).$$

Since $\alpha \in \mathcal{A}$ is arbitrarily chosen, we then get

$$w(t, z) \geq v(t, z), \quad \text{on } [0, T) \times \mathcal{S}. \quad (\text{B.9})$$

(b) By (2.35), we get the equality for (B.2) and then $w(t, z) = v(t, z)$ on \mathcal{B} .

Applying the arguments in (a) for $(t, z) \in [0, T) \times \mathcal{S}$ with

$$\hat{\alpha} := \left((\hat{\varphi}(s, Z_s^{\hat{\alpha}}))_{s \geq 0}, \left\{ (\hat{\tau}_j, \hat{\xi}_j) : j \in \mathbb{N}^+ \right\} \right) \in \mathcal{A}.$$

Then by (2.36) we get the equality for (B.7), and by (2.37) and (2.38) we get the equality for (B.8). We therefore obtain

$$w(t, z) = \mathbb{E} \left[w \left(\hat{w}_m, \check{Z}_{\hat{\tau}_m^-}^{t, z, (\hat{\alpha})} \right) \right],$$

and letting $m \rightarrow \infty$ yields $w(t, z) = J(t, z, \hat{\alpha})$, which combined with (B.9) finishes the proof.

C

APPENDIX FOR CHAPTER 3

C.1 PROOF OF PROPOSITION 3.23

In Scenario [S1], the agent posts a limit order at the best ask price ($l \geq 1$), and the best ask queue is depleted before the best bid queue ($\tilde{j} = +1$). Hence,

- the execution time of the best ask queue is less than that of the best bid queue;
- the limit order posted by the agent must get fully executed in the queueing race;
- the duration of the queueing race is the depletion time of the best ask queue.

Therefore, we can write

$$\begin{aligned}
\mathcal{Q}_{j,v,\alpha}(t, \tilde{j}, \tilde{z}) &= \mathbb{P}\left(X_{n+1} \leq t, J_{n+1} = +1 \mid J_n = j, (V_n^b, V_n^a) = (v^b, v^a), A_n = \alpha\right) \\
&\quad \times \mathbb{P}\left(Z_{n+1} = \tilde{z} \mid J_{n+1} = +1, L_n = l\right) \\
&= \bar{\mathbb{P}}(\tau_{B^b} > \tau_{A^l}, \tau_{A^l} \leq t) \mathbb{1}_{\{\tilde{z}=l\}} \\
&= \left\{ F_{A^l}(t) - \int_0^t f_{A^l}(u) F_{B^b}(u) du \right\} \mathbb{1}_{\{\tilde{z}=l\}}.
\end{aligned}$$

In Scenario [S2], the agent posts no limit order at the best ask price ($l = 0$). The dynamics of best ask queue can be then described by the process B^a , independent of that of the best bid queue. The proof is similar to that in Scenario [S1].

In Scenario [S3], the agent posts a limit order at the best ask price ($l \geq 0$), and the best bid queue is depleted before the best ask queue ($\tilde{j} = -1$), while the agent's limit order gets no execution ($\tilde{z} = 0$). Hence,

- the execution time of the best bid queue is less than that of one unit size of the agent's limit order together with the limit orders with higher time priority at the best ask price, and is therefore less than that of the entire best ask queue;
- the duration of the queueing race is the depletion time of the best bid queue.

We then have

$$\begin{aligned}
\mathcal{Q}_{j,v,\alpha}(t, \tilde{j}, \tilde{z}) &= \mathbb{P}\left(X_{n+1} \leq t, Z_{n+1} = 0 \mid J_n = j, (V_n^b, V_n^a) = (v^b, v^a), A_n = \alpha\right) \\
&\quad \times \mathbb{P}(J_{n+1} = -1 \mid L_n = l, Z_{n+1} = 0) \\
&= \bar{\mathbb{P}}(\tau_{C^1} > \tau_{B^b}, \tau_{B^b} \leq t) \\
&= F_{B^b}(t) - \int_0^t f_{B^b}(u) F_{C^1}(u) du.
\end{aligned}$$

In Scenario [S4], the agent posts a limit order of one unit size at the best ask price ($l = 1$), the best bid queue is depleted before the best ask queue

($\tilde{j} = -1$) and the agent's limit order gets executed ($\tilde{z} = 1$). According to Remark 3.20, we have $\mathcal{Q}_{j,v,\alpha}(t, \tilde{j}, \{0, 1\}) = \mathcal{Q}_{j,v,\alpha}(t, \tilde{j}, 0) + \mathcal{Q}_{j,v,\alpha}(t, \tilde{j}, 1)$, so that

$$\begin{aligned}
& \mathcal{Q}_{j,v,\alpha}(t, -1, 1) \\
&= \mathbb{P}\left(X_{n+1} \leq t, J_{n+1} = -1 \mid J_n = j, (V_n^b, V_n^a) = (v^b, v^a), A_n = (m, 1)\right) \\
&\quad - \mathcal{Q}_{j,v,\alpha}(t, -1, 0) \\
&= \overline{\mathbb{P}}(\tau_{A^1} > \tau_{B^b}, \tau_{B^b} \leq t) - \mathcal{Q}_{j,v,\alpha}(t, -1, 0) \\
&= F_{B^b}(t) - \int_0^t f_{B^b}(u) F_{A^1}(u) du - \left[F_{B^b}(t) - \int_0^t f_{B^b}(u) F_{C^1}(u) du \right] \\
&= \int_0^t f_{B^b}(u) [F_{C^1}(u) - F_{A^1}(u)] du.
\end{aligned}$$

In Scenario [S5], the best bid queue is depleted before the best ask queue ($\tilde{j} = -1$), while $\tilde{z} \in \{1, \dots, l-1\}$ out of $l > 1$ unit size of the agent's limit order gets executed when this queueing race terminates. Hence,

- the execution time of the best bid queue lies within the interval $[\tau_{C^{\tilde{z}}}, \tau_{C^{\tilde{z}}} + \Delta)$, where Δ is the execution time of one unit size of the agent's limit order when at the top of the queue, which is exponentially distributed with parameter μ_j^a and is independent of $\tau_{C^{\tilde{z}}}$;
- the duration of the queueing race is the depletion time of the best bid queue.

We then have

$$\begin{aligned}
& \mathcal{Q}_{j,v,\alpha}(t, \tilde{j}, \tilde{z}) \\
&= \mathbb{P}\left(X_{n+1} \leq t, Z_{n+1} = \tilde{z} \mid J_n = j, (V_n^b, V_n^a) = (v^b, v^a), A_n = \alpha\right) \\
&\quad \times \mathbb{P}(J_{n+1} = -1 \mid L_n^a = l, Z_{n+1} = \tilde{z}) \\
&= \bar{\mathbb{P}}\left(\tau_{C^{\tilde{z}}} \leq \tau_{B^b} < \tau_{C^{\tilde{z}}} + \Delta, \tau_{B^b} \leq t\right) \\
&= \int_0^\infty \int_0^\infty \bar{\mathbb{P}}(\tau_{B^b} \in [u, u + \nu), \tau_{B^b} \leq t) f_{C^{\tilde{z}}}(u) \bar{\mathbb{P}}(\Delta \in d\nu) du d\nu \\
&= \int_0^t \int_0^{t-u} [F_{B^b}(u + \nu) - F_{B^b}(u)] f_{C^{\tilde{z}}}(u) \bar{\mathbb{P}}(\Delta \in d\nu) d\nu du \\
&\quad + \int_0^t \int_{t-u}^\infty [F_{B^b}(t) - F_{B^b}(u)] f_{C^{\tilde{z}}}(u) \bar{\mathbb{P}}(\Delta \in d\nu) d\nu du \\
&= \mu_j^a \int_0^t e^{\mu_j^a u} f_{C^{\tilde{z}}}(u) \left(\int_u^t e^{-\mu_j^a \epsilon} F_{B^b}(\epsilon) d\epsilon \right) du \\
&\quad + e^{-\mu_j^a t} F_{B^b}(t) \int_0^t e^{\mu_j^a u} f_{C^{\tilde{z}}}(u) du - \int_0^t F_{B^b}(u) f_{C^{\tilde{z}}}(u) du \\
&= \mu_j^a \int_0^t F_{B^b}^*(\epsilon) \int_0^\epsilon f_{C^{\tilde{z}}}^*(u) du d\epsilon + \int_0^t [F_{B^b}^*(\epsilon)]' \int_0^\epsilon f_{C^{\tilde{z}}}^* du d\epsilon \\
&= \int_0^t f_{B^b}^*(\epsilon) \int_0^\epsilon f_{C^{\tilde{z}}}^*(u) du d\epsilon
\end{aligned}$$

where $f_{C^z}^*(\xi) := e^{\mu_j^a \xi} f_{C^z}(\xi)$, $f_{B^b}^*(\xi) := e^{-\mu_j^a \xi} f_{B^b}(\xi)$ and $F_{B^b}^*(\xi) := e^{-\mu_j^a \xi} F_{B^b}(\xi)$ for any $\xi \geq 0$ and $z \in \mathbb{N}^+$.

Finally, in Scenario [S6], according to Remark 3.20, for $(j, v^b, v^a, \alpha) \in \mathcal{K}'$ such that $l > 1$, we have

$$\mathcal{Q}_{j,v,\alpha}(t, -1, \{0, 1, \dots, l\}) = \mathcal{Q}_{j,v,\alpha}(t, -1, 0) + \sum_{z=1}^{l-1} \mathcal{Q}_{j,v,\alpha}(t, -1, z) + \mathcal{Q}_{j,v,\alpha}(t, -1, l),$$

which yields the result by using [S3] and [S5].

C.2 PROOF OF PROPOSITION 3.24

If $l = 0$ and $\mathfrak{z} = 0$, then

$$\begin{aligned} P(\mathfrak{z}|(e, \alpha), \lambda) &= \bar{\mathbb{P}}(\tau_{B^b} \wedge \tau_{B^a} > \lambda) \\ &= \bar{\mathbb{P}}(\tau_{B^b} > \lambda) \bar{\mathbb{P}}(\tau_{B^a} > \lambda) = \bar{F}_{B^b}(\lambda) \bar{F}_{B^a}(\lambda). \end{aligned}$$

If $l \geq 1$, $\mathfrak{z} = 0$, then

$$\begin{aligned} P(\mathfrak{z}|(e, \alpha), \lambda) &= \bar{\mathbb{P}}(\tau_{B^b} \wedge \tau_{A^l} > \lambda, \tau_{C^1} > \lambda) \\ &= \bar{\mathbb{P}}(\tau_{B^b} > \lambda) \bar{\mathbb{P}}(\tau_{C^1} > \lambda) = \bar{F}_{B^b}(\lambda) \bar{F}_{C^1}(\lambda). \end{aligned}$$

If $l > 1$ and $\mathfrak{z} \in \{1, \dots, l-1\}$, then

$$\begin{aligned} P(\mathfrak{z}|(e, \alpha), \lambda) &= \bar{\mathbb{P}}(\tau_{B^b} \wedge \tau_{A^l} > \lambda, \tau_{C^3} + \Xi > \lambda \geq \tau_{C^3}) \\ &= \bar{\mathbb{P}}(\tau_{B^b} > \lambda) \bar{\mathbb{P}}(\tau_{C^3} + \Xi > \lambda \geq \tau_{C^3}) \\ &= \bar{\mathbb{P}}(\tau_{B^b} > \lambda) \bar{\mathbb{P}}[1 - \bar{\mathbb{P}}(\tau_{C^3} > \lambda) - \bar{\mathbb{P}}(\tau_{C^3} + \Xi \leq \lambda)] \\ &= \bar{F}_{B^b}(\lambda) [F_{C^3}(\lambda) - (F_{C^3} * F_{\Xi})(\lambda)]. \end{aligned}$$

If $l \geq 1$ and $\mathfrak{z} = l$, then

$$\begin{aligned} P(\mathfrak{z}|(e, \alpha), \lambda) &= \bar{\mathbb{P}}(\tau_{B^b} \wedge \tau_{A^l} > \lambda, \tau_{C^l} \leq \lambda) = \bar{\mathbb{P}}(\tau_{B^b} > \lambda) \bar{\mathbb{P}}(\tau_{A^l} > \lambda \geq \tau_{C^l}) \\ &= \bar{\mathbb{P}}(\tau_{B^b} > \lambda) [1 - \bar{\mathbb{P}}(\tau_{C^l} > \lambda) - \bar{\mathbb{P}}(\tau_{A^l} \leq \lambda)] \\ &= \bar{F}_{B^b}(\lambda) [F_{C^l}(\lambda) - F_{A^l}(\lambda)]. \end{aligned}$$

By Remark 3.9, the terminal kernel has zero value in all other scenarios.

C.3 PROOF OF PROPOSITION 3.30

To prove Part (a) of the proposition, we can write the inequality

$$\begin{aligned} \|\mathcal{T}^\phi u\| \leq & \sup_{(e,\lambda) \in \mathcal{E} \times \mathbb{T}} |r(e, \phi(e, \lambda))| + \sup_{\substack{(e,\lambda) \in \mathcal{E} \times \mathbb{T} \\ \mathfrak{j} \in \{0, \dots, \bar{l}\}}} |w(e, \phi(e, \lambda), \mathfrak{j})| \\ & + \sup_{(e,\lambda) \in \mathcal{E} \times \mathbb{T}} \left| \sum_{\tilde{e} \in \mathcal{E}} \int_0^\lambda u(\tilde{e}, \lambda - t) Q(dt, \tilde{e} | (e, \phi(e, \lambda))) \right|, \end{aligned}$$

for any $\phi \in \Phi$ and $u \in \mathcal{U}$. The first two terms are bounded since the state space \mathcal{E} and the action space \mathcal{A} are finite. Regarding the last term, applying Lemma 3.29 yields

$$\begin{aligned} & \sup_{(e,\lambda) \in \mathcal{E} \times \mathbb{T}} \left| \sum_{\tilde{e} \in \mathcal{E}} \int_0^\lambda u(\tilde{e}, \lambda - t) Q(dt, \tilde{e} | (e, \phi(e, \lambda))) \right| \\ & \leq \|u\| \sup_{(e,\lambda) \in \mathcal{E} \times \mathbb{T}} \left| \sum_{\tilde{e} \in \mathcal{E}} \int_0^\lambda Q(dt, \tilde{e} | (e, \phi(e, \lambda))) \right| \\ & = \|u\| \sup_{(e,\lambda) \in \mathcal{E} \times \mathbb{T}} Q(\lambda, \mathcal{E} | (e, \phi(e, \lambda))) \\ & \leq \|u\| \sup_{\lambda \in \mathbb{T}} (1 - e^{-2\iota\lambda}) \\ & = \|u\| (1 - e^{-2\iota T}) < \infty. \end{aligned}$$

Therefore the codomain of \mathcal{T}^ϕ is \mathcal{U} . The contraction property follows directly from (3.16), since $\|\mathcal{T}^\phi u - \mathcal{T}^\phi v\| \leq (1 - e^{-2\iota T})\|u - v\|$ holds for all $u, v \in \mathcal{U}$, and the monotonicity follows from the properties of the semi-Markov kernel.

To prove Part (b), we can write, for any $(e, \lambda) \in \mathcal{E} \times \mathbb{T}$ and $\pi := \{\phi_0, \phi_1, \phi_2, \dots\} \in$

II,

$$\begin{aligned}
V^\pi(e, \lambda) &= \sum_{n=0}^{\infty} \mathbb{E}_{(e, \lambda)}^\pi \left[r(\mathcal{E}_n, \mathcal{A}_n) \mathbb{1}_{\{\Lambda_n \geq 0\}} + w(\mathcal{E}_n, \mathcal{A}_n, \mathfrak{Z}) \mathbb{1}_{\{0 \leq \Lambda_n < X_{n+1}\}} \right] \\
&= \mathbb{E}_{(e, \lambda)}^\pi \left[r(\mathcal{E}_0, \mathcal{A}_0) \mathbb{1}_{\{\Lambda_0 \geq 0\}} + w(\mathcal{E}_0, \mathcal{A}_0, \mathfrak{Z}) \mathbb{1}_{\{0 \leq \Lambda_0 < X_1\}} \right] \\
&\quad + \sum_{n=1}^{\infty} \mathbb{E}_{(e, \lambda)}^\pi \left[r(\mathcal{E}_n, \mathcal{A}_n) \mathbb{1}_{\{\Lambda_n \geq 0\}} + w(\mathcal{E}_n, \mathcal{A}_n, \mathfrak{Z}) \mathbb{1}_{\{0 \leq \Lambda_n < X_{n+1}\}} \right] \\
&= \mathbb{E}_{(e, \lambda)}^\pi \left[\mathbb{E}_{(e, \lambda)}^\pi \left[r(\mathcal{E}_0, \mathcal{A}_0) \mathbb{1}_{\{\Lambda_0 \geq 0\}} + \sum_{\mathfrak{z}=0}^{\infty} w(\mathcal{E}_0, \mathcal{A}_0, \mathfrak{z}) \mathbb{1}_{\{0 \leq \Lambda_0 < X_1, \mathfrak{z}=\mathfrak{Z}\}} \middle| H_0 \right] \right] \\
&\quad + \sum_{n=1}^{\infty} \mathbb{E}_{(e, \lambda)}^\pi \left[\mathbb{E}_{(e, \lambda)}^\pi \left[r(\mathcal{E}_n, \mathcal{A}_n) \mathbb{1}_{\{\Lambda_n \geq 0\}} + w(\mathcal{E}_n, \mathcal{A}_n, \mathfrak{Z}) \mathbb{1}_{\{0 \leq \Lambda_n < X_{n+1}\}} \middle| H_1 \right] \right] \\
&= r(e, \phi_0(e, \lambda)) + \sum_{\mathfrak{z}=0}^{\infty} w(e, \phi_0(e, \lambda), \mathfrak{z}) P(\mathfrak{z} | (e, \phi_0(e, \lambda)), \lambda) \\
&\quad + \sum_{n=1}^{\infty} \mathbb{E}_{(e, \lambda)}^\pi \left[\mathbb{E}_{(\mathcal{E}_1, \Lambda_1)}^{\pi^-} \left[r(\mathcal{E}_{n-1}, \mathcal{A}_{n-1}) \mathbb{1}_{\{\Lambda_{n-1} \geq 0\}} + w(\mathcal{E}_{n-1}, \mathcal{A}_{n-1}, \mathfrak{Z}) \mathbb{1}_{\{0 \leq \Lambda_{n-1} < X_n\}} \right] \right] \\
&= r(e, \phi_0(e, \lambda)) + \sum_{\mathfrak{z}=0}^{\infty} w(e, \phi_0(e, \lambda), \mathfrak{z}) P(\mathfrak{z} | (e, \phi_0(e, \lambda)), \lambda) + \mathbb{E}_{(e, \lambda)}^\pi [V^{\pi^-}(\mathcal{E}_1, \Lambda_1)] \\
&= r(e, \phi_0(e, \lambda)) + \sum_{\mathfrak{z}=0}^{\infty} w(e, \phi_0(e, \lambda), \mathfrak{z}) P(\mathfrak{z} | (e, \phi_0(e, \lambda)), \lambda) \\
&\quad + \sum_{\tilde{e} \in \mathcal{E}} \int_0^\lambda V^{\pi^-}(\tilde{e}, \lambda - t) Q(dt, \tilde{e} | (e, \phi_0(e, \lambda))),
\end{aligned}$$

according to Remark 3.18 and Theorem 3.16, which concludes the proof.

C.4 PROOF OF PROPOSITION 3.31

Let $\mathbf{i} := (0, 0, 0, 1, 0, 0)$ and $\mathbf{k} := (0, 0, 0, 0, 1, 0)$, so that $e = \bar{e} + \Delta_p \mathbf{i} + \Delta_z \mathbf{k}$, where $\Delta_p = p - \bar{p}$ and $\Delta_z := z - \bar{z}$. Define further $\hat{e} := \bar{e} + \Delta_z \mathbf{k}$. According to Proposition 3.30 and [31, Theorem 3], we can write

$$V^*(\hat{e}, \lambda) = \mathcal{A}V^*(\hat{e}, \lambda) = V^*(\bar{e}, \lambda) + \rho \Delta_z (\bar{p} - j). \quad (\text{C.1})$$

With the auxiliary function $u(\mathbf{e}, \lambda) := V^*(\mathbf{e} - \Delta_p \mathbf{i}, \lambda) + \rho \Delta_p (y + z)$ for $(\mathbf{e}, \lambda) \in \mathcal{E} \times \mathbb{T}$, simple calculations yield $\mathcal{A}u(\mathbf{e}, \lambda) = u(\mathbf{e}, \lambda)$ for any $(\mathbf{e}, \lambda) \in \mathcal{E} \times \mathbb{T}$, and Theorem 3.28 implies that $V^*(e, \lambda) = V^*(\hat{e}, \lambda) + \rho \Delta_p (y + z)$. Combining this with (C.1) concludes the proof.

C.5 MAXIMUM LIKELIHOOD ESTIMATION FOR THE POISSON PARAMETERS

Fix $\mathfrak{s} \in \{a, b\}$, $j \in \{+1, -1\}$ and denote the Poisson parameters $\mu_j^{\mathfrak{s}}, \kappa_j^{\mathfrak{s}}, \theta_j^{\mathfrak{s}}$ by μ, κ, θ respectively. Introduce the auxiliary parameters $\mu' := \mu S^l / S^m$ and $\theta' := \theta S^l / S^c$. Suppose we observe l_i times of limit order arrivals, m_i times of market order arrivals and c_i times of cancellations on the \mathfrak{s} side in the i -th queueing race, whose starting time is τ_i , duration is d_i and the volume in unit size at \mathfrak{s} price at time t is $\text{Vol}_i(t)$, for $i \in \{1, \dots, \#\Omega_j\}$. The likelihood functions are then constructed as:

$$\begin{aligned} \mathcal{L}(\mu' : m_1, \dots, m_{\#\Omega_j}, d_1, \dots, d_{\#\Omega_j}) &:= \prod_{i=1}^{\#\Omega_j} \frac{(\mu' d_i)^{m_i}}{m_i!} e^{-\mu' d_i}, \\ \mathcal{L}(\kappa : l_1, \dots, l_{\#\Omega_j}, d_1, \dots, d_{\#\Omega_j}) &:= \prod_{i=1}^{\#\Omega_j} \frac{(\kappa d_i)^{l_i}}{l_i!} e^{-\kappa d_i}, \\ \mathcal{L}(\theta' : c_1, \dots, c_{\#\Omega_j}, \Theta(d_1), \dots, \Theta(d_{\#\Omega_j})) &:= \prod_{i=1}^{\#\Omega_j} \frac{\Theta(d_i)^{c_i}}{c_i!} e^{-\Theta(d_i)}, \end{aligned}$$

where $\Theta(d_i) := \theta' \int_{\tau_i}^{\tau_i + d_i} \text{Vol}_i(t) dt$. Taking logarithms, and cancelling the derivatives yield the optima (3.21) with

$$N_{s,j}^{\varpi} = \sum_{i=1}^{\#\Omega_j} \varpi_i, \quad \text{for } \varpi \in \{m, l, c\} \quad D_{s,j} = \sum_{i=1}^{\#\Omega_j} d_i, \quad V_{s,j} = \sum_{i=1}^{\#\Omega_j} \int_{\tau_i}^{\tau_i + d_i} \text{Vol}_i(t) dt.$$

REFERENCES

- [1] J. Abate, G. L. Choudhury and W. Whitt. An introduction to numerical transform inversion and its application to probability models. *Computational Probability*, W. Grassman (ed.), Kluwer, Boston: 257-323, 1999.
- [2] J. Abate and W. Ward. Computing Laplace transforms for numerical inversion via continued fractions. *INFORMS Journal on Computing*, 11(4): 394-405, 1999.
- [3] J. Abate and W. Whitt. Numerical inversion of Laplace transforms of probability distributions. *ORSA Journal on Computing*, 7(1): 36-43, 1995.
- [4] A. Alfonsi, A. Fruth and A. Schied. Optimal execution strategies in limit order books with general shape functions. *Quantitative Finance*, 10(2): 143-157, 2010.
- [5] R. F. Almgren. Optimal execution with nonlinear impact functions and trading-enhanced risk. *Applied Mathematical Finance*, 10(1): 1-18, 2003.
- [6] R. F. Almgren and N. Chriss. Optimal execution of portfolio transactions. *Journal of Risk*, 3(2): 5-39, 2001.
- [7] R. B. Ash. *Real Analysis and Probability*. Academic Press, 2014.
- [8] E. Bayraktar and M. Ludkovski. Liquidation in limit order books with controlled intensity. *Mathematical Finance*, 24(4): 627-650, 2014.
- [9] P. A. Bernstein and E. Newcomer. *Principles of transaction processing*. Morgan Kaufmann, 2000.
- [10] R. Bloomfield, M. O'hara and G. Saar. Hidden liquidity: Some new light on dark trading. *The Journal of Finance*, 70(5): 2227-2274, 2015.

- [11] J. Bonart and M. D. Gould. Queue imbalance as a one-tick-ahead price predictor in a limit order book. *Market Microstructure and Liquidity*, 2(2): 1650006, 2016.
- [12] J. Bonart and M. D. Gould. Latency and liquidity provision in a limit order book. *Quantitative Finance*, 17(10): 1601-1616, 2017.
- [13] P. Brémaud. Point processes and queues: martingale dynamics. Springer-Verlag, 1981.
- [14] J. Brogaard, T. Hendershott and R. Riordan. High-frequency trading and price discovery. *Quantitative finance*, 27(8): 2267-2306, 2014.
- [15] J. Brogaard, T. Hendershott and R. Riordan. Price discovery without trading: Evidence from limit orders. [SSRN:2655927](#), 2016.
- [16] E. N. Brown, R. Barbieri, V. Ventura, R. E. Kass and L. M. Frank. The time-rescaling theorem and its application to neural spike train data analysis. *Neural computation*, 14(2): 325-346, 2002.
- [17] A. Carrion. Very fast money: High-frequency trading on the NASDAQ. *Journal of Financial Markets*, 16(4): 680-711, 2013.
- [18] Á. Cartea, R. F. Donnelly and S. Jaimungal. Enhancing trading strategies with order book signals. [SSRN:2668277](#), 2015.
- [19] Á. Cartea and S. Jaimungal. Optimal execution with limit and market orders. *Quantitative finance*, 15(8): 1279-1291, 2015.
- [20] A. Cartea, R Payne, J. Penalva and M. Tapia. Ultra-fast activity and market quality. [SSRN:2616627](#), 2016.
- [21] G. Cebiroğlu and U. Horst. Optimal order display in limit order markets with liquidity competition. *Journal of Economic Dynamics and Control*, 58: 81-100, 2015.
- [22] D. Challet and R. Stinchcombe. Analyzing and modeling 1+ 1d markets. *Physica A: Statistical Mechanics and its Applications*, 300(1): 285-299, 2001.

- [23] V. Choulakian, R. A. Lockhart and M. A. Stephens, Cramér-von Mises statistics for discrete distributions. *Canadian Journal of Statistics*, 22(1): 125-137, 1994.
- [24] A. Clauset, C. R. Shalizi and M. E. Newman. Power-law distributions in empirical data. *SIAM review*, 51(4): 661-703, 2009.
- [25] R. Cont, A. Kukanov and S. Stoikov. The price impact of order book events. *Journal of Financial Econometrics*, 12(1): 47-88, 2014.
- [26] R. Cont and A. De Larrard. Price dynamics in a Markovian limit order market. *SIAM Journal on Financial Mathematics*, 4(1): 1-25, 2013.
- [27] R. Cont, A. Kukanov. Optimal order placement in limit order markets. *Quantitative Finance*, 17(1): 21-39, 2017.
- [28] R. Cont, S. Stoikov and R. Talreja. A stochastic model for order book dynamics. *Operations Research*, 58(3): 549-563, 2010.
- [29] R. Cont and E. Voltchkova. A finite difference scheme for option pricing in jump diffusion and exponential Lévy models. *SIAM Journal on Numerical Analysis*, 43(4): 1596-1626, 2005.
- [30] K. Dayri and M. Rosenbaum. Large tick assets: implicit spread and optimal tick size. *Market Microstructure and Liquidity*, 1(1), 2015.
- [31] E. V. Denardo. Contraction mappings in the theory underlying dynamic programming. *Siam Review*, 9(2): 165-177, 1967.
- [32] R. Donnelly and L. Gan. Optimal Decisions in a Time Priority Queue. [SSRN:2911540](https://ssrn.com/abstract=2911540), 2017.
- [33] S. S. Dragomir. Approximating the Riemann-Stieltjes integral by a trapezoidal quadrature rule with applications. *Mathematical and Computer Modelling*, 54(1): 243-260, 2011.
- [34] P. Fodra and H. Pham. Semi-Markov model for market microstructure. *Applied Mathematical Finance*, 22(3): 261-295, 2015.

- [35] A. Garache, G. Disdier, J. Kockelkoren and J. P. Bouchaud Fokker-planck description for the queue dynamics of large tick stocks. *Physical Review E*, 88(3): 032809, 2013.
- [36] J. Gatheral, A. Schied and A. Slynko. Transient linear price impact and Fredholm integral equations. *Mathematical Finance*, 22(3): 445-474, 2012.
- [37] M. A. Goldstein, P. Kumar and F. C. Graves. Computerized and High-Frequency Trading. *Financial Review*, 49(2): 177-202, 2014.
- [38] F. Gonzalez and M. Schervish. Instantaneous order impact and high-frequency strategy optimization in limit order books. [arXiv:1707.01167](https://arxiv.org/abs/1707.01167), 2017.
- [39] M. Gould, M. Porter, S. Williams, M. McDonald, D. Fenn and S. Howison. Limit order books. *Quantitative Finance*, 13(11): 1709-1742, 2013.
- [40] A. Granas and J. Dugundji. Fixed point theory. Springer Science & Business Media, 2013.
- [41] O. Guéant, C. A. Lehalle and J. Fernandez-Tapia. Optimal portfolio liquidation with limit orders. *SIAM Journal on Financial Mathematics*, 3(1): 740-764, 2012.
- [42] F. Guilbaud and H. Pham. Optimal high-frequency trading with limit and market orders. *Quantitative Finance*, 13(1): 79-94, 2013.
- [43] B. Hagströmer and L. Norden. The diversity of high-frequency traders. *Journal of Financial Markets*, 16(4): 741-770, 2013.
- [44] J. Hasbrouck and G. Saar. Low-latency trading. *Journal of Financial Markets*, 16(4): 646-679, 2013.
- [45] N. Hautsch. Econometrics of financial high-frequency data. Springer Science & Business Media, 2011.
- [46] B. Hollifield. R. A. Miller and P. Sandås. Empirical analysis of limit order markets. *The Review of Economic Studies*, 71(4): 1027-1063, 2004.

- [47] N. Hautsch and R. Huang Limit order flow, market impact and optimal order sizes: evidence from NASDAQ TotalView-ITCH data. *Market Microstructure: Confronting Many Viewpoints*, 2012.
- [48] N. Hirschey. Do high-frequency traders anticipate buying and selling pressure? [SSRN:2238516](#), 2016.
- [49] W. Huang, C.-A. Lehalle and M. Rosenbaum. Simulating and analyzing order book data: The queue-reactive model. *Journal of the American Statistical Association*, 110(509): 107-122, 2015.
- [50] Y. Huang and X. Guo. Finite horizon semi-Markov decision processes with application to maintenance systems. *European Journal of Operational Research*, 212(1): 131-140, 2011.
- [51] R. Huang and T. Polak. LOBSTER: Limit order book reconstruction system. [SSRN:1977207](#), 2012.
- [52] M Ieda. An implicit method for the finite time horizon Hamilton-Jacobi-Bellman quasi-variational inequalities. *Applied Mathematics and Computation*, 265: 163-175, 2015.
- [53] A. Irle. Stochastic ordering for continuous-time processes. *Journal of Applied Probability*, 40(2): 361-375, 2003.
- [54] D. R. Jiang and W. B. Powell. An approximate dynamic programming algorithm for monotone value functions. *Operations Research*, 63(6): 1489-1511, 2015.
- [55] C. M. Jones. What do we know about high-frequency trading?. *Working Paper*, 2013.
- [56] A. Kirilenko, A. S. Kyle, M. Samadi and T. Tuzun. The Flash Crash: High-Frequency Trading in an Electronic Market. *The Journal of Finance*, 72(3): 967-998, 2017.
- [57] A. A. Kirilenko and G. Lamacie. Latency and asset prices. [SSRN:2546567](#), 2015.

- [58] A. A. Kirilenko and A. W. Lo. Moore's law versus murphy's law: Algorithmic trading and its discontents. *The Journal of Economic Perspectives*, 27(2): 51-72, 2013.
- [59] J. Lorenz and R. F. Almgren. Mean-variance optimal adaptive execution. *Applied Mathematical Finance*, 18(5): 395-422, 2011.
- [60] J. W. Mamer. Successive approximations for finite horizon, semi-Markov decision processes with application to asset liquidation. *Operations Research*, 34(4): 638-644, 1986.
- [61] S. Maslov and M. Mills. Price fluctuations from the order book perspective - empirical facts and a simple model. *Physica A: Statistical Mechanics and its Applications*, 299(1): 234-246, 2001.
- [62] A. J. Menkveld. The economics of high-frequency trading: Taking stock. *Annual Review of Financial Economics*, 8: 1-24, 2016.
- [63] A. J. Menkveld. High-Frequency Traders and Market Structure. *Financial Review*, 49(2): 333-344, 2014.
- [64] A. J. Menkveld. High-frequency trading as viewed through an electronic microscope. [SSRN:2875612](#), 2016.
- [65] C. C. Moallemi and K. Yuan. A model for queue position valuation in a limit order book. [SSRN:2996221](#), 2017.
- [66] J. M. Nascimento and W. B. Powell. An optimal approximate dynamic programming algorithm for the lagged asset acquisition problem. *Mathematics of Operations Research*, 34(1): 210-237, 2009.
- [67] A. A. Obizhaeva and J. Wang. Optimal trading strategy and supply/demand dynamics. *Journal of Financial Markets*, 16(1): 1-32, 2013.
- [68] M. O'Hara, G. Saar and Z. Zhong. Relative tick size and the trading environment. [SSRN:2463360](#), 2015.
- [69] M. O'Hara, C. Yao and M. Ye. What's not there: Odd lots and market data. *The Journal of Finance*, 69(5): 2199-2236, 2014.

- [70] M. O’Hara and M. Ye. Is market fragmentation harming market quality? *Journal of Financial Economics*, 100(3): 459-474, 2011.
- [71] B. Øksendal and A. Sulém. Applied stochastic control of jump diffusions (2nd ed.). Springer, 2005.
- [72] W. B. Powell. Approximate Dynamic Programming: Solving the curses of dimensionality, 703. John Wiley & Sons, 2007.
- [73] U.S. Securities and Exchange Commission. Concept release on equity market structure. *Federal Register*, 75(13): 3594-3614, 2010.
- [74] U.S. Securities and Exchange Commission. Equity market structure literature review Part II: High frequency trading. Staff of the Division of Trading and Markets, 2014.
- [75] E. Smith, J. D. Farmer, L. s. Gillemot and S. Krishnamurthy. Statistical theory of the continuous double auction. *Quantitative finance*, 3(6): 481-514, 2003.
- [76] S. Stoikov and R. Waeber. Optimal asset liquidation using limit order book information. [SSRN:2113827](https://ssrn.com/abstract=2113827), 2012.
- [77] L. Takács. Introduction to the Theory of Queues. Oxford University press, Chapman & Hall, 1959.
- [78] H. C. Tijms. A first course in stochastic models. John Wiley and Sons, 2003.
- [79] I. M. Toke and N. Yoshida. Modelling intensities of order flows in a limit order book. *Quantitative finance*, 17(5): 683-701, 2017.
- [80] T. W. Yang and L. Zhu. A reduced-form model for level-1 limit order books. *Market Microstructure and Liquidity*, 2(2): 1650008, 2016.
- [81] Ö. Yeniay. Penalty function methods for constrained optimization with genetic algorithms. *Mathematical and Computational Applications*, 10(1): 45-56, 2005.

- [82] L. Zhao. A model of limit-order book dynamics and a consistent estimation procedure. PhD thesis, Carnegie Mellon, 2010.